Institutional Repository - Research Portal
Dépôt Institutionnel - Portail de la Recherche
researchportal.unamur.be
University of Namur

THESIS / THÈSE

MASTER IN BIOMEDICINE PROFESSIONAL FOCUS

Role of the integrin α5β1 in cell migration in a model of metastatic breast cancer

Piñeros Leyton, Martha

Award date:
2019

Awarding institution:
University of Namur

Link to publication

General rights
Copyright and moral rights for the publications made accessible in the public portal are retained by the authors and/or other copyright owners and it is a condition of accessing publications that users recognise and abide by the legal requirements associated with these rights.

- Users may download and print one copy of any publication from the public portal for the purpose of private study or research.
- You may not further distribute the material or use it for any profit-making activity or commercial gain
- You may freely distribute the URL identifying the publication in the public portal ?

Take down policy
If you believe that this document breaches copyright please contact us providing details, and we will remove access to the work immediately and investigate your claim.

Download date: 26. Apr. 2024

Faculté de Médecine

ROLE OF THE INTEGRIN α5β1 IN CELL MIGRATION IN A MODEL OF METASTATIC BREAST CANCER

Mémoire présenté pour l'obtention
du grade académique de master en sciences biomédicales

Martha Liliana PIÑEROS LEYTON

Janvier 2019

Université de Namur
FACULTE DE MEDECINE
Secrétariat des départements
Rue de Bruxelles 61 - 5000 NAMUR
Téléphone: + 32(0)81.72.43.22
E-mail: manon.chatillon@unamur.be - http://www.unamur.be/

Role of the integrin α5β1 in cell migration in a model of metastatic breast cancer

PIÑEROS LEYTON Martha Liliana

Abstract

Background: Metastasis is the leading cause of breast cancer mortality and is the result of the interplay between cancer cells and the surrounding microenvironment, which is regulated by complex molecular networks and involved numerous genes. Matrix components and many extracellular matrix (ECM) proteins, such as fibronectin (FN), promote tumor progression and metastatic spread. Integrins are cell-surface adhesion receptors that interact with ECM components have been reported to contribute to tumor growth, cell adhesion, invasion, and metastasis.
Aim: The purpose of this study was to characterize the role of integrin α5 (ITGA5) and integrin β3 (ITGB3) in cell migration in a model of metastatic breast cancer.
Methods: ITGA5 and ITGB3 expressions were invalidated using siRNA in MDA-MB-231 cells. To achieve a stable knockdown, ITGA5 and ITGB3 invalidation as also performed using shRNA. First, the levels of mRNA and protein were assessed to confirm the effectiveness of the invalidation. Second, impacts of integrin invalidation were evaluated on phenotype characteristics, cytotoxicity, and migratory capacity.
Results: Effective invalidation of ITGA5 and ITGB3 using siRNA, with a strong effect on the migratory capacity in ITGB3 invalidated cells. On the other hand, the ITGA5 knockdown using shRNA was effective in the case of sh126, but it was not for sh124. No differences were observed at the morphological level. A difference in the confluency was observed without a toxicity effect, suggesting a decrease in cell adhesion. During the second part of the study a cell adhesion test was carried out, which did not show conclusive results. Additionally, ITGA5- and ITGB3-invalidated cells were further characterized on uncoated and FN-coated surfaces. A new ITGA5-targeting shRNA was tested, giving a very strong phenotype that did not allow cell characterization. ITGB3 knockdown was performed using shRNA previously tested in the PACMAN project, which covers this study. FN-coating showed an effect on the cells. It triggered the clusterization of ITGA5 and induced change in cell size, indicating a higher adhesion to the surface. Finally, cells were co-invalidated for ITGA5 and ITGB3, leading to a lower adhesion. Nevertheless, the focal adhesion formation was observed in all the cases studied.
Conclusion: ITGA5 invalidated cells did not show a significant difference in their migratory capacity. A further characterization of the role of the integrins in cell migration will allow to identify therapeutic/diagnostic targets against advanced breast cancer.
Keywords: *Cell migration, Integrins, α5β1, αvβ3, metastasis*

Mémoire de master en sciences biomédicales
Janvier 2018
Thesis Supervisor: C. Michiels

I would like to thank the people who were present this year during the development of my Master thesis and that made this an unforgettable experience.

First, I would like to thank my supervisor, Carine Michiels. Thank you for your guidance and support. Thank you for sharing your wisdom with your valuable advice.

Second, I would like to thank Sophie, who prepare and encourage me this year. Thank you for your patience, for always being willing to help me and guide me through this process.

I have a deep admiration for both of you and I could learn a lot from you during this work, not only at the academic level but also for my life.

Thanks to the TumHyp team for help me to grow as a researcher and for always give solutions in each part of the project.

Thank you also to all other members of the URBC who contributed in many ways to the development of this thesis, always within a good atmosphere. Thanks to Antoine, Catherine, Noële, Maude, Martine and Guy for being always available to help me and teach me something new.

Thanks to all the others thesis students that makes this period enjoyable. Especially to Christoph, Loïc, Sebastian for sharing with me their scientific knowledge and always being willing to answer my questions.

Thanks to all people from the Master. To Mr. Gillet who has advised me during this study and with who I have been able to learn a lot. To the Biomed students that accompanied me in all the period, specially Emilie and Bea.

Thanks to all the people that contributed to this scientific pathway. Thanks to Ana L, Natalia and Maria Mercedes.

Thanks to my family and friends that support me. Special thanks to Juanita, Rita, Pierre and Nancy.

I would like to thank my mom for her unconditional love and support in each step, that help me to reach my dreams.

Finally, thanks to Florent for being always present by my side, help me on this path and make my life so happy.

A-TUB	α-tubulin
BrdU	5-bromo-2'- deoxyuridine
BSA	Bovine serum albumin
CAF	Cancer-associated fibroblast
CAM	Cell adhesion molecule
CTC	Circulating tumor cell
ECM	Extra cellular matrix
EGFR	Epidermal growth factor receptor
EMT	Epithelial-mesenchymal transition
FA	Focal adhesion
FAK	Focal adhesion kinase
FN	Fibronectin
IF	Immunofluorescence
ITG	Integrin
ITGA5	Integrin alpha 5
ITGB3	Integrin beta 3
ITGB3 KO	Integrin beta 3 knock-out
ITGB6	Integrin beta 6
KO	Knock out
LDH	Lactate dehydrogenase
mRNA	Messenger RNA
MET	Mesenchymal- epithelial transition
MMP	Matrix metalloproteinase
MSC	Mesenchymal stem cell
PBS	Phosphate-buffered saline
PFA	Paraformaldehyde
PPT	Passage post-transduction
RISC	RNA-induced silencing complex
RT-qPCR	Reverse transcription - quantitative polymerase chain reaction
shRNA	Short hairpin RNA
siA5	siRNA ITGA5
siB3	siRNA ITGB3
siRF	siRNA RISC free
siRNA	Small interfering RNA
TAM	Tumor-associated macrophage
TGF-β	Transforming growth factor beta
TNM	TNM Classification of Malignant Tumours
UT	Untransfected/Untransduced
WNT	Wingless/Integrated
ZEB	Zinc finger E-box-binding homeobox

Table of contents

This thesis is written as the completion to the Master of Biomedical Sciences, at the University of Namur. This project was done at Laboratory of Cellular Biochemistry and Biology (URBC) within the TumHyp team lead by Prof. Carine Michiels.

This study focused on the role of the integrin α5β1 in cell migration in a model of metastatic breast cancer. In order to facilitate the understanding of the experiments and results obtained, this work will start with an introduction containing a series of information and theoretical notions relevant to the study.

First, with cancer being a leading cause of death worldwide, it is an important research focus in the medical field. Cancer is a group of diseases that can affect almost any part of the body. It is an uncontrolled growth, that often invades surrounding tissue and spread to other organs[1]. This latter process is denominated metastasis.

Chapter 1 contains the information about breast cancer, the study focused on this cancer type because is the most frequently diagnosed cancer, with approximately 2.09 million cases in 2018, and the leading cause of cancer death in women worldwide[1]. Then, to understand the cancer progression and metastasis, chapter 2 explains the cell adhesion process and the role of the actors involved. The chapter brings key information about the interaction of some cell adhesion molecules and the extracellular matrix. It also describes, how the abnormal functioning of those molecules could entail to different processes related to metastasis and alter the interactions with the different compounds of the microenvironment.

Following, chapter 3 talks about metastasis, which is a complex process with great importance because it remains to be a big problem in the clinical management of cancer since a major cause cancer mortality is associated with the disseminated disease rather than with the primary tumor[2]. Chapter 3 explains the steps involved in this process and its relevance within the frame of breast cancer. Afterward, chapter 4 presents integrins and their characteristics in cancer progression and metastasis. Integrins are some of these cell adhesion molecules to extracellular matrix (ECM). Specifically, this section elucidates the current knowledge about integrins α5 (ITGA5) and β3 (ITGB3) in relation to cancer, which are the focus of this study.

Finally, chapter 5 finishes with the description of the PACMAN (Peptide-Assisted Cellular Migration Along eNgineered surfaces) project, which is a research project aiming to characterize and compare the static and different migratory phenotypes in a way to identify pathways involved in cell migration induced by the activation of integrins α5β1 and αvβ3, and within which this thesis was developed.

I. INTRODUCTION

1. Breast cancer

Breast cancer results from the proliferation of malignant cells derived from epithelial cells that coat the breast ducts or lobules. This is a clonal and unique disease, where a cell, through a series of somatic or germline mutations, acquires the ability to divide without control, forming a tumor. The development of breast cancer involves a progression through intermediate stages. Then, it becomes severe as an invasive carcinoma, finally resulting in a metastatic disease, when it spreads to other parts of the body[3]. Breast cancer is characterized by heterogeneous cell populations. This heterogeneity causes different problems in therapeutic medicine. Notably due to its complex etiology and uncomplete understanding of its genesis[4].

1.1. Epidemiology and risk factors

Breast cancer is the cancer with the highest incidence among women worldwide. This disease is the most frequently diagnosed cancer and the leading cause of cancer death in that population[5]. Consequently, breast cancer is becoming a major public health problem[6]. According to Globocan statistics, over 1.7 million new breast cancer cases were diagnosed in 2012, accounting for 25% of all cancer morbidities among females worldwide[4]. Current predictions and statistics suggest that incidence and related mortality are on the rise around the world[7]. However, the incidence of breast cancer significantly varies around the world; for example, it is markedly higher in developed countries. Also, an estimated 60% of breast cancer deaths are now thought to occur in the developing world[6].

There are some risk factors for breast cancer. First, it is strongly related to age with only 5% of all breast cancers occurring in women under 40 years old[8]. Second, the lifestyle plays a major role. For example, the number of cases worldwide has significantly increased in the last 50 years. This phenomenon could be attributed to the modern lifestyle (obesity, drinking alcoholic beverages, smoking and exposure to ionizing radiation). Third, the increased exposure to endogenous estrogen due to reproductive factors such as a late menopause. Also, nulliparity, lack of breastfeeding or the use of combination estrogen-progesterone hormones after menopause have been shown to be associated with the diseace[9]. Finally, genetic susceptibility is the primary cause of 5–10% of all cases[10].

1.2. Classification

Breast cancer is classified by several grading systems. Histopathology, grade, stage, receptor status and DNA mutational status are such examples. The classification determines the prognosis, the selection of the best treatment and its response.

1.2.1. Histopathology

It is based on characteristics observed upon microscopy of biopsy specimens. The two most common histopathological types are carcinoma *in situ* and invasive carcinoma. First, in carcinoma *in situ*, cancer cells proliferate within the epithelial tissue without invade neighboring tissue. It accounts for 13% of breast cancers. Contrarily, invasive carcinoma can spread outside the breast to surrounding tissue. Invasive carcinoma divides in two types depending where it develops:

invasive ductal carcinoma, accounting for 55% of breast cancers, and invasive lobular carcinoma, accounting for 5% of the cases[11].

1.2.2. Stage

Cancer staging is the process of determining how much cancer is in the body and where it is located. It helps to describe the severity of an individual's cancer based on the magnitude of the original (primary) tumor as well as on the extent cancer has spread in the body[12]. The assessment uses the TNM staging system, that is a classification system developed as a tool for doctors to stage different types of cancer, based on certain, standardized criteria. The TNM staging system is based on the extent of the tumor (T), the extent of spread to the lymph nodes (N) and the presence of metastasis (M)[12]. Larger size, nodal spread and metastasis have a higher stage number and a worse prognosis[13]. The lowest stage is the stage 0, describing non-invasive cancers that remain within their original location, they are pre-cancerous, either ductal carcinoma *in situ* (DCIS) or lobular carcinoma *in situ* (LCIS). It is followed by the stages 1–3, those tumors are within the breast or regional lymph nodes. At last, stage 4 describes invasive cancers that have spread beyond the breast and regional lymph nodes to other parts of the body. These metastatic cancers have a less favorable prognosis[14].

1.2.3. Grade

This classification depends on the degree of differentiation of the tumor tissue. It refers to the semi-quantitative evaluation of morphological characteristics of the tumor malignancy and aggressiveness. Pathologists describe cells as well differentiated (low grade), moderately differentiated (intermediate grade) or poorly differentiated (high grade) as the cells progressively lose the features seen in normal breast cells[15].

1.2.4. Receptor status

Breast cancer cells express receptors on their surface and in their cytoplasm and nucleus. The estrogen receptor (ER) and progesterone receptor (PR) status is of critical interest in determining the prognosis of breast cancer patients and the potential benefit of adjuvant hormonal therapy[16]. Their status is routinely assessed as well as the Human epidermal growth factor receptor 2 (*HER2)* status that is also a prognosis marker, where HER2+ breast cancers are generally more aggressive than HER2- breast cancers. This marker, HER2+, determines patient eligibility to monoclonal antibody trastuzumab therapy[17]. Triple negative breast cancer is characterized by lack of expression of these three receptors: estrogen, progesterone and HER2 receptors, although these tumors frequently do express receptors for other hormones, such as androgen receptor and prolactin receptor[18]. Clinically, these cases are characterized by greater aggressiveness, frequent rate of local recurrence and organ metastases. They are associated with the occurrence of hereditary forms of breast cancer caused by pathogenic mutations in the BRCA1 gene or in rare cases, BRCA2[19] they are more common in younger women. Therefore, most triple-negative breast cancers are poor-prognosis tumors with a complex genomic landscape[20].

1.2.5. Mutational status

In cancer, some changes in DNA sequence, known as driver mutations, confer proliferative advantages to those cancer cells. Driver mutations can be inherited in the germline, but most of them appear in somatic cells during the lifetime of the patient. In addition, many temporary mutations that are not involved in cancer development also arise [21].

The cases due to a hereditary predisposition are just a small percentage. However, gene signatures have been developed as predictors of response to therapy and protein gene products. Those implicated genes have direct roles in driving the biology and clinical behavior of cancer cells and are potential targets for the development of novel therapeutics[22].

Two genes, BRCA1 and BRCA2, are linked to a rare familial form of breast cancer. Women whose families have mutations in these genes have a higher risk of developing breast cancer[23]. Additionally, the mutation of the p53 oncogene, characteristic of the Li-Fraumeni syndrome, has been connected to the disease[24]. These mutations would determine approximately 40% of the cases of hereditary breast cancer.

Other inherited mutations that increase the risk of cancer include mutations of the PTEN gene (Cowden syndrome) of STK11 (Peutz-Jeghers syndrome) of CDH1. The majority of breast cancer-susceptibility genes code for tumor suppressor proteins that are involved in critical processes of DNA repair pathways[25]. Its frequency and increased risk for breast cancer are not yet known exactly. In more than 50% of cases, the gene associated with inherited breast cancer is unknown.

To analyze the complete panorama, that involved inherited and non-inherited mutations, 560 genomes of patients with breast cancer were sequencing to study all classes of somatic mutation across exons, introns, and intergenic regions. As a result, five new cancer genes were identified (MED23, FOXP1, MLLT4, XBP1, and ZFP36L1)[21]. This study highlights the repertoire of cancer genes and mutational processes.

1.3. Prognosis

The stage of the breast cancer is the most important component of conventional classification methods of breast cancer, because it has a greater effect on the prognosis than the other classification. This disease heterogeneous in clinical, pathological and genetical characteristics shows that the poor prognosis and the cause of death in the majority of patients are related to the metastatic lesions[26]. Despite major advances in understanding the molecular and genetic basis of cancer, metastasis remains the cause of the vast majority of cancer-related mortality[27]. The spread of cancer cells throughout the body represents the central clinical challenge of solid tumor treatment. A deeper understanding of the mechanisms underlying the metastatic process and the complex interactions between tumor and host during disease progression has been widely recognized and will be critical for developing efficient therapeutic interventions and diagnostic tools[28].

2. Cell adhesion

Cell adhesion is an essential process for tissue development, structure, and maintenance in multicellular organisms[29]. Also, cell adhesion is involved in cell migration and proliferation. Cell-to-cell and cell-to-matrix adhesion are the interactions by which cells attach to other cells or to extracellular components through specialized molecules of the cell surface[29]. Additionally, cell adhesion provides a mechanism for intercellular communication and signal transduction, in order to detect and respond to changes in the microenvironment. Alteration in cell adhesion can affect different cellular processes and lead to a diverse kind of diseases, including cancer[30]. Understand its complexity is crucial for the study of cancer progression and metastasis.

2.1. Cell adhesion molecules

Cell adhesion molecules (CAMs) are transmembrane glycoproteins that mediate cell-cell and cell-matrix interactions and also serve as the receptor for different kinds of virus[31]. They are essential for transducing intracellular signals responsible for the cytoskeletal organization, cell growth, differentiation, site-specific gene expression, morphogenesis, immunologic function, inflammation, adhesion, migration, invasion, angiogenesis, and organ-specific metastasis[32].

Four of the major groups of cell adhesion molecules are the immunoglobulin superfamily (Ig-CAMs), the integrins, the selectins, and the cadherins. CAMs bind to other cells or matrix components through their interaction with the corresponding ligands. In some cases, those ligands can be CAMs themselves[33] (Figure 1).

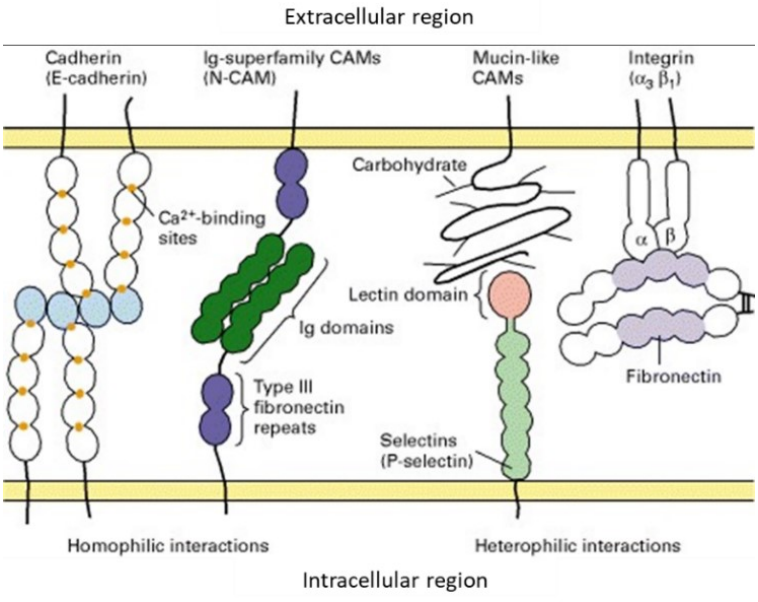

Figure 1. Major families of cell-adhesion molecules (CAMs). The main groups that mediate cell-cell and cell-matrix adhesion: the immunoglobulin superfamily (ig-CAMs), the integrins, the selectins, and the cadherins. Adapted from Lodish et al. Molecular cell biology (2000).

2.1.1. Immunoglobulin superfamily

The immunoglobulin superfamily (Ig-CAMs) is the most diverse superfamily of CAMS. They are expressed in many different cell types, including cells of the nervous system, leukocytes and epithelial, and endothelial cells. This characteristic implies the wide variety of biological processes that Ig-CAMS have in the organism, such as brain development, immune responses, tissue sorting, epithelial morphogenesis and the development of the vascular network[34]. This family is characterized by the presence of one or more Ig-like domains in the extracellular region of the protein. Additionally, the ectodomain can have fibronectin type III (FNIII) repeats[33].

2.1.2. Cadherins

This superfamily is the main mediator of calcium-dependent cell-cell adhesion. This process is accomplished by homophilic protein-protein interactions between two cadherin molecules at the surface of the respective cell, with a link to the actin filament network[34]. They are the principal components of adherent junctions and desmosomes. Their biological functions are diverse and include the regulation of cell recognition, tissue morphogenesis, tumor progression, synapse formation and synaptic activity[32]. Cadherins play an important role in the migration of cells during the epithelial-mesenchymal transition (EMT). For example, E-cadherin is an epithelial marker and N-cadherin is a mesenchymal marker of the EMT process[31].

2.1.3. Selectins

Selectins (E-selectin, P-selectin, and L-selectin) are a family of heterophilic CAMs that are dependent on fucosylated carbohydrates. Those indispensable for binding of circulating leukocytes to vascular endothelium during the inflammatory response to injury or infection[33].

2.1.4. Integrins

Integrins are the major cell-surface adhesion receptors to the extracellular matrix (ECM). They are a family of 24 transmembrane heterodimers constituted of 18 α and 8 β subunits[35] (Figure 2). Integrins mediate cell adhesion and directly interact with ECM components, providing anchorage for cell adhesion, proliferation, motility, survival and invasion[36]. Integrins are classified into receptors recognizing Arg- Gly-Asp (RGD) peptide motifs, collagen receptors, laminin receptors and leukocyte-specific integrins[37]. Integrin expression is dynamic during the multiple cellular processes where they take part, including cell adhesion, migration, proliferation, survival and the activation of growth factor receptors[36]. In cancer, integrins contribute to tumor growth, cell adhesion, invasion and metastasis[38]. Their role during these processes will be described in chapter 4.

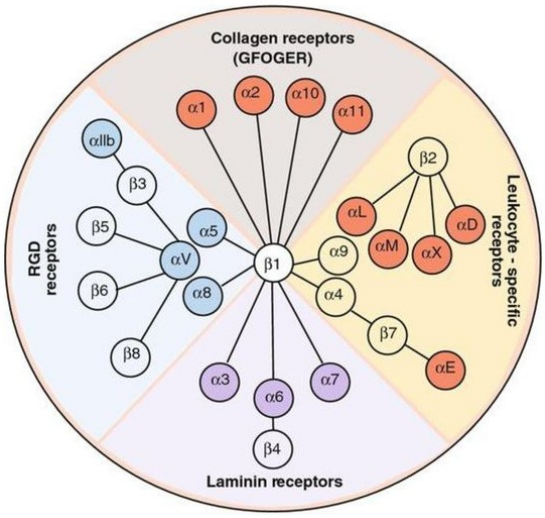

Figure 2 Integrins subunits interactions. The integrin family contains 24 heterodimers constituted of 18 α and 8 β subunits. From Li, Y. et al. Breast Cancer Res (2015).

2.1. Cell-cell interactions

Cell-cell adhesion is indispensable for the physiological function of a cell and its integration in functional structures, such as organ epithelia or stroma[34]. The intercellular junctional complex is compound by three types of adhesion junction: tight junctions, adherens junctions and desmosomes (Figure 3).

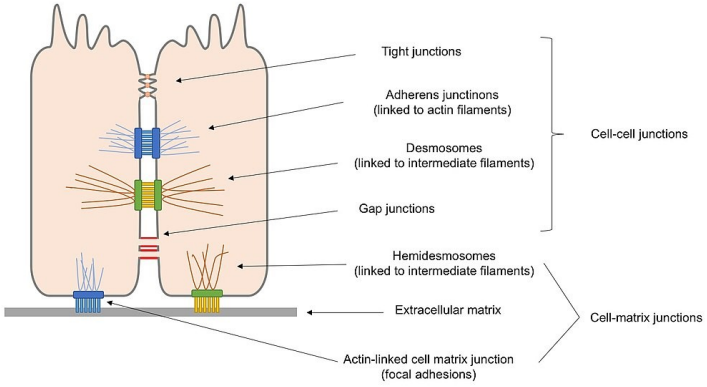

Figure 3. Cell-cell and cell-matrix junctions present in epithelial cells. Representation of the main cell-cell junctions: tight junctions, adherens junctions, desmosomes and gap junctions. Also, the main actors in cell-matrix adhesion are also illustrated: hemidesmosomes, extracellular matrix and focal adhesion. From Lu.qianhe. Cell adhesion (2018).

2.2. Cell-matrix interactions

Cell-matrix interactions are essential for many processes, including normal development, migration and proliferation. They are mediated by CAMs, including integrins, selectins, cadherins, the Ig superfamily and CD44[39]. Other actors involved in cell-matrix adhesion are the focal adhesions, actin and actin-binding proteins, and scaffolding proteins[40].

2.2.1. Extracellular matrix

The extracellular matrix (ECM) is composed of a variable and dynamic network that regulates cell behavior and the development and maintains tissue homeostasis. The protein composition of the ECM assembles into a three-dimensional structure with specific biochemical and biomechanical properties that characterize the cellular microenvironment. Those characteristics determine processes like cell growth, survival, motility and differentiation by the interaction with CAMs. One important feature of the ECM is that it can be dynamically remodeled and specifically tailored to the structure and function of each tissue. Deregulation of the ECM can have serious consequences that lead to pathological conditions like cancer.

Specific matrix components promote tumor progression and metastatic spread[41]. Some of these components, such as fibrillar collagens, fibronectin (FN), hyaluronan and matricellular proteins, have been identified as important constituents of the tumor microenvironment and the metastatic niche. Additionally, therapeutic resistance has been found related to specific ECM molecules, their receptors or enzymatic modifiers[42]. Amongst the ECM compound, FN plays a role with particular interest for this study.

2.2.2. Fibronectin

Fibronectin (FN) is an extracellular glycoprotein, synthesized by diverse cell types like fibroblasts, smooth muscle cells and endothelial cells[43]. The proportion of FN in the ECM is variable depending on the type of tissue and the conditions of such tissue. This protein is a dimer of subunits. Each monomer has a molecular weight of 250 kDa and is composed of three types of modules: FNI, FNII, and FNIII[44] (Figure 4). They have binding affinity for some ECM proteins, heparin/heparan sulfate moieties, and cell surface integrin receptors[43]. Binding to integrins is dependent on an Arg-Gly-Asp (RGD) sequence[45].

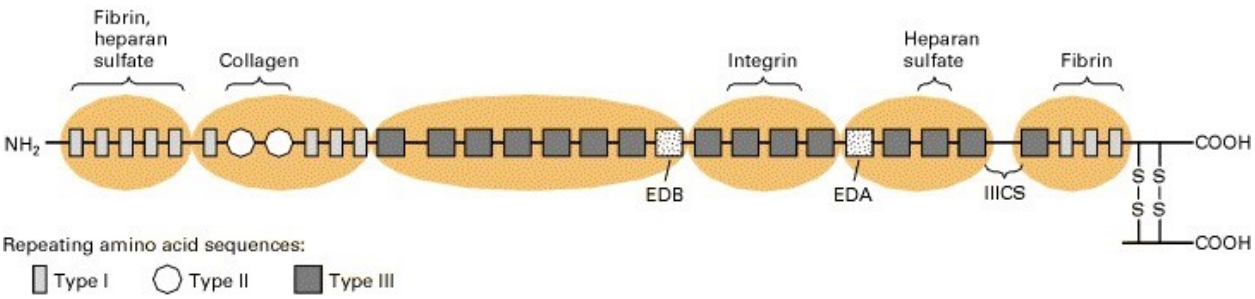

Figure 4. Structure of fibronectin chains. Representation of one of the two chains present in the dimeric fibronectin molecule, composed for the three modules and the binding sites. From Zipursky, L. B. Molecular Cell Biology (2000).

FN plays a major role in the regulation of many cellular and developmental functions. Some of them are cell adhesion, migration, growth, differentiation and proliferation. Also, FN is important for processes such as wound healing and embryotic development[43].

Alteration of FN expression has been associated with different pathologies, including multiple types of cancer. It has been implicated as one of the main elements in promoting cell survival, proliferation, migration, oncogenic transformation and invasion in metastatic models[46]. For example, in breast cancer, FN is expressed to a higher level and with an altered distribution compared to normal breast parenchyma[46]. FN influences cell adhesion and migration because of its interaction with integrins and its role as organizer of ECM.

2.2.3. Focal adhesions

Focal adhesions (FA) are contact points between ECM and cytoskeleton, where integrins attach fibronectin or other extracellular matrix compounds to actin filaments inside cells by a complex of proteins, such as talins, vinculins, α-actinins and filamins[47] (Figure 5). That process generates the driving force necessary for cell migration and other processes, such as cell-cell contacts.
Focal adhesion kinase (FAK), part of this protein complex of FA, is a cytoplasmic nonreceptor tyrosine kinase essential for the organization of focal contacts and maturation into FA[48]. FAK can be activated (by its phosphorylation) by growth factor receptors or integrins and is a crucial mediator their signaling. The overexpression of that kinase has been linked to cancer cell migration, proliferation and survival[49].

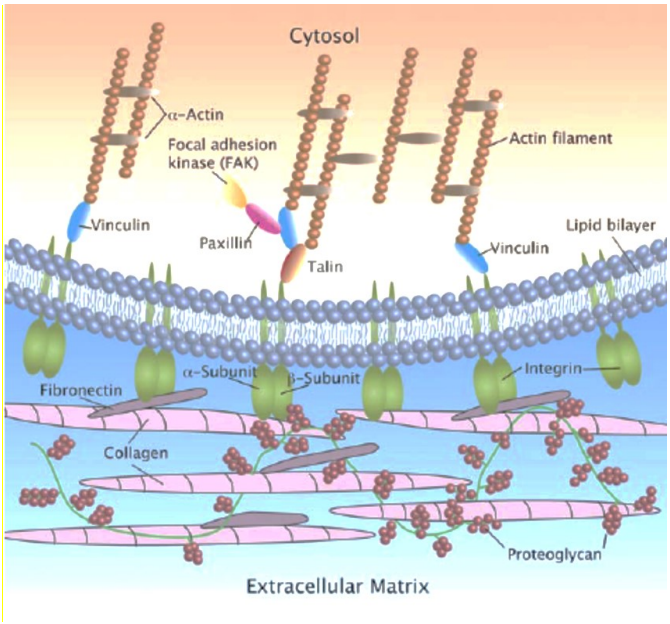

Figure 5. Formation of focal adhesion. Integrin-mediated adhesion of fibronectin in the extracellular matrix and the actin in the cytoskeleton, through the focal adhesion protein complex. From Variola, F. et al. Nanoscale (2011).

2.3.Cell adhesion in cancer

Multiple and diverse cell adhesion molecules are part of the different steps in cancer progression. Alterations in the intercellular and cell-extracellular matrix interactions play a pivotal role in the development of invasive and distant metastasis. The metastatic cascade is a complex process where cancer cells and other interacting cells have flexible adhesive properties. For example, one of the characteristic events is the loss of adhesion between cells at the beginning of the cascade. It results in the dissociation of the cell from the primary tumor, degradation of the extracellular matrix and acquisition of a motile and invasive phenotype via changes in the cell-matrix interaction and composition[31]. Finally, cells attach with a specific tissue tropism and proliferate at a new location to produce the secondary tumor, after extravasation and intravasation processes. The study of cell adhesion and the multiple molecules involved allows their targeting for the development of cancer therapy and diagnostic tools for this pathology.

3. Metastasis

Metastasis refers to the spread of malignant cells to a distant site from a primary cancer location, that allows cancer cells to progressively colonize distant organs[50]. Cancer cells interact with metastatic microenvironment to alter antitumor immunity and the extracellular microenvironment. This is often associated with genomic instability, survival signaling, chemotherapeutic resistance and proliferative cycles[51].

Metastasis also has organ specificity. Different types of cancer have characteristic tendencies to metastasize to particular sites. Additionally, it depends upon properties of the host as well as alterations in the cancer cells[52]. This metastatic process follows three different routes. The first is lymphatic metastasis, which involves colonization of the regional lymph nodes. The second is travel via open cavities such as the pleural cavity or abdominal cavity (peritoneal metastasis). The third is travel through the bloodstream or hematogenous metastasis[52].

Metastasis is a major contributor to the deaths of cancer patients. Therefore, prevention of the initiation of metastasis in high-risk patients is a major therapeutic objective[2].

3.1. Metastasis in breast cancer

The majority of deaths from breast cancer are not due to the primary tumor as the main cause, but are the result of metastases to other organs in the body. Among women diagnosed with breast cancer, only a minority is classified with stage IV disease, which is nearly always incurable. It happens when some patients initially present with distant metastasis or other patients without detectable metastasis at the time of diagnosis. However, around 30% of the patients initially diagnosed with an early-stage disease will develop metastatic lesions within months or even years later[53].

The development of breast cancer involves a progression through a series of intermediate processes, starting with ductal hyperproliferation, followed by subsequent evolution to carcinoma *in situ*, invasive carcinoma, and finally into metastatic disease[54]. Breast cancer metastasis is the result of the interplay between cancer cells and the surrounding microenvironment, which is regulated by complex molecular networks and involved numerous genes. Currently, two processes that have a main role into the metastatic cascade have been pinpointed as a focus of investigation: epithelial-mesenchymal transition (EMT) and tumor microenvironment interactions where cell adhesion molecules play a major role.

3.2. Metastatic cascade

The metastatic cascade is a complex process, that comprises a series of sequential steps. This process is considered highly inefficient, a failure to complete any of these steps will arrest the process. However, because of the high mortality associated with metastasis, the metastatic cascade has been under intense investigation in hopes to eliminate distant spread and reduce their cancer-associated mortality[55].

During carcinoma metastasis, stationary epithelium-derived cancer cells must first become migratory and invasive in order to disseminate from the primary tumor site, and at that point,

cancer cells are disseminated into the bloodstream or lymphatic vessels to distant organs[56]. Upon surviving the transport, some circulating tumor cells (CTCs) undergo cell cycle arrest and adhere to capillary beds within the target organ. After, they manage to extravasate out of the vasculature into the organ parenchyma, proliferating and promoting angiogenesis within the organ and initiate distant metastasis colonization. Simultaneously to these steps, the cancer cells must evade the host's immune response and apoptotic signals (anoikis) in order to survive[57]. At distant sites, disseminated cancer cells need to adapt to the new microenvironment and create a metastatic supportive niche, and switch back from the migratory mode to proliferation mode to repeat the process to produce secondary metastases[55] (Figure 6).

3.2.1. Invasion

Metastasis begins with the invasion of cancer cells into the surrounding host tissue. Degradation of the ECM allows the penetration into tissue boundaries, following by invasion. The cell-to-cell adhesion and cell-ECM adhesion are also altered by the invasive cancer cells[58]. For example, the cadherin family plays a predominant role in breast cancer metastasis. The down-regulation of E-cadherin, which maintains cell-cell junctions, is a determinant in the outgrowth of metastatic breast cancer cells and reflects its progression and metastasis associated with poor prognosis. Epithelial-mesenchymal transition (EMT) plays a major role in tumor progression by assisting invasion and intravasation into the bloodstream or lymphatic vessels, and inducing proteases involved in the degradation of the ECM. As markers of the process are E-cadherin and N-cadherin. First, the down-regulation of E-cadherin results in the loss of cell-cell adhesion between epithelial breast cancer. Second, the increase in N-cadherin or other mesenchymal cadherins, enables the adhesion of cancer cells to stromal cells, promoting the invasion of cancer cells into the stroma[34]. Additionally, some mutations in E-cadherin which lead to its functional loss were discovered in lobular breast carcinoma. In some systems, host cells such as macrophages, fibroblasts and the coagulation system are required for efficient invasion and metastasis[59].

3.2.2. Migration and mobility

Cancer cells need to migrate from the primary site in order to achieve an invasive phenotype. Those cells are able to migrate either singly or coordinately[60]. Primary, cancer cells that migrate collectively need the presence of intercellular junctions and after invasion and intravasation, they commonly circulate as emboli in the blood or lymphatic vessels. On the other hand, single cancer cells migrate in two ways, mainly by protease-dependent mesenchymal movement, where EMT is a critical pathway, or via the protease-independent amoeboid movement[26]. For being able to leave the primary tumor and invade the surrounding tissue, cancer cells need to reduce their cell-cell adhesion. This action allows disaggregation of cancer cells from the primary site to initiate dissemination. In most cases, EMT mechanism is followed by single cells leaving the primary tumor site[61].

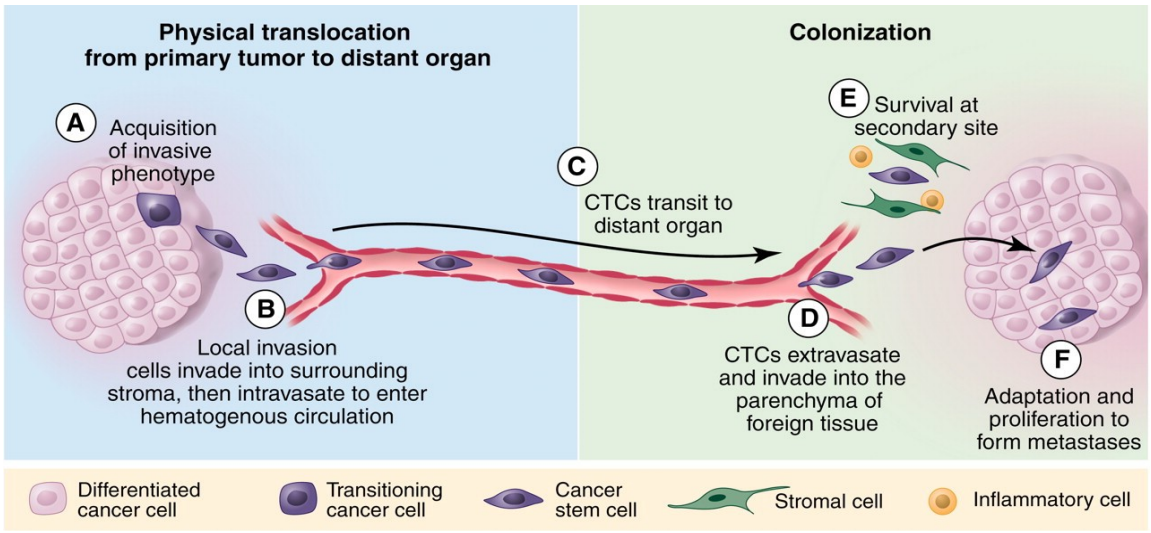

Figure 6. The metastatic cascade. Metastasis is a process that occurs in two major phases: (i) physical translocation of cancer cells from the primary tumor to a distant organ and (ii) colonization of the translocated cells within that organ. (**A**) Cancer cells acquire a invasive phenotype to begin the metastatic cascade, (**B**) Cancer cells invade into the surrounding matrix, and then they intravasate to enter into blood vessels (**C**) Circulating tumor cells (CTCs) travel through the circulation to distant organ. They display properties of anchorage-independent survival. (**D**) At the distant organ, CTCs extravasate and invade into the microenvironment of the foreign tissue. (**E**) At that foreign site, cancer cells must be able to survive, evading the innate immune response as a single cell (or as a small cluster of cells). (**F**) Cancers cell must be able to adapt to the microenvironment and initiate proliferation. From Chaffer and Weinberg, Science (2011).

3.3. Epithelial-mesenchymal transition

Two of the main cell types in mammals are epithelial and mesenchymal cells. Epithelial cells are characterized by cohesive interactions among cells that facilitate the formation of continuous cell layers, presenting three membrane domains (apical, lateral and basal), tight junctions between apical and lateral domains, apicobasal polarized distribution of the various organelles and cytoskeleton components and a lack of mobility of individual epithelial cells with respect to their local environment. On the other hand, multicellular mesenchymal architectures are characterized by loose or no interactions among cells - so that no continuous cell layer is formed - no clear apical and lateral membranes, no apicobasal polarized distribution of organelles and cytoskeleton components and motile cells that may even have invasive properties[62].

Some cells can switch from an epithelial to a mesenchymal status by a regulated process defined as the epithelial to mesenchymal transition (EMT), which is a highly complex and dynamic process with numerous overlapping pathways, cellular and molecular events. The EMT program is a spectrum of cell states in transition, where epithelial cells could undergo a partial EMT and present a partial epithelial and mesenchymal characteristics[55]. In some cases, EMT is reversible and cells undergo the reciprocal mesenchymal to epithelial transition (MET) (Figure 7).

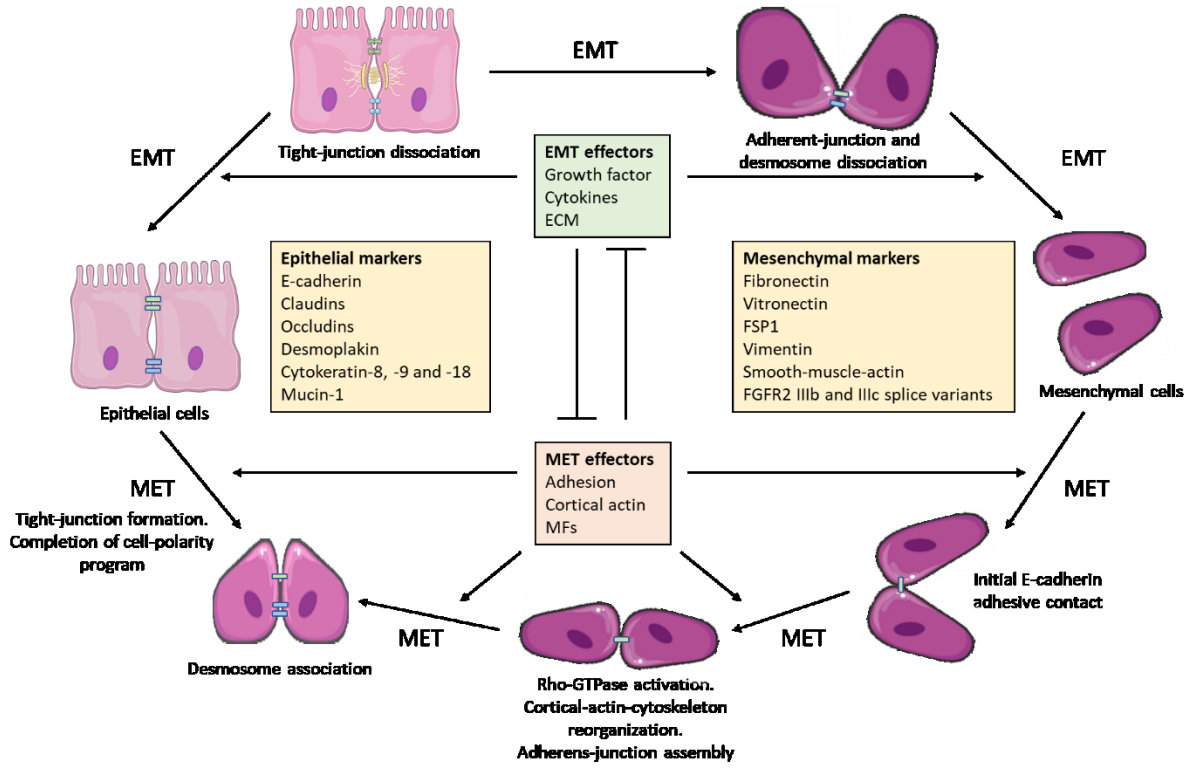

Figure 7. Cycle of events during EMT (epithelial–mesenchymal transition) and the reverse process MET (mesenchymal–epithelial transition). The different stages during EMT and MET are regulated by effectors of EMT and MET, which influence each other. Important events during the progression of EMT and MET, including the regulation of the tight junctions and the adherens junctions, are indicated. Additionally, a number of markers that have been identified as characteristics of either epithelial or mesenchymal cells and these markers. E-cadherin, epithelial cadherin; ECM, extracellular matrix; FGFR2, fibroblast-growth-factor receptor-2; FSP1, fibroblast-specific protein-1; MFs, microfilaments. Adapted from Thiery and Sleeman, Nature Reviews (2006).

EMT was originally described as an integral part of morphogenesis in embryonic development and later was observed in several pathogenesis events, including wound healing, fibrosis and cancer metastasis[55]. It is associated with tumorigenesis, invasion, metastasis, tumor stemness and resistance to therapy[46]. During the EMT process, cells lose their epithelial characteristics and acquire mesenchymal features, which enable them to migrate more efficiently and invade the underlying mesenchyme.

EMT starts with the disintegration of cell-cell adhesion by losing epithelial markers, such as E-cadherin, and expressing mesenchymal markers, such as N-cadherin, fibronectin and vimentin, in order to leave the primary tumor site and invade the surrounding tissue. Therefore, the expression of transcriptional repressors of E-cadherin is associated with poor prognosis in breast carcinoma[64]. Some of them include zinc finger E-box-binding homeobox 1 (ZEB1), zinc finger E-box-binding homeobox 2 (ZEB2), twist-related protein (Twist), zinc finger protein, Snail and Slug. There are involved in signaling pathways such as transforming growth factor-β (TGF-β), the wingless-type MMTV integration site family, (WNT) cascade and the phosphatidylinositol 3' kinase-serine/threonine kinase (PI3K/AKT) axis, all linked to the EMT programs (Figure 8)[62]. Following the loss of cell adhesion, at both levels of cell-cell and cell-ECM adhesion, cell physical polarity

is altered from apical-basal polarity to front-rear polarity to initiate cell migration through reorganization in cortical actin and actin stress fibers, that induces cytoskeleton remodeling. Finally, increased cell protrusions and expression of metalloproteinases (MMPs) result in ECM degradation, cell migration and invasive behavior[55].

After all these processes, these cells are loosely attached to the ECM, lose cell polarity and move through the paths of least resistance. Some of these cells, which have undergone EMT, have an elongated fibroblast-like shape and their movement is facilitated by matrix-degrading enzymes, such as MMPs, which are released through channels in the ECM. Contrarily, cells with amoeboid movement are round cells like unicellular organisms. The last ones rely mostly on shape deformations and structural changes in the ECM composition rather than actual degradation of the matrix. Also, that modification in the ECM composition depends on the cell phenotype. Some of those modifications help the cell migration; for example, the increase in fibronectin (FN) type III expression for amoeboid and FN type I expression for migrating cells. The mechanical force used is generated by active myosin/actin contractions and cortical actin *via* signaling pathways such as RhoA/Rho kinase (ROCK)[63].

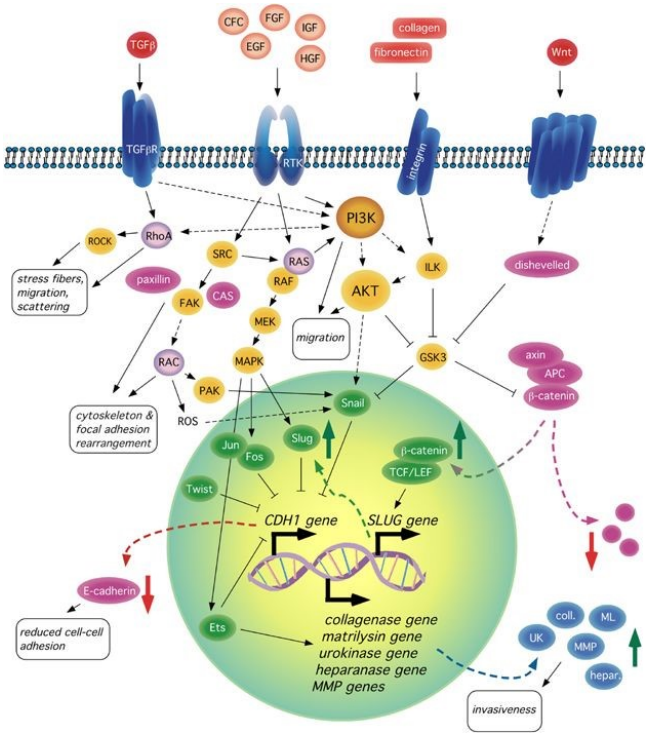

Figure 8. Signal transduction pathways associated with epithelial–mesenchymal transition. End points of EMT are boxed. RTK: receptor tyrosine kinase; ROS: reactive oxygen species. From Larue and Bellacosa, Oncogene (2005).

3.4. Tumor microenvironment

The tumor microenvironment appears to play a role in metastatic potential and is critical for cancer cell proliferation. An appropriate microenvironment is a requirement for establishing tumor growth and malignant progression. Many different specialized cells, including stromal cells,

immune cells - such as fibroblast, macrophages, natural killer cells, endothelial cells - together with all types of tumor cells, the ECM, and the lymphatic and vascular systems[65] create the microenvironment that supports tumor progression[59] (Figure 9).

The cell-matrix and cell-cell interactions into this microenvironment imply a number of specific cell surface-associated molecules, including the family of integrin receptors, the cadherins, the immunoglobulin (IgG) superfamily, a 67-kDa laminin-binding protein, and the CD44 receptor, that interact with hyaluronic acid and also with other ligands, such as osteopontin, collagens and MMPs[44]. Those interactions also affect the metastatic potential and build the way for the progression from *in situ* cancer to metastatic cancer.

The migratory and invasive abilities are the crucial parameters of cancer cells, as well as the interaction with the ECM[61]. Those adhesion receptors of the cancer cell surface play an important role in one of the earlier steps of metastasis, the migration of cells through the basement membrane and ECM surrounding the tumor.

Cancer cells secrete substances prior to metastasis to establish a pre-metastatic niche supporting future metastatic sites. These signals from the primary tumor also could determine and promote preferential invasion of cancer cells to a particular site. Indeed, breast cancer has been observed to preferentially metastasize to the bone and lungs and less frequently to other organs such as the liver and brain. Gene expression signatures accounting for the preferential metastasis of breast cancer cells to the bone marrow and lung have been identified, providing evidence that metastasis exhibits tissue tropism[66].

Angiogenesis is another important aspect in metastasis, establishing tumor vasculature and subsequent metastasis growth. Genetic mutations, mechanical stresses, inflammatory processes, tumor expression of angiogenic proteins and hypoxia are believed to cause the angiogenic process, that is a critical microenvironmental adaptation for tumors and is regarded as a hallmark of cancer progression[67].

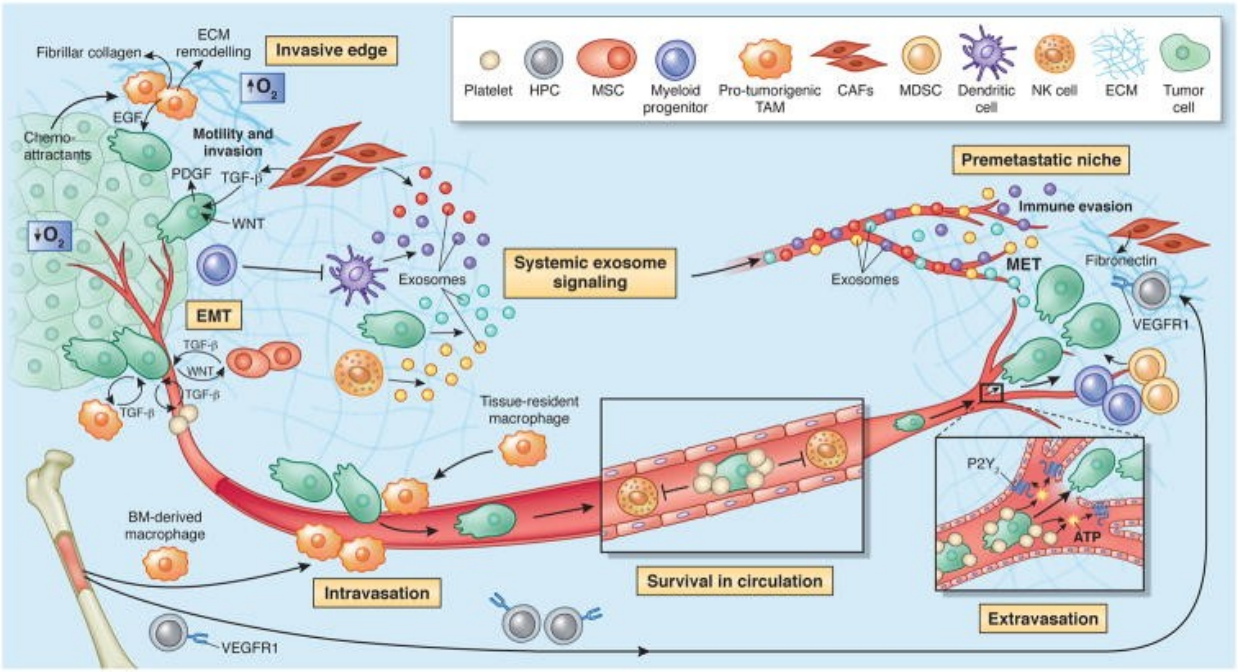

Figure 9. The microenvironment supports metastatic dissemination and colonization at secondary sites. Some cells such as macrophages, platelets, and mesenchymal stem cells (MSCs) contribute to EMT at primary sites, allowing for cancer cells to separate from neighboring epithelial cell-cell contacts and acquire a mobile/invasive phenotype. One major mediator of this event is TGF-β. Tumor-associated macrophages (TAMs), cancer-associated fibroblasts (CAFs) and myeloid progenitor cells also tend to cluster at the invasive/leading edge of the primary tumor, where they play an immunosuppressive role by interfering with dendritic cell differentiation. Macrophages help during the intravasation of cancer cells into circulation. In the circulation, platelets and components of the coagulation system support cancer cell survival by protecting them from cytotoxic immune cell recognition. At secondary sites such as the lung, fibroblasts upregulate fibronectin, which serves to the arrival of cancer cells. Immunosuppressive cell types also populate premetastatic niches where they help to direct metastatic dissemination by creating a niche permissive to tumor colonization. Factors contained in exosomes have the capacity to direct organ tropism, modulate immune evasion, support mesenchymal-to-epithelial transition (MET), and are predictive of metastasis and patient outcome. From Quail and Joyce, Nature Medicine (2013).

4. Integrins in cancer progression and metastasis

Integrins are expressed on epithelial cells and because many tumors originate from epithelial cells, they are also expressed in cancer cells[30]. Additionally, integrin are the main cellular adhesion receptor and they have multifaceted roles and implication in cell migration. These characteristics implicate them in almost every step of cancer progression and metastasis, as it is illustrated in Figure 10.

Nevertheless, due to the complexity of integrins, their study in order to find new therapeutic targets or diagnosis predictor has been a challenge. First, they have adaptable and even antagonist roles in cancer cells and tumor microenvironment. Another interesting characteristic is that some integrins can interact with just one specific ECM ligand, such as fibronectin, vitronectin, laminin, or collagen; but others can bind to multiple ligands. It is for example the case for the integrins of interest for this study, ITGA5 that binds specifically to FN. Moreover, the interaction of different integrin heterodimers with the same ligand can trigger a totally different signaling in the cell. Because of that, integrin expression on the cell surface is key to determining cell response to microenvironmental influences[37].

Studies correlate integrin expression levels in cancer cells with metastatic progression in many types of cancer like melanoma, breast carcinoma, prostate and pancreatic and lung cancer. Some of the integrins identified with those pathological outcomes are $\alpha v\beta 3$, $\alpha v\beta 5$, $\alpha 5\beta 1$, $\alpha 6\beta 4$[36].

For example, one of the α integrins, αv, dimerizes with the specific β integrin subunits has been implicated in the pathophysiology of malignant tumors (Figure 2)[68]. Especially, integrin αvβ3 has been coupled to EMT and metastasis, induced cancer cell migration, and for maintaining a mesenchymal phenotype of these cells[69]. Interactions with the ECM through integrin adhesion receptors provide cancer cells with physical and chemical signals that act together with growth factors to support survival and proliferation[44]. The major adhesion receptor for FN is α5β1 integrin, implying a relationship between the expression of the integrin and tumor metastasis.

Moreover, some of these studies are contradictory in the information about the same type of cancer or the role of the same integrin in different cancer types[37]. For this reason, the mechanism by which integrins can enhance cancer progression is still unclear.

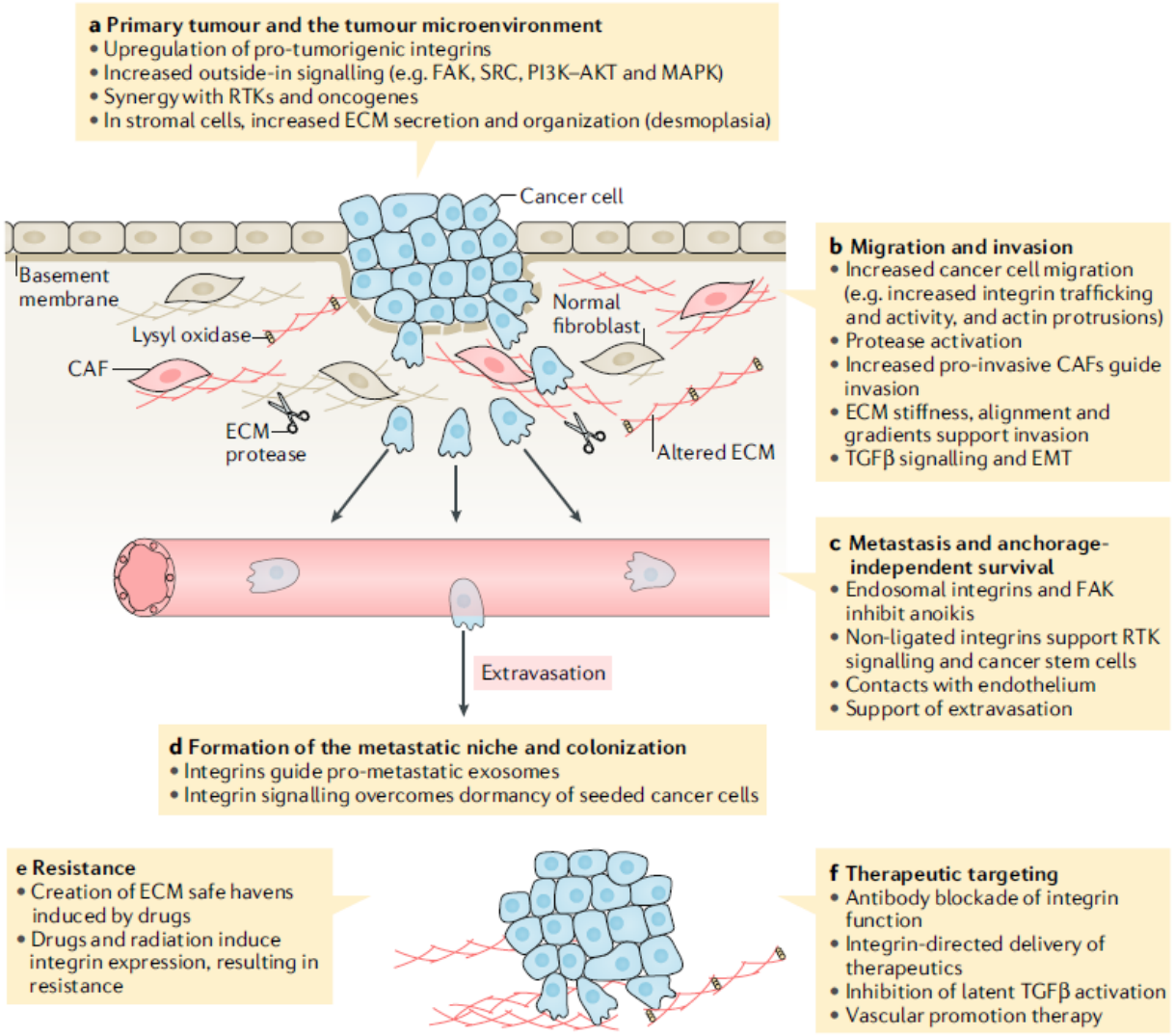

Figure 10. Integrins involved in different steps of cancer progression. Integrin expression have been implicated in the different stages of cancer development and metastasis (parts a-d). Also, they have been related to the acquisition of drug resistance (part e). Because all of that, integrins are considered attractive as new therapeutic targets against cancer (part f). From Hamidi and Ivaska, Nature Reviews (2018).

5. PACMAN Project

The different pathways implied in cell migration and invasion are in continuous study. How they are related to cancer progression and metastasis still unclear, as well as the role of integrins in those processes. One of the challenges is the difficulty of isolate non-migrating cells from migrating cells present within the same sample, in a way to analyze their gene expression and to identify the pathways involved in metastasis formation. Additionally, recreate the complexity of the complete tumor microenvironment *in vitro* is another challenging task.

The PACMAN (Peptide-Assisted Cellular Migration Along eNgineered surfaces) project is a research project that through PACMAN surfaces aims to separate MDA-MB-231 cells regarding their migrating phenotype (Figure 11). The static and the different migratory phenotypes are characterized and compared in a way to identify pathways involved in the metastatic process.

To this aim, this project focusses on ECM composition and particularly on the role of FN motifs in distal migration in breast cancer model, and more particularly on the role of integrins ITGA5 and ITGB3. These integrins can be extrinsically activated by a highly conserved sequence of FN type I (IGDQ motif) or intrinsically by the activation of the EGFR pathway.

Previous results from our laboratory, obtained in the PACMAN project, showed that IGDQ-exposing (Iso-Gly-Asp type I FN motif) monolayers (SAMs) sustain the adhesion of MDA-MB-231 cells, a metastatic breast cancer cell line, by triggering FAK, similarly to the analogous RGD-terminating (Arg-Gly-Asp type III FN motif) surfaces[70], with migrating cells at the cm-subscale for IGD and only proliferation for RGD. Further analysis of these ECM proteins and the downstream ECM mediated signaling pathways may provide a range of possibilities to identify therapeutic/diagnostic targets against advanced breast cancer.

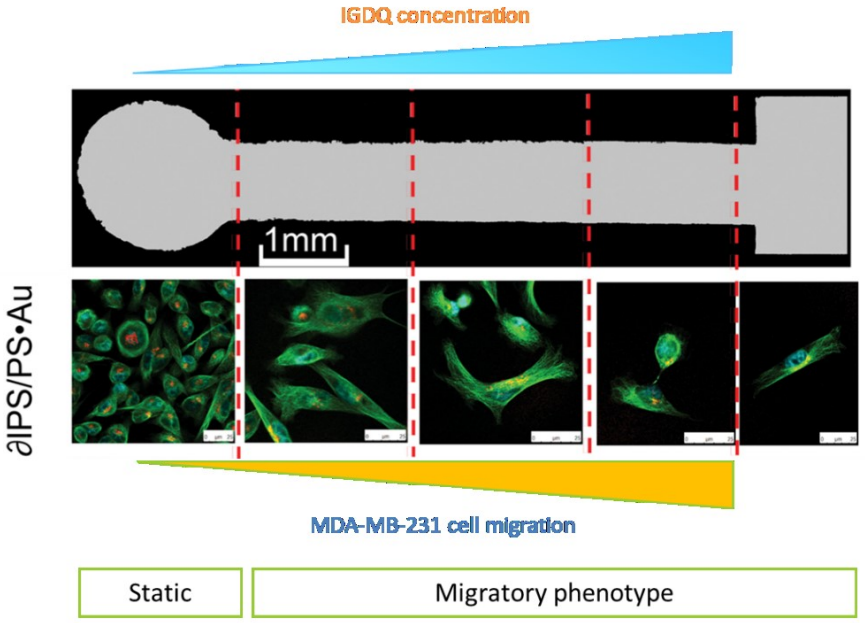

Figure 11. Breast cancer cells migrating on PACMAN IGDQ-exposing surface. Modified from V. Corvaglia & al. Small (2015).

II. OBJECTIVES

Objectives

Although the importance of breast cancer has been recognized due to its high incidence in women around the world, and the metastatic process has been widely studied in order to prevent and treat this disease; metastasis is still the leading cause of breast cancer mortality. For this reason, it is important to understand the relationship between cancer cells and the surrounding microenvironment, which is regulated by complex molecular networks and involving numerous genes amongst which are integrins.

The purpose of this study was to characterize the role of ITGA5 and ITGB3 in cell migration using an in vitro model of metastatic breast cancer. Given that matrix components and many ECM proteins, such as FN, promote tumor progression and metastatic spread, and that integrins are cell-surface adhesion receptors that interact with ECM components and have been reported to contribute to tumor growth, cell adhesion, invasion, and metastasis.

We chose to use MDA-MB-231 cells because they are originating from one metastasis of a triple-negative breast cancer.

³⁸This thesis is part of Sophie Ayama's work that aims to characterize and compare the different phenotypes of MDA-MB-231 cells regarding their migration in order to identify pathways involved in cell migration. A special focus is put on integrins α5β1 and αvβ3, using PACMAN surfaces and single cell deep RNA sequencing.

The first part of this project consisted in invalidating the expression of ITGA5 or ITGB3 using siRNA. Additionally, ITGA5 was invalidated using shRNA in order to allow a stable and long-term invalidation of the target gene. To assess the effectiveness of this invalidation, mRNA and protein expression levels were analyzed by RT-qPCR and by western blotting and immunofluorescence labeling, respectively. Characterization of control and invalidated cells were performed by morphological observations. Also, cytotoxicity was evaluated. Finally, cell migratory capacity was assessed to determine the role of the integrins in cell migration.

For the second part of the thesis, other ITG-targeting shRNA were tested, and invalidated cells were characterized with the same methods. In addition, cell adhesion capacity was evaluated. Furthermore, a co-invalidation of ITGA5 and ITGB3 was performed and its importance on migratory capacity was evaluated.

The results highlighted that integrins influence some of the features of metastatic breast cancer cells and evidence the need for a further characterization of the role of integrins in cell migration.

III. MATERIAL AND METHODS

1. Cell culture

1.1. Cellular model

The model used during this thesis is the MDA-MB-231 cell line (ATCC® HTB-26™) (ATCC, USA). It is a human breast cancer cell line, derived from the pleural effusion of a metastatic site. They are mesenchymal-like epithelial adherent cells that express epidermal growth factor (EGF) and transforming growth factor alpha (TGF alpha).

1.2. Culture conditions

MDA-MB-231 cells were cultured in 75 cm^2 polystyrene cell culture flasks (T75) (Corning, USA) containing 15 mL of RPMI-1640 medium (Gibco, USA) supplemented with 10% fetal bovine serum (FBS) (Gibco, USA). Cells were maintained under standard culture conditions in a humidified 5% CO_2 atmosphere at 37 °C.

MDA-MB-231 cells were subcultured every 2 to 3 days according to the following protocol: the culture medium was removed from the flask and cells were rinsed with 10 mL of homemade sterile phosphate buffer saline (PBS) (Table 1) to remove all traces of serum. After discarding the PBS, cells were detached using 1.5 mL 0.05% trypsin-EDTA (Gibco, USA) for 5 minutes at 37 °C. After cell detachment, cells were recovered with 8.5 mL of complete medium in order to inhibit the trypsin via the protease inhibitors contained in the serum and then placed in a 15 mL centrifuge tube (Sigma-Aldrich, USA). The tube was centrifuged for 5 minutes at 1000 rpm to pellet the cells. Next, the supernatant was discarded, and the cell pellet was resuspended with 5 mL of media which were then divided into one or more T75 flasks. Finally, fresh medium was added to obtain a final volume of 15 mL and the flasks were replaced into the CO_2 incubator.

Table 1. Phosphate buffer saline (PBS) homemade: preparation for 1 L.

Reagent	Quantity
Phosphate buffer KH_2PO_4 0.5 mM at pH 7.4 (Merck, Germany)	20 mL
NaCl 99% (Carl Roth, Germany)	9 g

1.3. Cell counting

After the centrifugation step for 5 minutes at 1000 rpm to pellet the cells, the supernatant was discarded, and the cell pellet was resuspended with RPMI-1640-10% FBS medium in a 15 mL centrifuge tube. 10 µL of the sample were added to 10 µL of trypan blue stain 0.4% (NanoEntek, Korea) and mixed gently by pipetting up and down. Then 10 µL of the sample mixture were added to the chamber ports on one side of the Countess™ cell counting chamber slides (Invitrogen, USA). The slide was inserted into the slide inlet on the Countess™ automated cell counter (Invitrogen, USA), the parameters were set and the instrument counted cells in each sample. The number of living cells and the percentage of survival were recorded.

2. siRNA knockdown

The previous day of the transfection, MDA-MB-231 cells were seeded in 25 cm^2 polystyrene cell culture flasks (T25) (Corning, USA) at a density of 700 000 cells per flask in 5 mL RPMI-1640 medium (Gibco, USA) supplemented with 10% FBS (Gibco, USA). The flasks were incubated at 37 °C in a humidified 5% CO_2 atmosphere.

SMART-Pool-ON-TARGET human single siRNAs were purchased from Dharmacon and the final siRNA concentration was 50 nM per sample (siRiscFree (siRF), ITGB3-targeting siRNA (siB3), ITGA5-targeting siRNA (siA5)). As negative controls, siRF and untransfected cells (UT) were used. After 24 hours of incubation, cells were transfected in duplicate with siRNA DharmaFECT transfection reagent (Dharmacon, USA). First, in separate tubes, 10 µL of the siRNA was diluted (Tube 1) in 390 µL of serum-free medium Opti-MEM (Gibco, USA) and 8 µL of the appropriate DharmaFECT transfection reagent (Tube 2) with 392 µL of the same serum-free medium. Second, the content of the tubes was gently mixed by pipetting carefully up and down and incubated for 5 minutes at room temperature. Third, the content of the tube 1 was added to the tube 2, mixed by pipetting and incubated for 20 minutes at room temperature. Finally, the culture medium was removed from the flasks and the siRNA mix was added into RPMI-1640-10% FBS medium to achieve a volume of 4 mL.

After cells were incubated 24 hours at 37 °C in 5% CO_2, the medium was replaced by complete medium RPMI-10% FBS. Gene silencing efficiency was determined by RT-qPCR and Western blot analysis.

3. shRNA knockdown

3.1. Bacterial culture and plasmid purification

The bacterial amplification was performed with transformed MISSION shRNA bacterial glycerol stocks (Sigma-Aldrich, USA). The plasmids contained the SHC001 expression vector for the integrin α5 shRNA 126 or shRNA 124, or integrin β3 shRNA 236 or shRNA 237, sequences with ampicillin resistance marker for prokaryote selection. A 15 mL centrifuge tube (Sigma-Aldrich, USA) was prepared for each treatment with 5 mL of sterilized LB medium, 20 µL of the bacteria in glycerol stock and 5 µL of ampicillin 50 mg/mL (Roche, Germany). The solution was incubated for 8 h at 37 °C on a shaker at 125 rpm. After that, for each sample in a 500 mL Erlenmeyer were added 125 mL of LB medium, 125 µL of ampicillin 50 mg/mL and the content in the first pre-amplified bacterial tube. They were incubated for 24 h at 37 °C, 125 rpm.

Afterward, the plasmids were purified using the Plasmid Plus Maxi kit (Qiagen, Germany) following the protocol for high-copy plasmid, according to the manufacturer's instructions. The quality and the quantity of the plasmids were determined by Nanodrop spectrophotometer N-100 (Isogen Life Science, The Netherlands) by measuring the absorbance at 260 nm. And then the samples were kept at -20 °C.

3.2. Lentiviral particle production

Lentivirus-based vector expressing integrin α5 shRNA 126 or shRNA 124 sequence was generated by transient co-transfection of HEK293T cells with a plasmid encoding the gag, pol, rev, and envelope genes and 2X hepes buffered saline (HeBS), adjusted to pH 7.05 and 7.12. HEK293T cells were seeded one day before the transfection in 75 cm^2 polystyrene cell culture flasks (T75) (Corning, USA) at a density of 1 million cells per flask. Briefly, a T75 flask of non-confluent (40-60%) cells were transfected with 3.34 µg of Δ8.3(pol), 1.67 µg of VSV-G (env) and 5 µg of lentiviral vector plasmid mixed with the diluent (720 µL ddH_2O, 110 µL $CaCl_2$ 2.5 M). 840 µL HeBS 2X (Table 2) were added dropwise to the mix, vortexed immediately and incubated at room temperature (RT) for 20 min. Following the incubation, the mixture was added to partially confluent HEK 293T cells with DMEM medium (Gibco, USA) supplemented with 10% FBS

(Gibco, USA) and glutamine. The medium was changed 24h post-transfection. 48 h post-transfection, lentivirus-containing supernatant was harvested and used for the following experiments.

Table 2 HeBS homemade: preparation for 500mL.

Reagent	Quantity
NaCl 274 mM	8g
KCl 10 mM	0.37g
Na_2 $HPO_4.2H_2O$ 1.5mM	0.1065g
Dextrose (glucose)	1g
Hepes 50mM	5g

3.3. shRNA transduction

MDA-MB-231 cells were seeded the previous day of the transduction in 25 cm^2 polystyrene cell culture flasks (T25) (Corning, USA) at a density of 300 000 cells per flask. Cells were transduced with shRNA targeting integrin α5 (sh126 or sh124) or integrin β3 (sh236 and sh237) with shRNA lentiviral particles produced in HEK293T cells. The transduction was performed for each lentivirus at two different dilutions (12 and 1/5) in fresh RPMI-1640 medium (Gibco, USA) supplemented with 10% FBS (Gibco, USA) containing protamine sulfate (60 µL/flask) (Sigma-Aldrich, USA) as the transducing agent. Two different controls were performed, untransduced cells and shRNA Ctrl cells, the latter were transduced with lentiviral particles Empty Vector (Sigma-Aldrich, USA) with a multiplicity of infection (MOI- number of particles per cell) of 5 in the same conditions of fresh medium containing protamine sulfate (0.06 mg/mL). 48 hours after the transduction, the medium was replaced by fresh medium supplemented with puromycin (2 µg/mL) (Sigma-Aldrich, USA) to select cells that were infected by the lentiviral particles and having incorporated the vector into their genome. The selection was maintained from 5 to 6 days while the cells were amplified in 75 cm^2 polystyrene cell culture flasks (Corning, USA). After the selection, a dilution ½ was chosen for further experiments and cells were frozen in RPMI-1640-10% FBS medium– 5% dimethylsulfoxid (DMSO) (Carl Roth, Germany) in liquid nitrogen.

4. Immunofluorescence labeling

Cells were seeded on sterile glass coverslips (Glaswarenfabrik Karl Hecht KG, Germany) in 24-well plates (Costar, USA) at a density of 30 000 cells per well in RPMI-1640 medium (Gibco, USA) supplemented with 10% FBS (Gibco, USA). First, after 48 hours of incubation at 37 °C in 5% CO_2, the medium was removed, and cells were fixed during 10 minutes at RT with PBS-PFA 4% (paraformaldehyde) (PFA 0.04 g/mL (Merck, Germany) in PBS non-sterile (Table 1) before being washed 3 times with PBS. Second, cells were permeabilized with PBS-Triton X 100 1% (Triton X-100 0.01 g/mL (Carl Roth, Germany) in PBS non-sterile) for 5 minutes at RT, followed by 3 washes for 10 minutes each with PBS-BSA 2% (bovine serum albumin) (VWR, USA). Third, the cells were incubated with the primary antibody overnight at 4°C (Table 1) in the dark and in a humid chamber. The next day, cells were rinsed 3 times for 10 minutes each with PBS-BSA 2% and incubated for 1 hour with the secondary antibody and/or probe (Table 3) and simultaneously with the Hoechst #H-21491 (Thermo Fisher Scientific, USA) diluted at 2 µg/mL PBS-BSA 2% at RT in the dark. Afterward, cells were washed 2 times with PBS-BSA 2% and 2 times with PBS. Finally, the coverslips were mounted on microscope slides (VWR, USA) with Mowiol mounting solution (Sigma-Aldrich, USA) prewarmed at 56°C. Slides were kept at 4°C protected from light

before the observation with the confocal laser scanning fluorescence microscope TCS SP5 (Leica, Germany).

Samples obtained after the immunofluorescence labeling were scanned by confocal microscope TCS SP5 (Leica, Germany) to obtain z-series image stacks to determine the cell size on the z-axis, in order to analyze cell adhesion.

Table 3 Antibodies used for immunofluorescence labeling.

Protein	Primary antibody	Secondary antibody
Integrin α5	Anti-integrin alpha 5 Rabbit, 1/100 (Abcam, UK)	Alexa 488 nm Anti-rabbit, A-11008, 1/1000 (Thermo Fisher Scientific, USA)
Integrin β3	Anti-integrin beta 3 Mouse, 1/50 (BD Biosciences, USA)	Alexa 568 nm Anti-mouse, A-11004, 1/1000 (Thermo Fisher Scientific, USA)
pFAK	Anti-pFAK Mouse, 1/100 (BD Biosciences, USA)	Alexa 568 nm Anti-mouse, A-11004, 1/1000 (Thermo Fisher Scientific, USA)
Phalloidin probe (F-actin)		Alexa fluor Phalloidin 568 nm A-12380, 1/100 (Thermo Fisher Scientific, USA)

5. Total RNA extraction and RT-qPCR

5.1. Total RNA extraction

Cells were seeded in 25 cm^2 polystyrene cell culture flasks (T75) (Corning, USA) at a density of 400 000 cells per flask and incubated for 48 hours at 37°C with 5% CO_2 in a humidified atmosphere. Then, the medium was discarded, cells were scraped in 600 µL of PBS (Table 1) and collected in a 1.5 mL Eppendorf (Qiagen, Germany). Afterwards, the tube was centrifuged for 5 min at 1200 RPM and 4°C. The supernatant was removed and 600 µL of RLT Lysis Buffer of the RNeasy Mini Kit (Qiagen, Germany) were added to lyse the cells in a 2 mL Eppendorf (Qiagen, Germany). Total RNA was then extracted using the RNeasy Mini Kit and the automate QIAcube (Qiagen, Germany) under conditions “Large sample with DNase” with an elution volume of 30 µL. The samples were kept at -80°C. Total RNA concentration was quantified using Nanodrop spectrophotometer N-100 (Isogen Life Science, Netherlands) by measuring the absorbance at 260 nm.

5.2. Retro-transcription of mRNA into cDNA

The retro-transcription of the mRNA to cDNA was performed using the GoScript reverse transcription kit (Promega, USA). 1 µg of total RNA was diluted with RNase-free water to a volume of 12 µL. The samples were then incubated at 70 °C for 5 minutes. A reaction mixture of 8 µL containing 4 µL of GoScript buffer mix with random primers (Promega, USA), 2 µL of GoScript enzyme mix (Promega, USA) and 2 µL of nuclease-free water was added to each sample to obtain a final volume of 20 µL. The samples underwent a thermal cycle of 5 minutes at 25 °C, then 60 minutes at 42 °C and finally, 15 minutes at 70 °C. The cDNA sample tubes obtained were directly placed on ice and stored at -20 °C.

5.3. Real time PCR

In a qPCR 96-well reaction plate (Thermo Fisher Scientific, USA) were added 4 µL of cDNA diluted at 1/100 and 16 µL of the reaction mix per well. This qPCR mix was prepared with 5.56 µL of MilliQ water, 0.22 µL of each forward and reverse primers (Integrated DNA Technologies, USA) to 300 nM (Table 4) and 10 µL GoTaq® qPCR Master Mix (Promega USA). After the wells were filled, the plate was sealed and centrifuged for 1 minute at 600 rpm.

The amplification was quantified using the threshold cycle (Ct) method using ViiA 7 Real-Time PCR System (Thermo Fisher Scientific, USA). Thermal cycling conditions were composed of an initial denaturation step at 95°C for 5 min, followed by 40 cycles at 95°C for 30 seconds and 60°C for 1 min.

Gene expression was determined using the ΔΔCt method with tubulin as the housekeeping or reference gene. For each sample, the Ct of the reference gene is subtracted from the Ct of the gene of interest in order to normalize the amount of cDNA loaded into each well:

ΔCt = Ct gene of interest - Ct reference gene

ΔΔCt = ΔCt of the gene in a condition - ΔCt of the gene in the control condition

$2^{-\Delta\Delta Ct}$ = level of induction or repression of the gene in comparison to the control condition

Table 4 Primers used for qPCR.

Gen	Primer	Sequence	%GC	Tm °C	Amplicon size (bp)
ITGB3	ITGB3-F-h	CCGTGACGAGATTGAGTCA	52.63	56.91	132
	ITGB3-R-h	AGGATGGACTTTCCACTAGAA	42.86	55.69	
ITGA5	ITGA5-F-h	TGCAGTGTGAGGCTGTGTACA	52.38	61.91	88
	ITGA5-R-h	GTGGCCACCTGACGCTCT	66.67	62.01	
A-Tubulin	Tub-178F	CCCGAGGGCACTACACCAT	63.16	60	108
	Tub-323R	CAGGGAGGTGAACCCAGAAC	60	60	

6. Protein extraction and Western blotting

6.1. Protein extraction

Cells were seeded in 25 cm^2 polystyrene cell culture flasks (T75) (Corning, USA) at a density of 400 000 cells per flask and incubated for 48 hours at 37°C with 5% CO_2 in a humidified atmosphere. Then, the medium was discarded, cells were scraped in 600 µL of PBS (Table 1) and collected in a 1.5 mL Eppendorf (Qiagen, Germany). Afterwards the tube was centrifuged for 5 min at 1200 RPM and 4°C. The supernatant was removed and the cell pellet was resuspended in 30 µL of lysis buffer solution (Table 5). After being incubated 15 min on ice, the sample was sonicated for 10 seconds 3 times and stored at -80°C.

Table 5 Reagents of lysis buffer solution

PIC (Phosphatase Inhibitor Cocktail)	A tablet of Complete protease inhibitor cocktail 25X (Roche, Germany) dissolved in 2 mL of water
PIB (Phosphatase Inhibitor Buffer)	- Na_3VO_4 25 mM (Sigma-Aldrich, USA) - PNPP (Para-NitroPhényl Phosphate) 250 mM (Sigma-Aldrich, USA) - β-glycerophosphate 250 mM (Sigma-Aldrich, USA) - NaF 125 nM (Merck, Germany)
Lysis buffer stock	- 929 mg of Tris (Trizma Base) 40 mM (ICN Biomedicals, USA) - 2.23 g of KCl 150 mM (Merck, Germany) - 74.44 mg d'EDTA (Tritriplex III) 2 mM (Merck, Germany)
Lysis buffer	- 1 mL of lysis buffer stock - 2 µL of β-mercaptoethanol - 40 µL of PIC - 40 µL of PIB

6.2. Determination of protein concentration

Quantification of proteins was carried out using Pierce 660 nm Protein assay (Thermo Fisher Scientific, USA), that allows assessing the protein concentration of a sample through a colorimetric analysis where the absorbance of the samples is measured spectrophotometrically at 660 nm.

To determine the protein concentration as a function of the absorbance, a calibration curve was performed obtaining the absorbance of different concentrations of BSA (stock at 2 µg/µL) (Sigma-Aldrich, USA) diluted in water. 10 µL of each diluted sample (1 µL of sample + 9 µL of water) were placed in a 96-wells plate (Costar, USA), as the blank of lysis buffer, in order to be able to subtract its absorbance from the absorbance of the samples. 150 µL of Pierce solution was added to each well and the plate was then placed in the dark between 5 to 20 minutes. Absorbance was measured at 660 nm using a spectrophotometer (Bio-Rad, USA) to calculate the protein concentration of the samples based on the equation of the calibration curve ($y = ax + b$) with y representing the absorbance and x the protein concentration.

6.3. Gel electrophoresis

Proteins were separated using a 10% homemade polyacrylamide gel. First, the 10% separation gel (running gel) was poured and a thin layer of SDS 0.1% was added to isolate the gel from oxygen and promote polymerization. Second, after 40 minutes of polymerization at RT, the gel was rinsed with milliQ water. Then, the 4% concentration gel (stacking gel) was poured, a comb comprising 10 or 15 wells was inserted and the gel polymerized for 30 minutes (Table 6).

For each sample, 7 µg of proteins from cell lysates were mixed with MilliQ water and 6 µL of loading blue 5X (Table 6) to achieve a final volume of 30 µL. The samples were heated for 5 minutes at 100 °C and then span briefly.

30 µL of sample or 2 µL of molecular-weight size marker (New England Biolabs, USA) were loaded into the wells of the gel placed in a tank of migration in which 1 L of running buffer 1X was added. The migration was performed at 200 V, 400 mA and 15 W per gel, until the migration front reached the bottom of the gel.

Table 6 Preparation of gel electrophoresis

Concentration buffer	For 100 mL: - 0.5 M: Tris (Carl Roth, Germany) = 6.06 g - 0.4 %: SDS 20% (ITW Reagents, Spain) = 2 mL Adjust to pH 6.8 with HCl
Separation buffer	For 200 mL: - 1.5 M: Tris (Carl Roth, Germany) = 36.3 g - 0.4 %: SDS 20% (Carl Roth, Germany) = 4 mL Adjust to pH 8.8 with HCl
Separation or running gel 10%	- 1.2 mL of separation buffer - 1.7 mL of acrylamide 30% (Bio-Rad, USA) - 2.1 mL of water - 25 µL of APS 10% (Bio-Rad, USA) - 5 µL of TEMED (Bio-Rad, USA)
Concentration or stacking gel 3.75%	- 1.25 mL of concentration buffer - 0.5 mL of acrylamide 30% (Bio-Rad, USA) - 2.25 mL of water - 50 µL of APS 10% (Bio-Rad, USA) - 5 µL of TEMED (Bio-Rad, USA)
Home-made gel (3.75-10 %)	- 10 mL of running gel 10% - 3 mL of stacking gel
Running buffer 10X	For 1 L : - 30.28 g of Tris (25mM) (ICN Biomedicals, USA) - 144 g of glycine (0.192 M) (Merck, Germany) - 50 mL of SDS 20 % (ITW Reagents, Spain) pH 8.7
Loading blue 5X	- 10 mL of concentration buffer - 10 mL of SDS 20% (ITW Reagents, Spain) - 5 mL of β-mercaptoethanol (Fluka Biochemika, Sigma-Aldrich, USA) - 10 mL of glycerol (Merck, Germany) - 17.5 mg of bromophenol blue (Merck, Germany) pH 6.8

6.4. Transfer

When the electrophoresis was finished, the gel was demolded to transfer the proteins onto a PVDF membrane (Bio-Rad, USA). This membrane was previously hydrated in methanol 100% (VWR, USA) for 1 minute and then in the transfer buffer (Table 7) for at least 3 minutes. Also, both transfer stacks (Bio-Rad, USA) must also be immersed in transfer buffer for at least 3 minutes. The different elements were placed in the center of the Trans-Blot Turbo transfer cassette (Bio-Rad, USA) in the precise order according to the protocol, from bottom to top: a transfer stack, the membrane, the gel and a transfer stack. The transfer was executed for 7 minutes at 2.5 A and 25 V.

6.5. Treatment of membranes and revelation

After the transfer step, the membrane was incubated for 1 hour at RT with stirring with a blocking solution composed of diluted Odyssey blocking buffer (Li-Cor Biosciences, USA) 2x in PBS (Table 1) to saturate all non-specific binding sites of antibodies on the membrane. After that, the membrane was incubated overnight at 4 °C in the presence of the primary antibody (Table 7) diluted appropriately in the Li-Cor solution with Tween 20 0.1% (Merck, Germany). The next day,

the membrane were rinsed 3 times for 5 minutes each with PBS-Tween 20 0.1% and was then incubated with the secondary antibody (Table 7) coupled to a fluorochrome diluted in a Li-Cor solution containing 0.1% Tween for 1 hour at RT. After incubation, the membrane was washed again 3 times for 5 minutes each with PBS-Tween 20 0.1% and then 2 times in PBS alone. Finally, the membrane was dried in the dark in a hot chamber at 37 °C for one hour before being scanned with the Odyssey Infrared Imaging system (LI-COR Biosciences, USA). The fluorescence was quantified using the Odyssey V3.0 Imaging Software from the Odyssey Infrared Imager (Li-Cor Biosciences, USA). Relative protein expression was standardized to the abundance of tubulin.

Table 7 Antibodies used for western blot analysis.

Protein	Primary antibody	Secondary antibody
Integrin α5	Anti-integrin alpha 5 Rabbit, 1/1 000 (Abcam, UK)	Alexa 488 nm Anti-rabbit, A-11008, 1/10 000 (Thermo Fisher Scientific, USA)
Integrin β3	Anti-integrin beta 3 Mouse, 1/1 000 (BD Biosciences, USA)	Alexa 568 nm Anti-mouse, A-11004, 1/10 000 (Thermo Fisher Scientific, USA)
α-Tubulin	Anti-Alpha tubulin Mouse, 1/1000 (Sigma-Aldrich, USA)	IRDye 680RD Anti-mouse, 1/10 000 (Li-Cor Biosciences, USA)

7. Scratch assay

MDA-MB-231 cells were seeded at a density of 800 000 cells/well with RPMI-1640 medium (Gibco, USA) supplemented with 10% FBS (Gibco, USA) in a 35mm x 10mm polystyrene cell culture dish (Corning, USA) to form a confluent monolayer and incubated for approximately 24 h at 37°C. The layer of cells was scraped to create a wound of ~1 mm width. Cellular debris was removed with the medium and 3 mL of fresh serum-starved medium were added, following by treatment with mitomycin C (Sigma-Aldrich, USA) 10 µg/mL to block the proliferation. The dish was placed under the Cytonote (Iprasense, France) at 37 °C to monitor the images of the wounds (LabCeTi). Cell migration quantification of pictures was assessed by imaging processing of the area that corresponds to the number of cells in the central gap. It is represented by Migration distance, that follows an arbitrary scale (u). The relative speed of migration was expressed in relative quantity after being normalized to the corresponding control.

An additional test was carried out to assess the effect of the mitomycin on the migratory capacity. Variations in the protocol of the addition of mitomycin C were tested, and all of them kept the concentration of 10 µg/mL. First, the case is described previously, after the scratch is done, the debris was removed with the medium and 3 mL of fresh serum-starved medium with mitomycin were added. Second, mitomycin was added 3 hours before performing the scratch and removed from the new media. Third, mitomycin was added 3 hours before doing the scratch and kept within the new media. Cell migration quantification was measured as described in the previous paragraph.

8. Fibronectin-coating

The fibronectin-coating was done with a fibronectin solution at 10 µg/mL in PBS sterile (Table 1) from the fibronectin human plasma 1 mg/mL (Sigma-Aldrich, USA). The glass coverslips (Glaswarenfabrik Karl Hecht KG, Germany) in 24-well plates (Costar, USA) were coated with 150 µL and the 35mm x 10mm polystyrene cell culture dish (Corning, USA) with 500 µL for the immunolabeling and the scratch assay, respectively. The solution was dried under sterile conditions before to seed the cells for the different experiments.

9. LDH Assay

Cells were seeded in 24-well plate (Costar, USA) at a density of 15 000 cells per well. 48 hours later, the supernatant of each well was collected in two 1.5 mL microtubes labeled as "Pellet". 250 µL of PBS-Triton 4% (Triton X-100 0,04 g/mL (Carl Roth, Germany) in PBS non-sterile (Table 1) were added to the adherent cells in each well and the plates were slightly agitated at RT for 10 minutes. The "Pellet" microtubes were centrifuged for 5 minutes at 2000 rpm at 4°C. The supernatant of the "Pellet" microtubes was transferred into microtubes called "Supernatant" while the pellets were resuspended in 250 µL of PBS-Triton 4%. The cell lysate remained in the wells. 100 µL of each sample were placed in a 96-well plate, except for the "Lysate" samples of which 5 µL are diluted in 95 µL of PBS-Triton 4 %. 100 µL of Cytotoxicity Detection Kit (Roche Applied Science, Switzerland) were added in each well and after 15 minutes of reaction, the optic density was read with a spectrophotometer (Bio-Rad, USA) at 490 nm and 655 nm every 15 minutes until at least one value reached 2. The percentage of cytotoxicity was then calculated as follows:

$$\%\ cytotoxicity = \frac{(Pellet-Blank)+((Supernatant-Blank)*4)}{(Pellet-Blank)+\big((Supernatant-Blank)*4\big)+((Lysate-Blank)*20)}$$

10. Adhesion test

Following the cell culture protocol (see 1.2), after cells were trypsinized and centrifuged for 5 minutes at 1000 rpm, the supernatant was discarded, the cell pellet was resuspended and counted to have one million cells per each sample in 2 mL of RPMI-1640 (Gibco, USA) medium supplemented with10% FBS (Gibco, USA) in a 15 mL centrifuge tube (Sigma-Aldrich, USA). Then, 10 µL calcein-AM 1 mM (Invitrogen, USA) were added to the solution, that was incubated for 30 minutes at 37 °C with stirring each 5 minutes. To rinse the probe, the cell suspension was centrifuged at 1000 rpm for 5 minutes and the cell pellet resuspended in fresh medium, twice. After that, the cells were counted and seeded at 150 000 cells/well in 6-well plate (Costar, USA) in triplicate for labeled cells and one well for the control of non-labeled cells. After incubation for 1.5 hours in the dark, pictures of the samples were taken with a inverted phase contrast microscope (Leica, Germany) before and after rise 3 times the cells with PBS (Table 1), to analyze the confluence related to the adhesion. Next, the cells were lysed using 200 µL/well of the diluted Passive Lysis Buffer 1X (Promega, USA) for 15 minutes with agitation in the dark. 80 µL/ well were placed in a black 96-well polypropylene plate (Thermo Fisher Scientific, USA), likewise the lysis buffer as a blank. The fluorescence was read by the Fluoroskan Ascent ((Thermo Fisher Scientific, USA) at excitation 494 nm and emission 517 nm. The percentage of adhesion was then calculated as follows:

$$\%\ of\ Adhesion = \frac{shRNA\ ITGA5\ or\ ITGB3}{shCtrl}\ x\ 100$$

Two alternatives of the assay were tested. At the lysis step, the procedure was done using 50 µL/well of the diluted Passive Lysis Buffer 1X (Promega, USA) or 20 µL of lysis buffer solution (Table 5) for 15 minutes. After that, the quantification of proteins was achieved using Pierce 660 nm Protein assay (Thermo Fisher Scientific, USA) (see 6.2.).

11.PACMAN surfaces

The surfaces and the cell migration assessment on them were performed by Sophie Ayama using a procedure adopted from 70.

12. Statistical analysis

Data from mRNA, protein, cell migration and cell size analyses are presented as mean ± SD. Two-way ANOVA was performed followed by the post-hoc Bonferroni test (GraphPad Prism 7). A p-value of 0.05 was considered significant (*$p < 0.05$; **$p < 0.01$; ***$p < 0.001$).

IV. RESULTS

MDA-MB-231 breast cancer cells were chosen for this study. This cell line is epithelial with a mesenchymal-like phenotype that had already experienced the EMT, they are therefore highly metastatic[71]. Because of that, it is frequently used to study cell migration and metastasis formation. In order to assess and characterize the role of the ITGA5 and ITGB3 in cell migration, their expression was invalidated using RNA interference (siRNA) or short hairpin RNA (shRNA).

Initially, as a confirmation of previous results, gene and protein expression of ITGA5 and ITGB3 were assessed in samples coming from earlier studies of the PACMAN project. There were ITGA5-silenced or ITGB3-silenced MDA-MB-231 cells using siRNA, and ITGA5 knockdown cells using shRNA. The quantification of the mRNA and the protein levels were performed by RT-qPCR and Western Blot analysis, respectively.

1. Characterization of ITGA5- and ITGB3-silencing using siRNA in MDA-MB-231 cells

RNA interference was used to investigate the function of ITGA5 and ITGB3 in cell migration. Cells were transfected with ITGA5-targeting (siA5) or ITGB3-targeting (siB3) siRNA. Untransfected cells (UT) and transfected cells with siRNA RISC-Free (siRF) were used as control. siRF provides a reliable baseline for cellular response to lipid-RNA complexes. To evaluate the effectiveness of the ITG-invalidation, the mRNA relative expression was quantified by RT-qPCR using α-tubulin (A-TUB) as the house-keeping gene, and the protein expression was quantified by Western Blot analysis using A-TUB as the loading control. The values were normalized based on the levels obtained from UT control. The analyses were performed 72h post-transfection in four independent biological replicates.

The gene expression analysis showed that the mRNA level of ITGB3 for ITGA5 knockdown cells rose slightly by about 27% (Figure 12A). Also, ITGA5 knockdown led to a significant decrease to 16% ($p < 0.01$) in the mRNA level of the ITGA5-targeted gene (Figure 12B). On the other hand, the ITGB3 mRNA level decreased to 9% ($p < 0.01$) in ITGB3-silenced cells, without effect on the ITGA5 mRNA expression.

In order to investigate whether the effect observed at the mRNA level was translated at the protein level, Western blotting and immunofluorescence labeling were performed at 72 h post-transfection (Figure 13). The results showed that protein level of ITGA5 was strongly reduced in cells transfected with siA5 to 7% ($p < 0.001$). Unexpectedly, siB3 induced a significant reduction of the protein ITGA5 to 58% ($p < 0.01$), while the mRNA level for that protein did not show a significant variation. We also aimed to assess the protein levels of ITGB3, but the anti-ITGB3 antibody did not have the expected performance and the outcomes of the Western Blot and the immunofluorescence labeling could not be analyzed (data not shown).

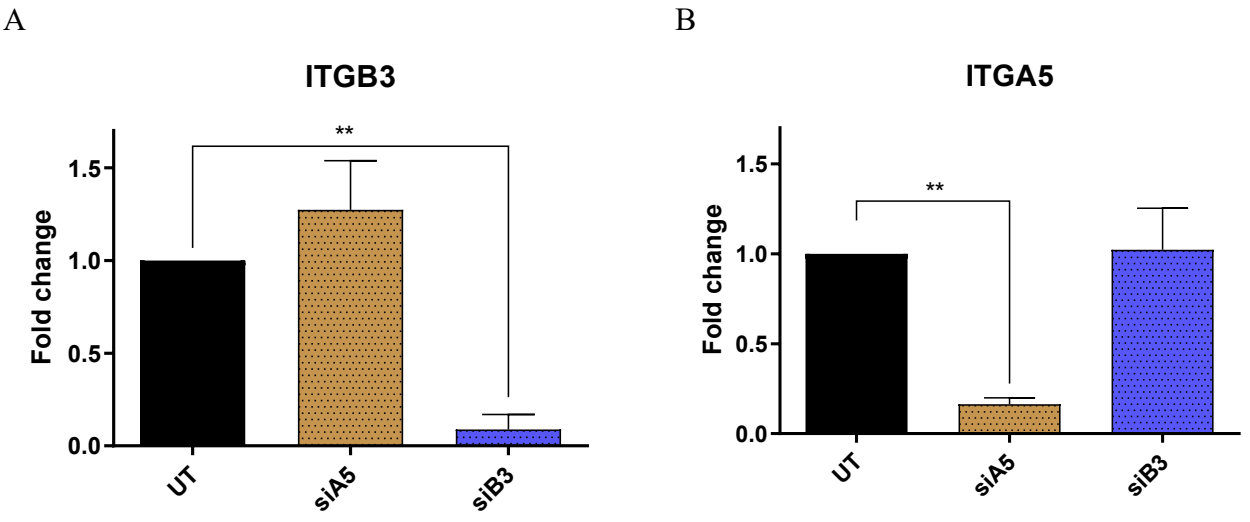

Figure 12. Gene expression of ITGA5 and ITGB3 in MDA-MB-231 cells. MDA-MB-231 cells were non-transfected (UT) or transfected using ITGA5-targeting (siA5) or ITGB3-targeting siRNA (siB3). 72 hours post-transfection, the mRNA levels of ITGA5 (A) and ITGB3 (B) were measured by RT-qPCR using α-tubulin as house-keeping gene. Results are expressed in fold change after being normalized to the reference condition (UT), and they represent the mean of three independent replicates (n = 3). Statistical significance was determined by two-way ANOVA; *p < 0.05; **p < 0.01; ***p < 0.001.

Figure 14A confirm the effectiveness of the invalidation of ITGA5 in cells transfected with siA5. Immunofluorescence labeling evidenced a decrease in the labeling intensity of this protein, compared to UT cells, siRF or siB3-transfected cells. However, the morphology of the microfilaments, determined by the labeling of F-Actin, did not seem to be influenced by ITGA5 or ITGB3 silencing.

Additionally, the phosphorylation and localization of FAK were analyzed because of the importance of FAK in the formation of focal adhesion. Furthermore, FAK is involved in the interaction with cell-surface adhesion receptors, such as integrins. The immunofluorescence labeling evidenced the formation of pFAK clusters and its abundance in all focal adhesion complexes. However, neither pFAK abundance, nor its subcellular localization were modified in the invalidated cells in comparison to UT or siRF-transfected cells (Figure 15A).

Then, MDA-MB-231 cells were characterized on 2D fibronectin-coated (FN-coated) surfaces by immunolabeling of ITGA5, pFAK, and F-actin (Annexe 1). This experiment was performed based on previous studies that highlighted the major role of ITGA5 in cells seeded onto FN-coated surfaces in comparison to uncoated surfaces. In these studies, ITGA5 and pFAK were observed in clusters formed by the focal adhesion complexes.

A

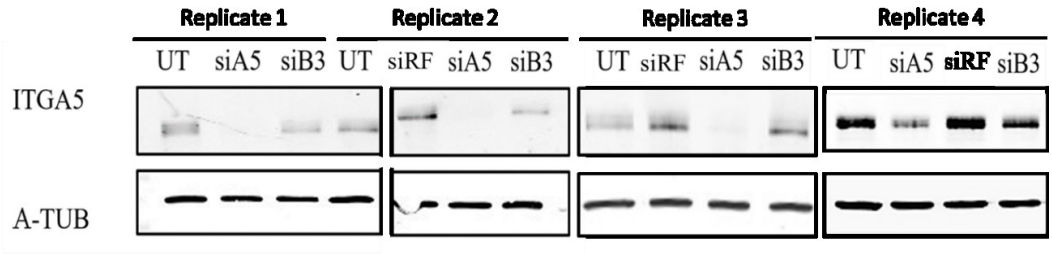

B

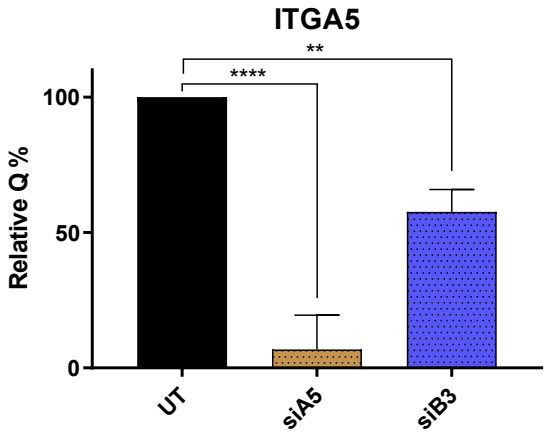

Figure 13. Protein level of ITGA5 in MDA-MB-231 cells after control, siITGB3 or siITGA5. MDA-MDA-MB-231 cells were non-transfected (UT) or transfected using ITGA5-targeting (siA5) or ITGB3-targeting (siB3) siRNA. 72 hours post-transfection, the protein level of ITGA5 was detected by Western Blotting and α-tubulin was used as the loading control. Results are expressed in relative quantity after being normalized to the reference condition (UT), and they represent the mean of independent replicates (n = 4). (A) Western blotting images. (B) Relative quantification. Statistical significance was determined by two-way ANOVA; *p < 0.05; **p < 0.01; ***p < 0.001.

A

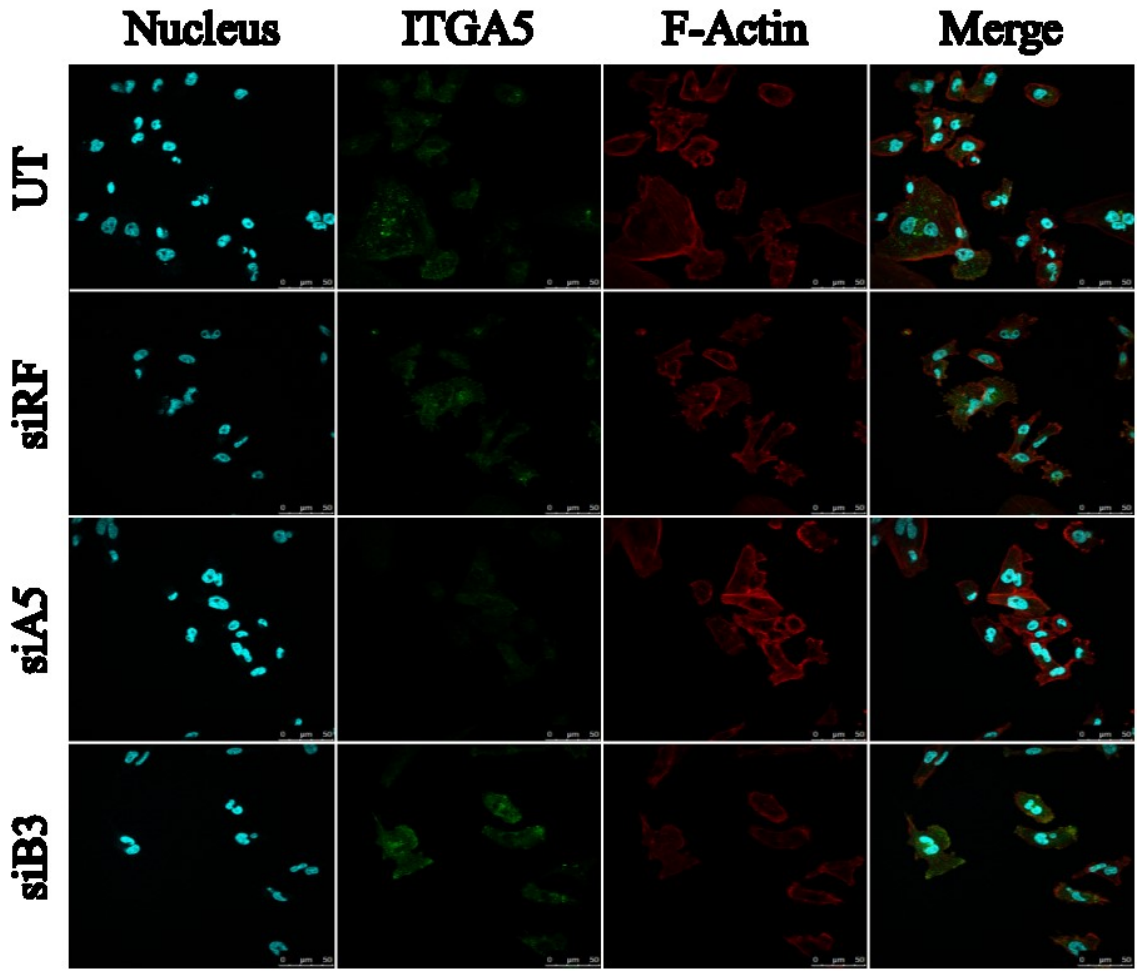

B

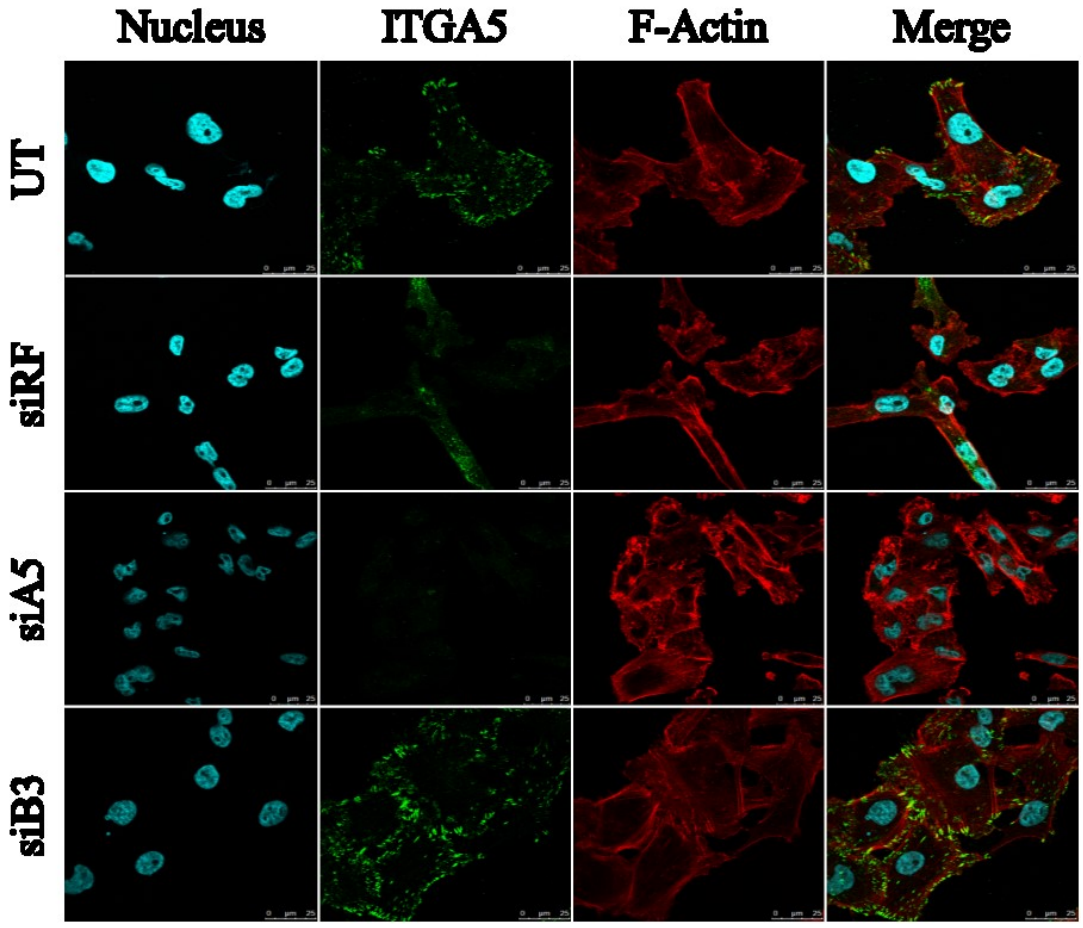

Figure 14. Immunofluorescence microscopy for ITGA5 and F-Actin in MDA-MB-231 cells. MDA-MDA-MB-231 cells were non-transfected (UT) or transfected using RISC-Free control (siRF), ITGA5-targeting (siA5) or ITGB3-targeting siRNA (siB3). Immunofluorescence labeling was performed at 72 h post-transfection: ITGA5 (green), F-actin (red) and Hoechst (blue). Scale bar = 25 µm. (A) Immunofluorescence microscopic images on uncoated surfaces. (B) Immunofluorescence microscopic images on fibronectin-coated surfaces.

In order to complement the characterization of ITGA5- or ITGB3-invalidated cells, ITGA5, pFAK, and F-actin abundance and subcellular localization were assessed by immunolabeling in cells cultured on fibronectin (Figure 14B and Figure 15B). In cells seeded on FN-coated surfaces, ITGA5 presented the cluster formation, which differed markedly from the images of cells seeded on uncoated-surfaces. Likewise, pFAK is grouped in clusters and present in all focal adhesion complexes, as was seen previously in cells seeded on uncoated surfaces. The cell morphology did not differ between the conditions. Furthermore, the effectiveness of the invalidation was also confirmed on those FN-coated surfaces since the fluorescence intensity associated to ITGA5 labeling was strongly decreased.

Taken together, these results indicate an effective invalidation of ITGA5 mRNA and protein in cells transfected with ITGA5-targeting siRNA as well as an effective invalidation of ITGB3 mRNA in cells transfected with ITGB3-targeting siRNA.

A

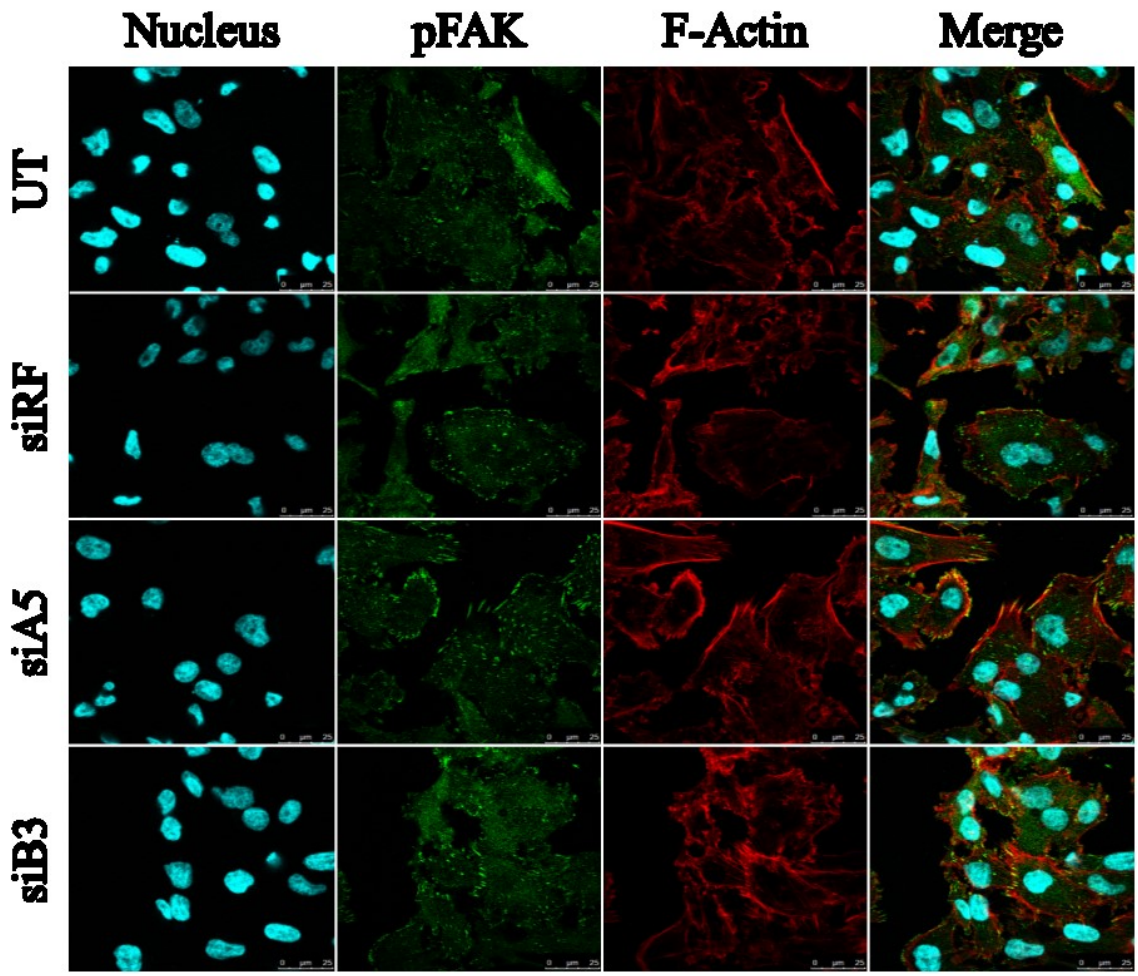

B

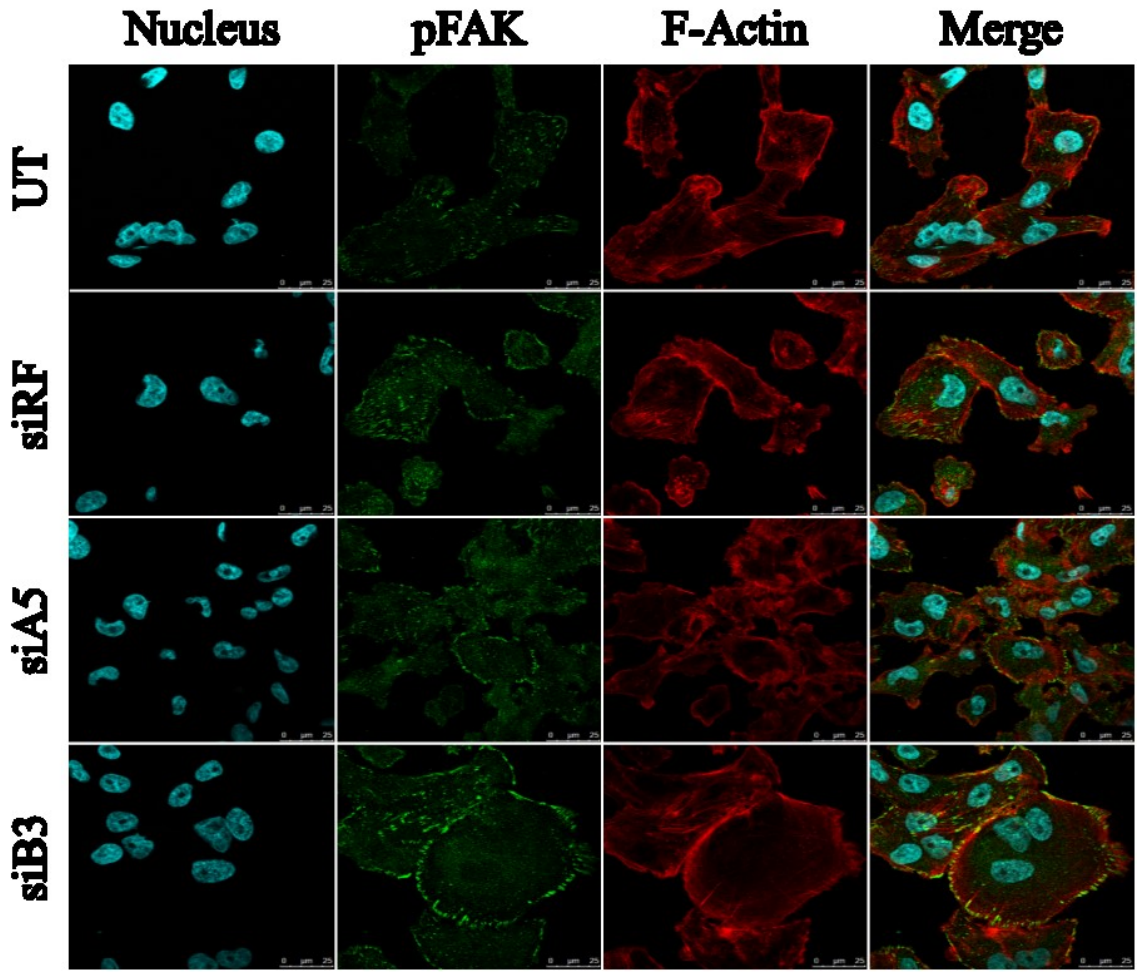

Figure 15. Immunofluorescence microscopy for pFAK and F-Actin in MDA-MB-231 cells. MDA-MDA-MB-231 cells were non-transfected (UT) or transfected using RISC-Free control (siRF), ITGA5-targeting (siA5) or ITGB3-targeting siRNA (siB3). Immunofluorescence labeling was performed at 72 h post-transfection: pFAK (green), F-actin (red) and Hoechst (blue). Scale bar = 25 µm. (A) Immunofluorescence microscopic images on uncoated surfaces. (B) Immunofluorescence microscopic images on fibronectin-coated surfaces.

To characterize the role of the ITGA5 in cell migration, a wound healing assay was performed in cells invalidated for ITGA5 or ITGB3 using siRNA, on both uncoated and FN-coated surfaces.

First, the relative speed of the cells to close the scratch on uncoated surfaces, compared to siRF-transfected cells, was markedly reduced (to 38%) in cells silenced for ITGB3. Similarly, the relative speed of migration was diminished by ITGA5 silencing, to 57% (Figure 16B). On FN-coated surfaces, the decrease in the migratory capacity was also observed, but to a lesser extent. The relative speed for ITGB3- and ITGA5-silenced cells decreased to 87% and 77% (Figure 16D).

For all the experiments, the migration of siRF-transfected cells was no different from the one of untransfected cells, indicating that the transfection by itself did not influence cell migration capacity.

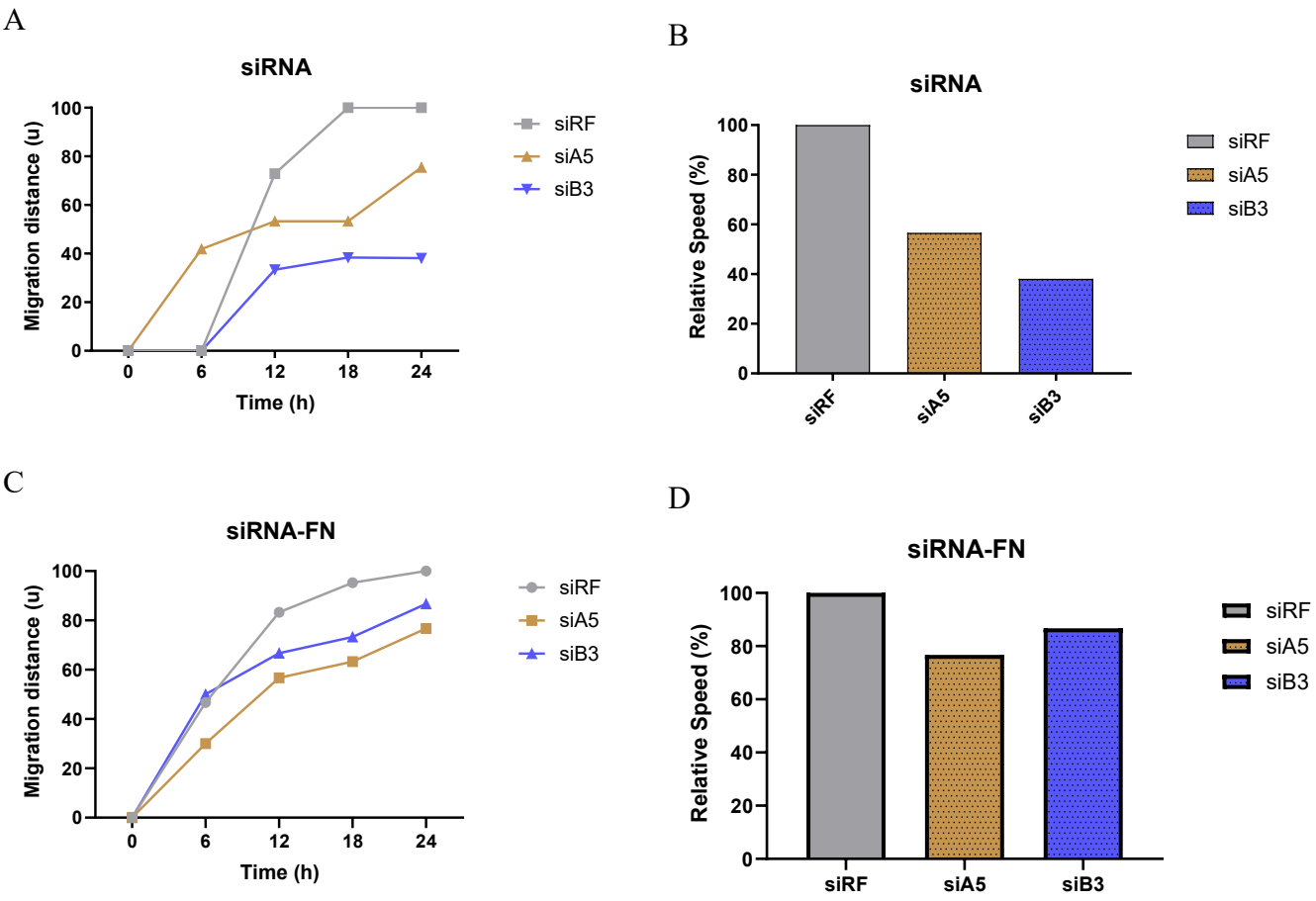

Figure 16. Effects of ITGA5 or ITGB3 knockdown on the migratory capacity of MDA-MB-231 cells seeded on uncoated or FN-coated surfaces. Scratch assay was performed to assess the effects of ITGA5-silencing and ITGB3-silencing using siRNA on the migratory capacity of MDA-MB-231 cells seeded on uncoated surfaces (A and B) or on FN-coated surfaces (C and D). Cell migration quantification of pictures was assessed by imaging processing and it is represented by Migration distance (u), that follows an arbitrary scale (A, C). The relative speed of migration is expressed after being normalized to the corresponding control (B, D).

2. Characterization of ITGA5 and ITGB3 knockdown using shRNA in MDA-MB-231 cells

Cell transduction with a viral vector expressing shRNA allows a stable and long-term invalidation of the targeted gene, through its insertion in the cellular DNA. This technique has shown to be more powerful to study gene function than the siRNA transitory knock-down[72]. In the second part of this master thesis, MDA-MB-213 cells were thus transduced using lentiviral particles designed to express one shRNA. This shRNA was synthesized and cloned in the vector SHC001 (Annexe 2). This part of the study was divided in two parts. First, in order to achieve ITGA5 knockdown, cells were transduced with an empty vector used as a control (shRNA Ctrl) or one of the two ITGA5-targeting shRNA (shRNA 126 or shRNA 124) (Annexe 2). Then, we aimed to confirm the characterization of ITGA5 knockdown using another ITGA5-targeting shRNA (shRNA 635). Secondly, we characterized ITGB3 knockdown cells using two different ITGB3-targeting shRNA (sh236 or sh237). shCtrl transduced cells were used as control cells.

2.1. ITGA5 invalidation

To assess the effectiveness of the ITGA5-invalidation using sh126 and sh124, ITGA5 expression has been evaluated at seven different passages post-transduction (PPT): PPT6, PPT7, PPT10, PPT12, PPT15, PPT18 and PPT21. The mRNA relative expression was evaluated by RT-qPCR using A-TUB as the house-keeping gene, and the protein expression was quantified by Western Blot analysis using A-TUB as the loading control.

The results indicate that the ITGB3 mRNA levels from sh126 or sh124 knockdown cells did not show a significant difference (Figure 17B). Nevertheless, cells transduced with sh124 displayed an increased level of ITGB3 mRNA as the number of PPTs increased from PPT7 to PPT12 (Figure 17A).

On the other hand, cells transduced with sh126 demonstrated a decrease in the ITGA5 mRNA level to 28% ($p < 0.001$) (Figure 17D). Also, ITGA5 protein expression in the cells transduced with sh126 was dramatically decreased to about 20% ($p < 0.001$) in comparison to shCtrl (Figure 18C). Contrarily, for the first four PPT analyzed, cells transduced with sh124 ITGA5 mRNA level was significantly increased by around 50% (Figure 17A), but no difference in the protein level of ITGA5 was observed (Figure 18B).

Similarly, a large reduction of the abundance of ITGA5 in the sh126-transduced cells was evidenced by immunolabeling, but no change in the abundance of the protein was observed for sh124-transduced cells (Figure 19A). That assay confirms the effective invalidation of ITGA5 using sh126 and the ineffective invalidation using sh124. For this reason, the characterization using sh124 was stopped at PPT12.

In addition, the immunolabeling allowed to assess the phosphorylation of FAK and its subcellular localization in transduced cells and to characterize the phenotype of ITGA5-targeting sh126 and sh124 transduced MDA-MB-231 cells in comparison to shCtrl transduced cells. At the morphological level, evaluated by the labeling of the microfilaments with F-actin, no differences were observed in ITGA5-knockdown cells in comparison to control cells. Moreover, neither the

phosphorylation of FAK nor its subcellular localization was affected by ITGA5 invalidation (Figure 19B).

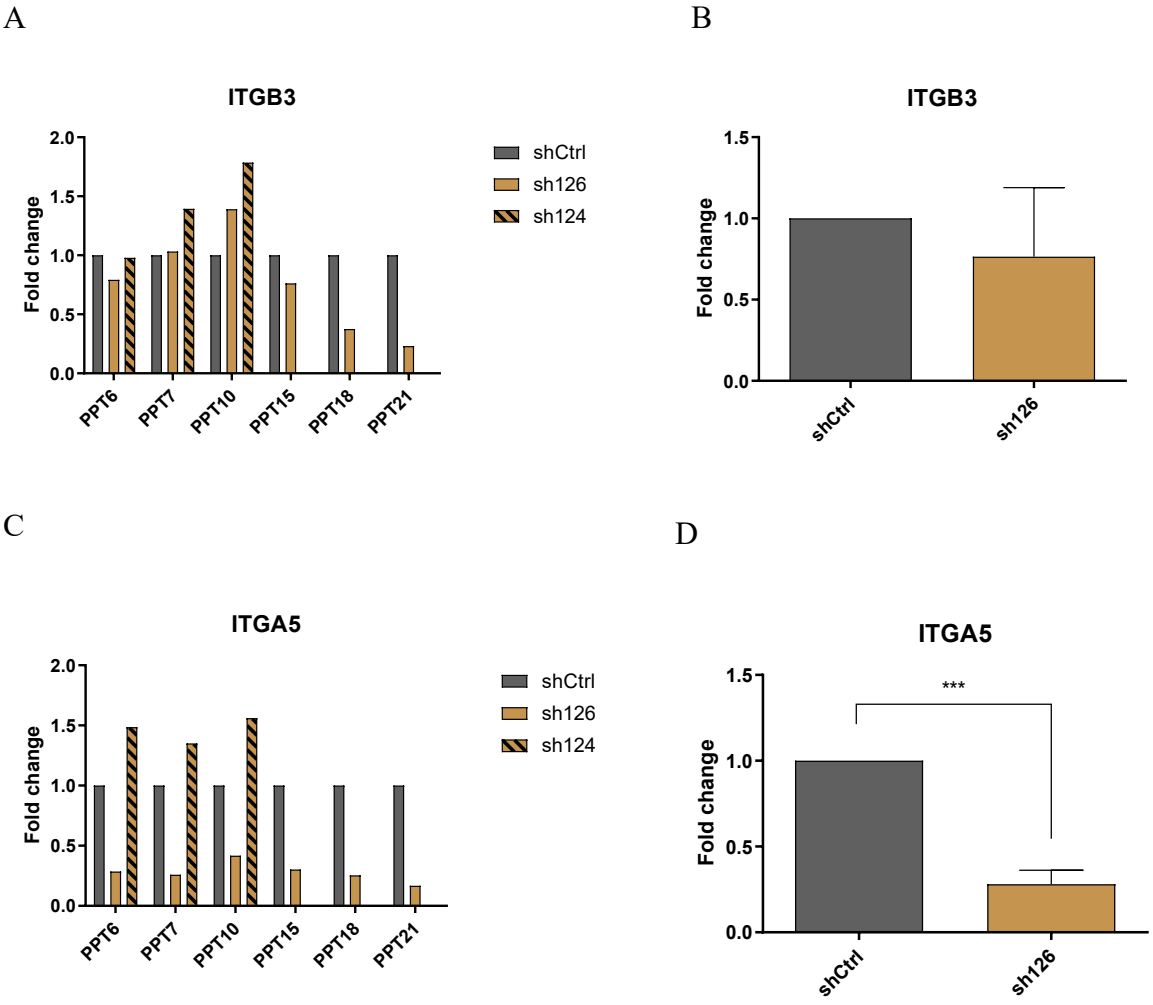

Figure 17. Gene expression of ITGA5 and ITGB3 in control cells and ITGA5 knockdown MDA-MB-231 cells. MDA-MB-231 cells were transduced with empty vector shC001 (shCtrl) or ITGA5-targeting shRNA (sh126 or sh124). At the passages post transduction (PPT) 6, 7, 10, 15, 18, and 21. The mRNA levels of ITGB3 (A and B) and ITGA5 (C and D) were measured by RT-qPCR using α-tubulin mRNA as house-keeping gene. Results are expressed in fold change after being normalized to the reference condition (shCtrl). For (B and D), results are the mean ± SD (standard deviation) of the passages (n = 6). Statistical significance was determined by two-way ANOVA; *$p < 0.05$; **$p < 0.01$; ***$p < 0.001$.

A

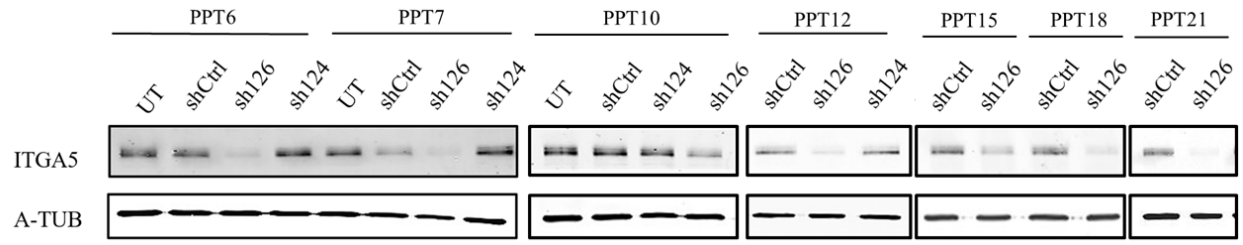

B

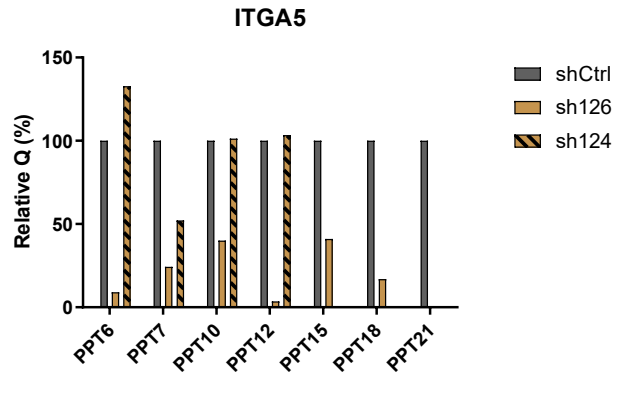

C

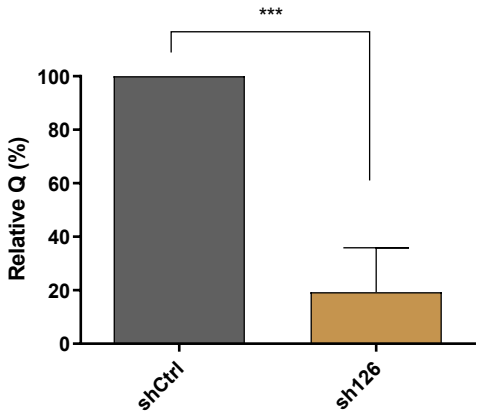

Figure 18. Protein level of ITGA5 in control cells and ITGA5 knockdown MDA-MB-231 cells. MDA-MB-231 cells were transduced with empty vector shC001 (shCtrl), ITGA5-targeting shRNA (sh126 or sh124) at the passages post transduction (PPT) 6, 7, 10, 15, 18, and 21. Protein levels of ITGA5 (A and B) were detected by Western Blotting (C) and α-tubulin was used as loading control. Results are expressed in relative quantity after being normalized to the reference condition (shCtrl). For (B), results are the mean ± SD (standard deviation) of the three passages (n = 6). Statistical significance was determined by two-way ANOVA; *p < 0.05; **p < 0.01; ***p < 0.001.

A

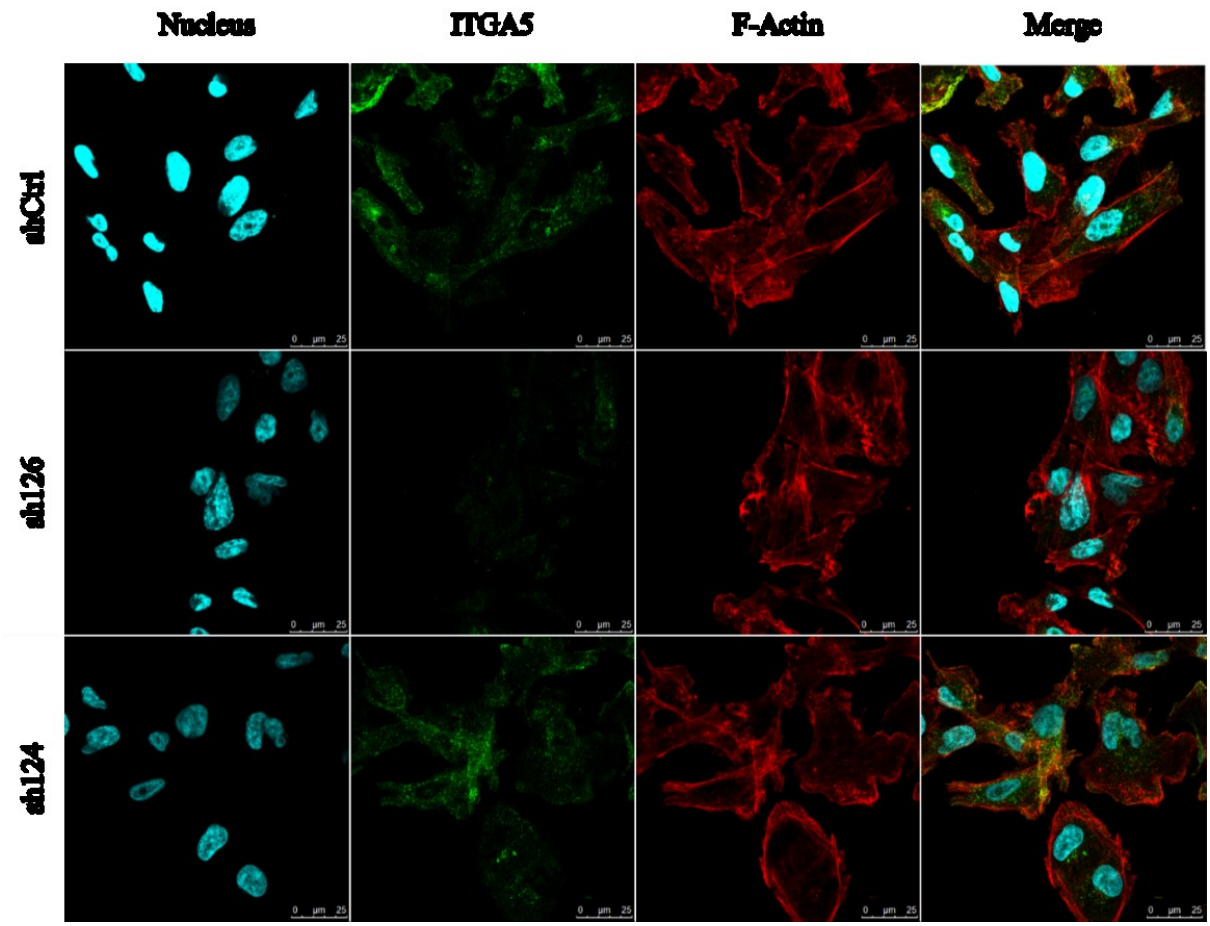

B

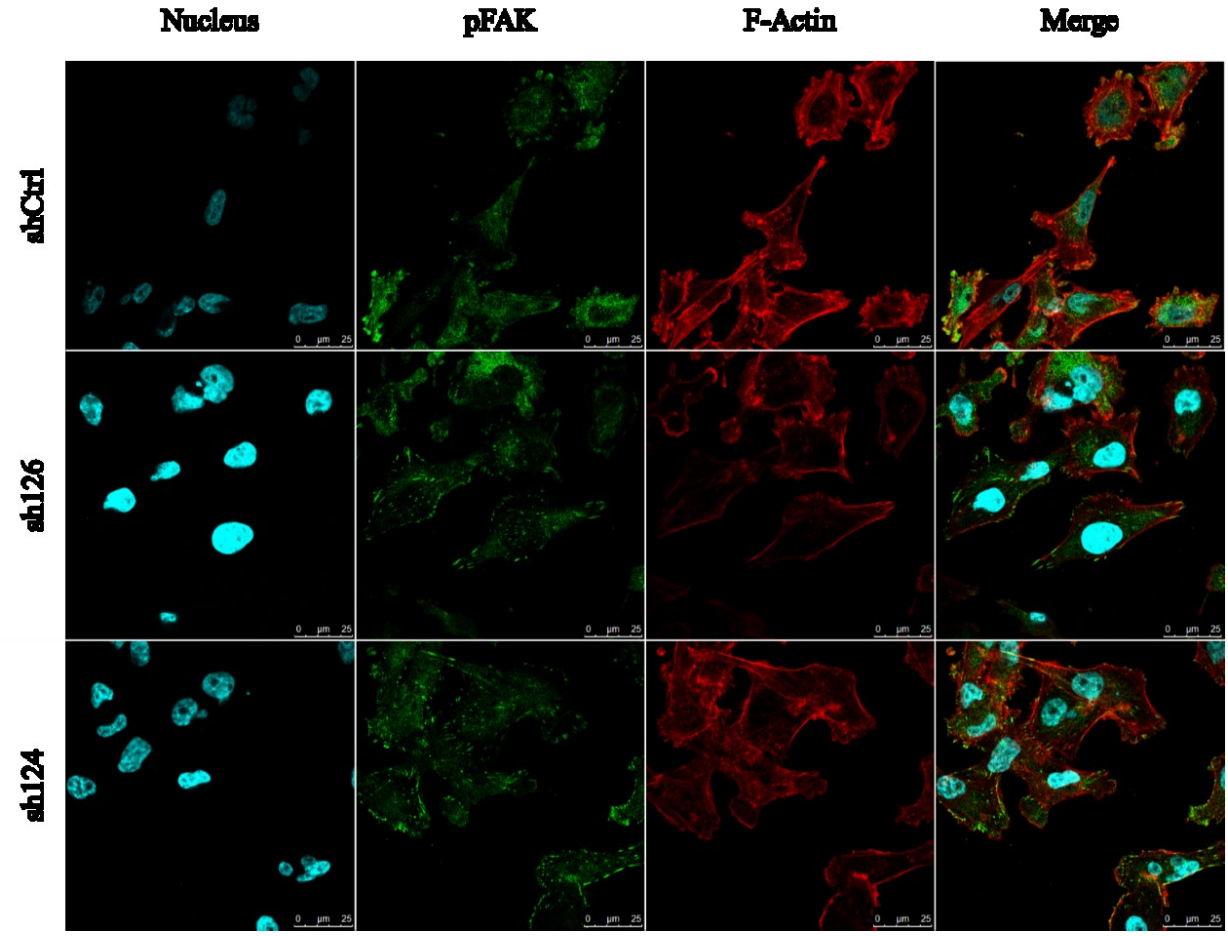

Figure 19. Immunofluorescence microscopy for ITGA5, pFAK and F-Actin in MDA-MB-231 cells. MDA-MB-231 cells were transduced with empty vector shC001 (shCtrl) or ITGA5-targeting shRNA (sh126 or sh124). Immunofluorescence labeling was performed at PPT12 post-transduction: F-actin (red) and Hoechst (blue). Scale bars: 25 µm. (A) Immunofluorescence microscopic images for ITGA5 (green). (B) Immunofluorescence microscopic images for pFAK (green).

Nevertheless, a difference in the confluence of the cells transduced with sh126 was observed. To evaluate if it can be explained by a cytotoxicity due to the transduction with ITGA5-targeting shRNA, at the PPT7, PPT10, PPT12, PPT15 and PPT18, the cells in 24-well plate were incubated for 48 hours in normal medium, and then, a LDH assay was performed. (Figure 20) shows that there was no considerable level of cytotoxicity, based on the threshold of 20%, neither in control cells, nor in the transduced cells.

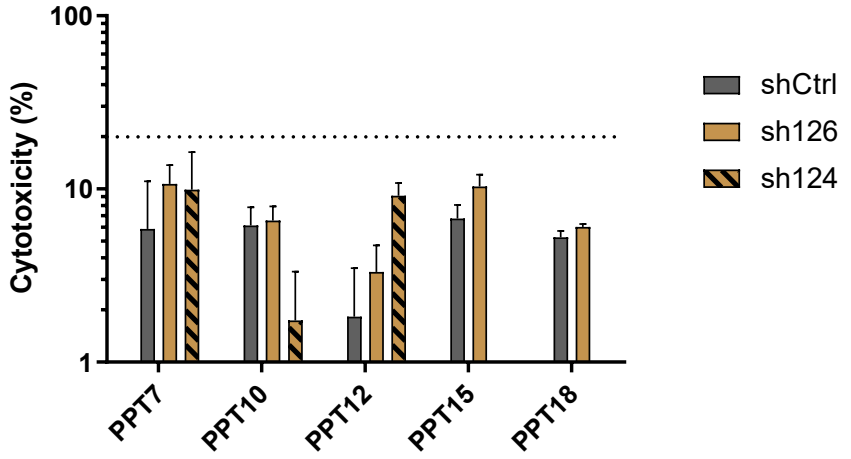

Figure 20. Lactate dehydrogenase cytotoxicity assay in control cells and ITGA5 knockdown MDA-MB-231 cells. MDA-MB-231 cells were transduced with empty vector shC001 (shCtrl) or ITGA5-targeting shRNA (sh126 or sh124). At the passages post transduction (PPT) 7, 10, 12, 15 and 18; cells were seeded in in 24-well plate and incubated for 48 hours with the RPMI-1640 medium supplemented with 10% fetal bovine serum, and then the assay was performed. The results are presented as the percent cytotoxicity of the maximum LDH release control according to the manufacturer's instructions, where values of 100% indicate total cellular toxicity and the non-cytotoxicity threshold is under 20%. The assay was done on five biological independent replicates (n = 5), each one with three technical replicates (n = 3).

The characterization was stopped at PPT21, because the cells transduced using sh126 diverged (Annexe 3). However, the quantification of the mRNA and protein level of ITGA5 at PPT21 confirm the continuous invalidation up to this last passage.

For all the experiments, shCtrl-transduced cells were no different from the one of untransfected cells. Additionally, the specific shCtrl control had the advantage to ensure that the effects observed after the transduction are the result of gene silencing and not merely the result of the introduction of the shRNA, like toxicity or gene expression changes due to activation of different pathways. Because of that, the use of untransfected cells was stopped at PPT8 and shCtrl was used as the only control.

Additionally, cells were transduced with sh635, another ITGA5-targeting shRNA, to confirm the results obtained using sh126. This shRNA was already validated in the cell line MCH58 with a mean knockdown level of 80% (Sigma information). Nevertheless, the phenotype obtained after the invalidation was very strong with a total loss of cell adhesion to the culture flasks. Cells were presenting low confluence that did not allow to achieve enough number of cells in usual cell culture conditions to characterize them (Annexe 4).

Finally, the role of ITGA5 in the migratory capacity of the shRNA ITGA5 knockdown cells was evaluated. Due to the ineffective invalidation of ITGA5 in cells trtansduced with sh124, the scratch assay was performed to compare sh126 to shCtrl. The cells with the invalidation of ITGA5 did not present a significant difference in the relative speed of migration compared to shCtrl. This observation was done both using uncoated or FN-coated surfaces (Annexe 5).

2.2. ITGB3 invalidation

During the second part, cells were invalidated for ITGB3 using two different ITGB3-targeting shRNA (sh236 or sh237). The test of sh236 had to be stopped at PPT7 because of contamination. First, to estimate the effectiveness of the invalidation, ITGA5 and ITGB3 expression was evaluated at three different passages post-transduction (PPT): PPT7, PPT10, and PPT12.

The results indicate that for ITGB3-invalidated cells using sh237, the level of ITGB3 strongly diminished, to 19% ($p < 0.05$) (Figure 21B). However, for these ITGB3-invalidated cells, we observed that the level of ITGA5 rose substantially, by around 56% ($p < 0.05$) (Figure 21D). In parallel, we observed a significant increase in ITGA5 protein level, which was two-fold higher than the control value, up to about 210% ($p < 0.05$) (Figure 22C). The overexpression of the protein ITGA5 in sh237-transduced cells was also detected in the immunofluorescence labeling of cells seeded on uncoated surfaces, as well as on FN-coated surfaces, in which it was observed in clusters (Figure 23).

In second place, the phosphorylation of FAK and its subcellular localization in transduced cells were evaluated using immunolabeling. Also, the phenotype of the sample cells was characterized in comparison to shCtrl transduced cells. At the morphological level, analyzing the microfilaments by the labeling of F-actin, no difference was observed in ITGB3-knockdown cells. Furthermore, neither the phosphorylation of FAK, nor its subcellular localization was changed in comparison to control cells seeded on uncoated or FN-coated surfaces (Figure 24). However, cells seeded on uncoated surfaces seemed to be smaller than on FN- coated surfaces, for each sample. To confirm the observation, cell sizes were measured by confocal microscopy (Annexe 6) and for all the conditions, cell sizes were lower for cells seeded on uncoated surfaces than for cells seeded on FN-coated surfaces.

Through the PPTs, difference of confluence between the control cells and the invalidated cells, for both ITGA5 and ITGB3 silencing, was observed (Annexe 7). Since cytotoxicity did not explain the lower confluence of sh126-transduced cells, a pilot test to evaluate the detachment of the cells was performed. The results obtained by the different methods did not allow to conclude that the lower confluence in the ITG-invalidated cells was due to a lack of adhesion capacity (Annexe 8).

A

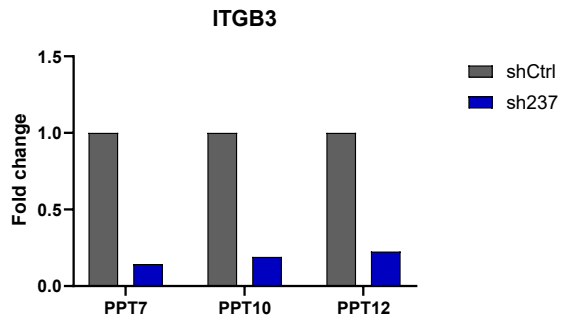

B

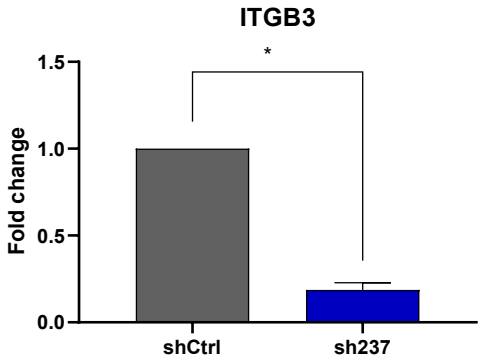

C

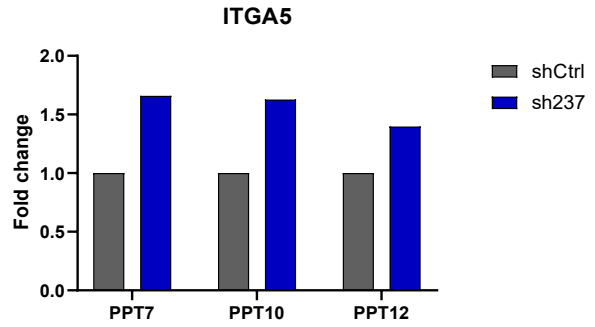

D

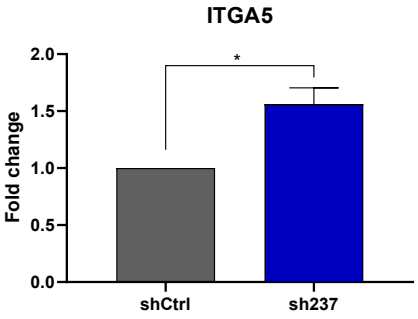

Figure 21. Gene expression of ITGA5 and ITGB3 in control cells, ITGA5 or ITGB3 knockdown MDA-MB-231 cells. MDA-MB-231 cells were transduced with empty vector shC001 (shCtrl) or ITGB3-targeting shRNA (sh237). At the passages post transduction (PPT) 7, 10 and 12, the mRNA levels of ITGB3 (A and B) and ITGA5 (C and D) were measured by RT-qPCR using α-tubulin mRNA as house-keeping gene. Results are expressed in fold change after being normalized to the reference condition (shCtrl). For (B and D), results are the mean ± SD (standard deviation) of the three passages (n = 3). Statistical significance was determined by two-way ANOVA; *p < 0.05; **p < 0.01; ***p < 0.001.

A

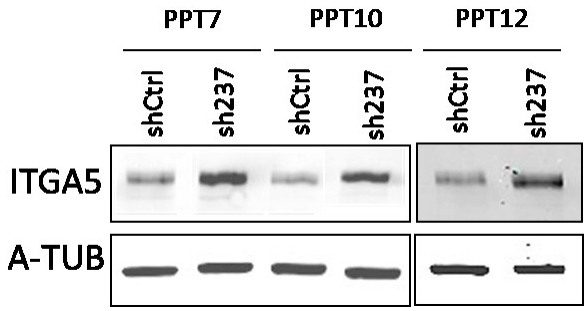

B

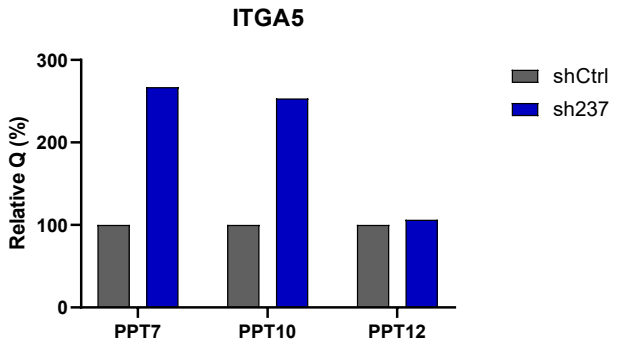

C

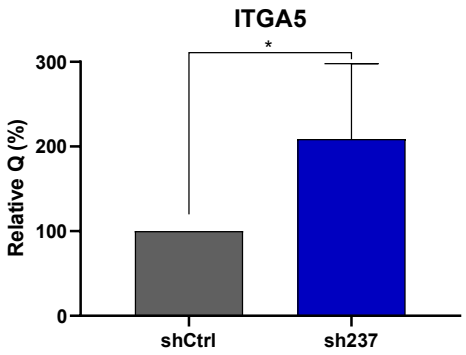

Figure 22. Protein level of ITGA5 in control cells, ITGA5 or ITGB3 knockdown MDA-MB-231 cells. MDA-MB-231 cells were transduced with empty vector shC001 (shCtrl) or ITGB3-targeting shRNA (sh237) at the passages post transduction (PPT) 6, 7 and 10. Protein levels of ITGA5 (A and B) were detected by Western Blotting (C) and α-tubulin was used as loading control. Results are expressed in relative quantity after being normalized to the reference condition (shCtrl). For (B), results are the mean ± SD (standard deviation) of the three passages (n = 3). Statistical significance was determined by two-way ANOVA; *p < 0.05; **p < 0.01; ***p < 0.001.

A

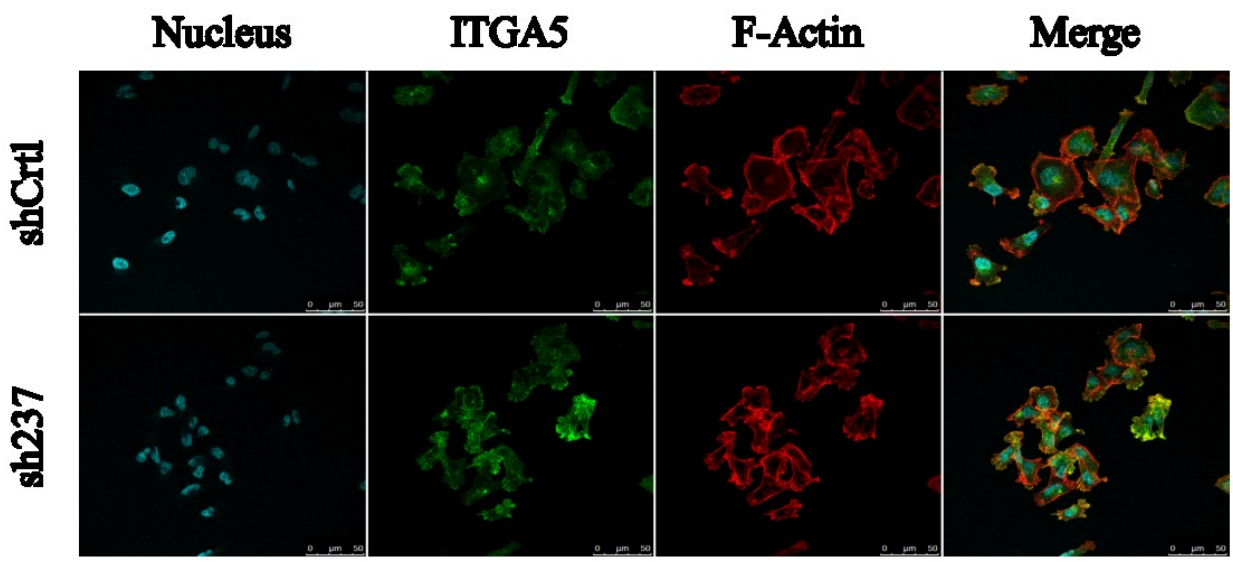

B

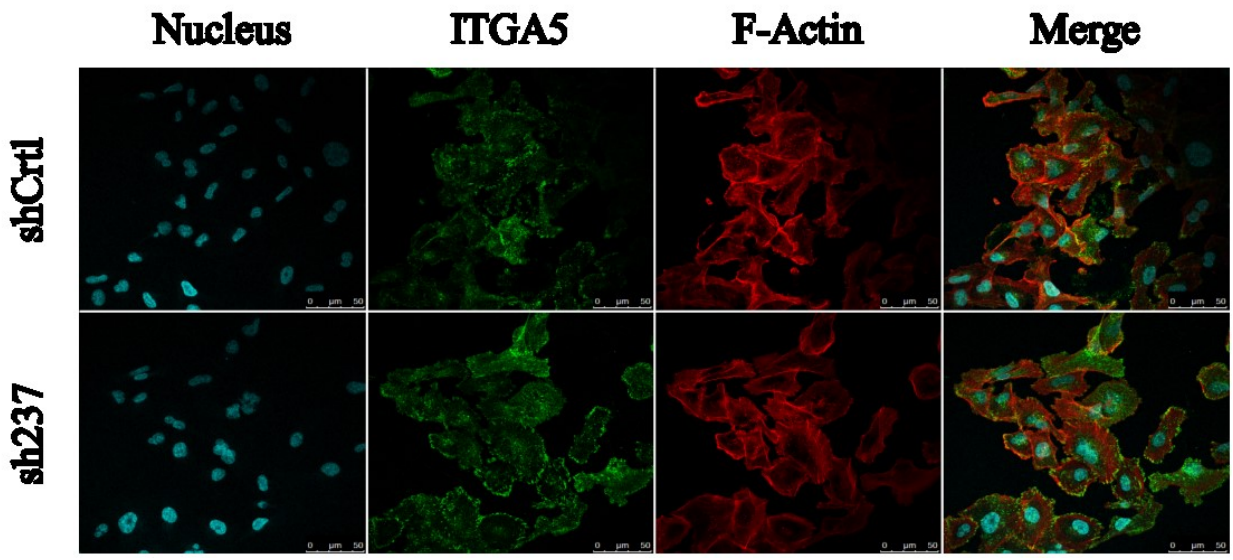

Figure 23. Immunofluorescence microscopy for ITGA5 and F-Actin in MDA-MB-231 cells. MDA-MB-231 cells were transduced with empty vector shC001 (shCtrl) or ITGB3-targeting shRNA (sh237). Immunofluorescence labeling was performed at passage post-transduction (PPT) 13: ITGA5 (green), F-actin (red) and Hoechst (blue). Scale bars: 25 µm. (A) Immunofluorescence microscopic images on uncoated surfaces. (B) Immunofluorescence microscopic images on fibronectin-coated surfaces.

A

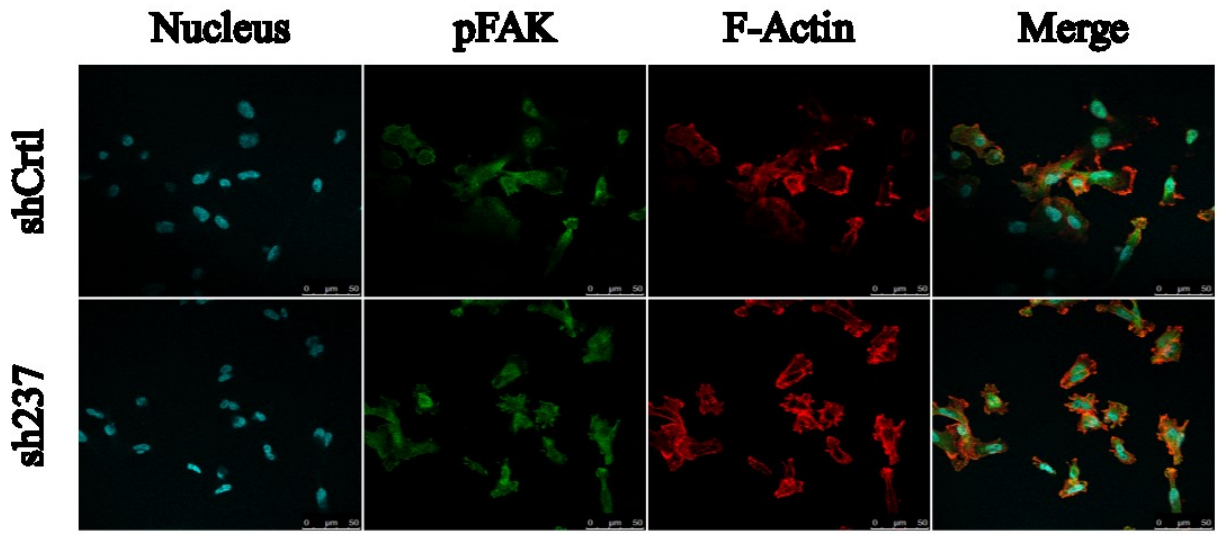

B

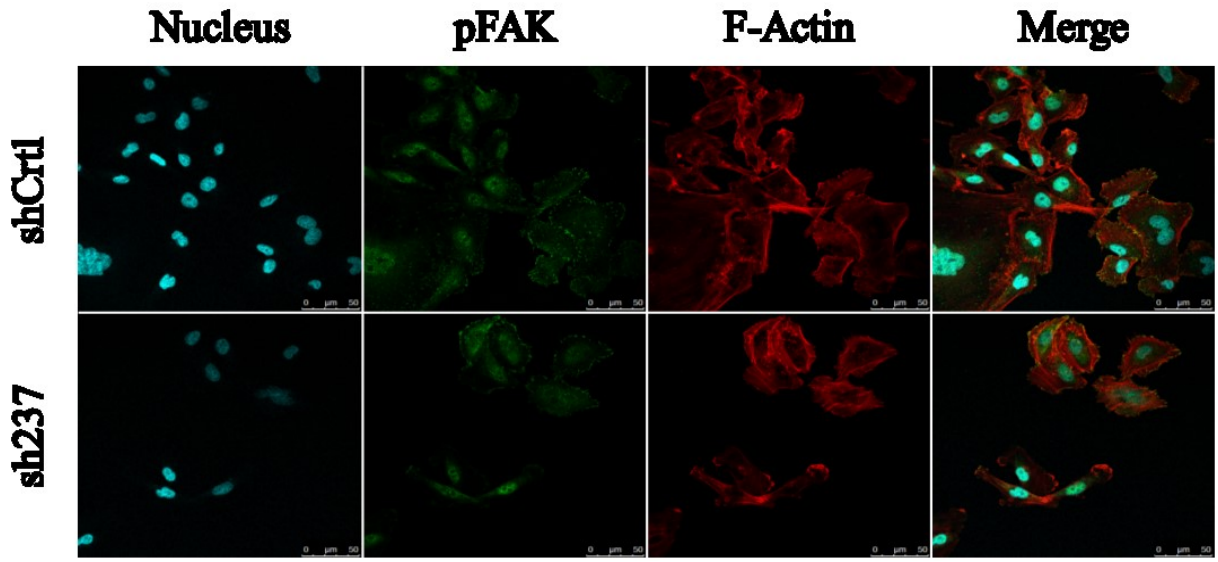

Figure 24. Immunofluorescence microscopy for pFAK and F-Actin in MDA-MB-231 cells. MDA-MB-231 cells were transduced with empty vector shC001 (shCtrl) or ITGB3-targeting shRNA (sh237). Immunofluorescence labeling was performed at passage post-transduction (PPT) 13: pFAK (green), F-actin (red) and Hoechst (blue). Scale bars: 25 µm. (A) Immunofluorescence microscopic images on uncoated surfaces. (B) Immunofluorescence microscopic images on fibronectin-coated surfaces.

3. Characterization of ITGA5 and ITGB3 co-invalidated MDA-MB-231 cells

Based on the current knowledge of the interaction and regulation between these two integrins, ITGA5 and ITGB3 and since we observed an influence of ITGB3 invalidation on ITGA5 expression, we though that co-invalidation of both integrins would be interesting.

First, to evaluate the effectiveness of the co-invalidation, ITGB3-invalidated cells using sh237 were invalidated for ITGA5 using siRNA (ITGB3 KO-siA5), ITGA5 and ITGB3 expression were assessed at 72 h post-transfection. ITGB3-invalidated cells using sh237 (ITGB3 KO) were used as a control, as well as transfected cells with siRNA RISC-Free (ITGB3 KO-siRF) that were used as the transfection control. The mRNA relative expression was evaluated by RT-qPCR using A-TUB as the house-keeping gene, and the protein expression was quantified by Western Blot analysis using A-TUB as the loading control.

The results indicate that the co-invalidation was effective because ITGB3 KO-siA5 cells displayed a substantially decrease in the ITGA5 mRNA level, to 15% and a reduced level of the ITGA5 protein level (to 1%) compared to ITGB3 KO-siRF control cells. For ITGB3 mRNA level, ITGB3 KO-siA5 cells did not show a significant difference from the ITGB3 KO-siRF control cells (Annexe 9). Similarly, a large reduction of the abundance of ITGA5 in co-invalidated cells was evidenced by immunolabeling in cells seeded on both uncoated and FN-coated surfaces compared to ITGB3 KO control cells (Figure 25).

Additionally, the transfection seemed to have an effect by itself because ITGB3 KO control cells displayed a decrease in the ITGA5 mRNA level (to 60%) in comparison to ITGB3 KO-siRF cells. That effect was also seen at protein level, since ITGB3 KO cells had a lower protein level of ITGA5 by around 20% compared to ITGB3 KO-siRF control cells (Annexe 10). The overexpression of ITGA5 protein in ITGB3 KO-siRF control cells was also observed by immunofluorescence labeling.

On the other hand, the phosphorylation of FAK and its subcellular localization did not differ in co-invalidated cells compared to the corresponding control cells when seeded on uncoated or FN-coated surfaces (Figure 26). Nevertheless, the cell phenotype on FN-coated surfaces differ from the one of cells seeded on uncoated-surfaces because they had a significant smaller size, as was seen in the second part of the shRNA characterization (Annexe 11).

In addition, cell migratory capacity was evaluated in the cells co-invalidated for the two integrins of interest. In this case, the ITGB3 KO-siRF control cells or ITGB3 KO-siA5 co-invalidated cells had a decrease in the relative speed in comparison to ITGB3 KO control. Nevertheless, the migratory relative speed of ITGB3 KO-siA5 cells did not have a significant reduction compared with the transfection control ITGB3 KO-siRF (Annexe 12).

Finally, the migratory capacity of MDA-MB-231 cells was assessed under three different protocols of exposition to the mitomycin (See Material and Methods). The results did not evidence any important difference (Annexe 13).

A

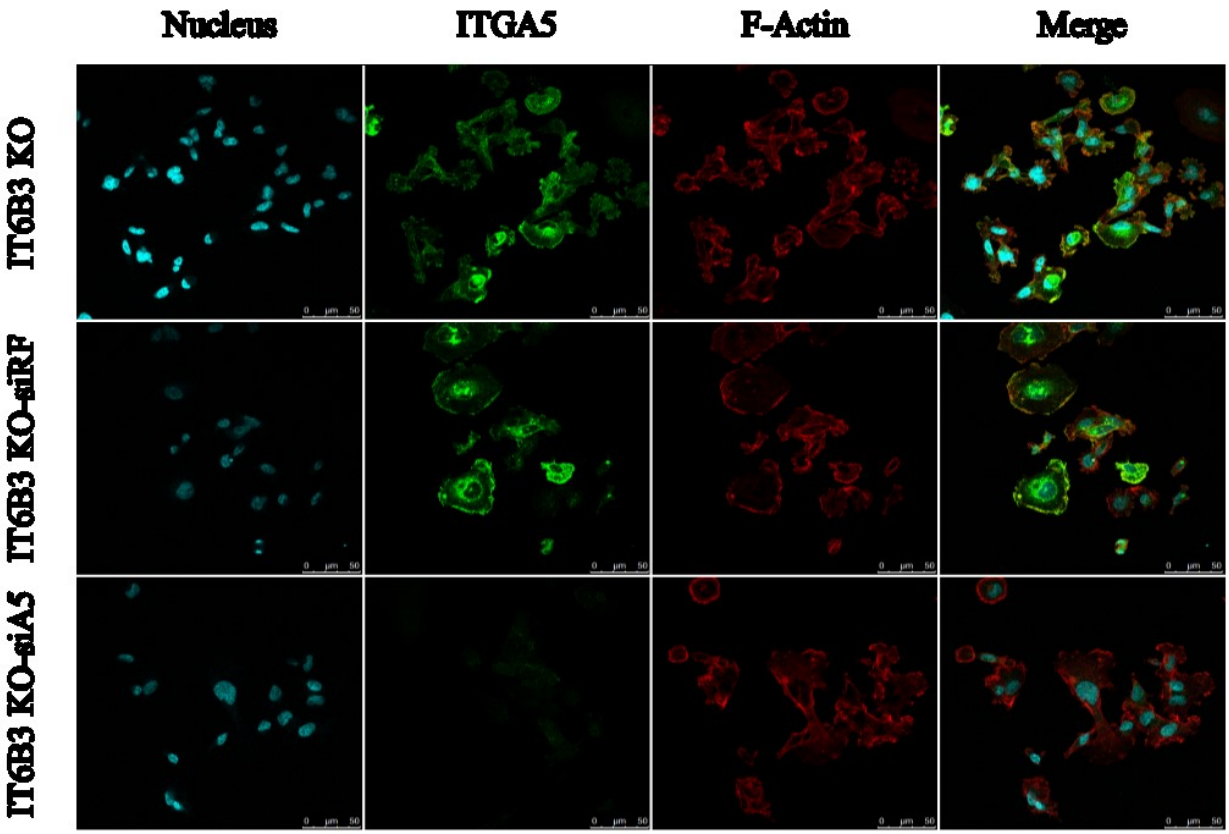
Nucleus
ITGA5
F-Actin
Merge
IT6B3 KO
IT6B3 KO-siRF
IT6B3 KO-siA5

B

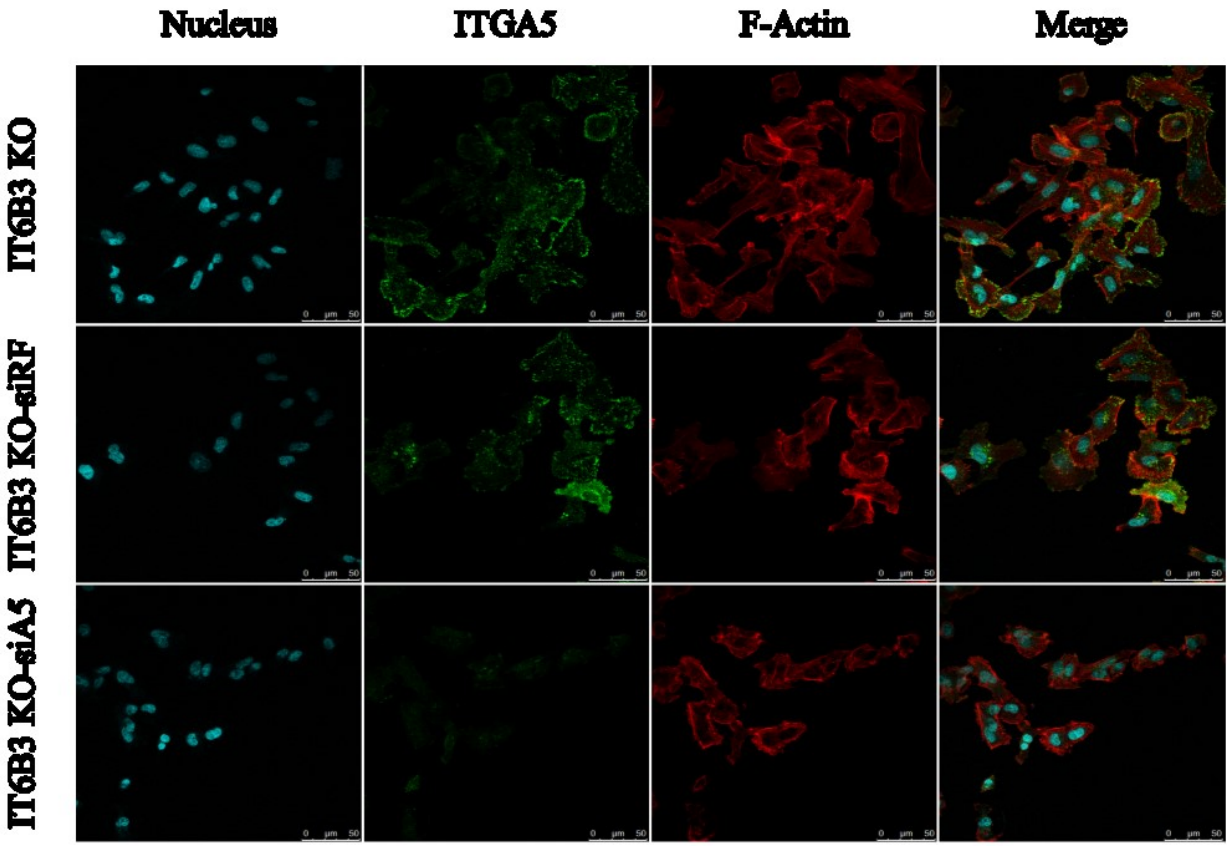

Figure 25. Immunofluorescence microscopy for ITGA5 and F-Actin in MDA-MB-231 cells upon co-invalidation. ITGB3-invalidated MDA-MB-231 cells transduced with ITGB3-targeting shRNA (sh237) were non-transfected (UT) or transfected using RISC-Free control (siRF) or ITGA5-targeting (siA5). Immunofluorescence labeling was performed at 72 h post-transfection: ITGA5 (green), F-actin (red) and Hoechst (blue). Scale bar = 25 µm. (A) Immunofluorescence microscopic images on uncoated surfaces. (B) Immunofluorescence microscopic images on fibronectin-coated surfaces.

A

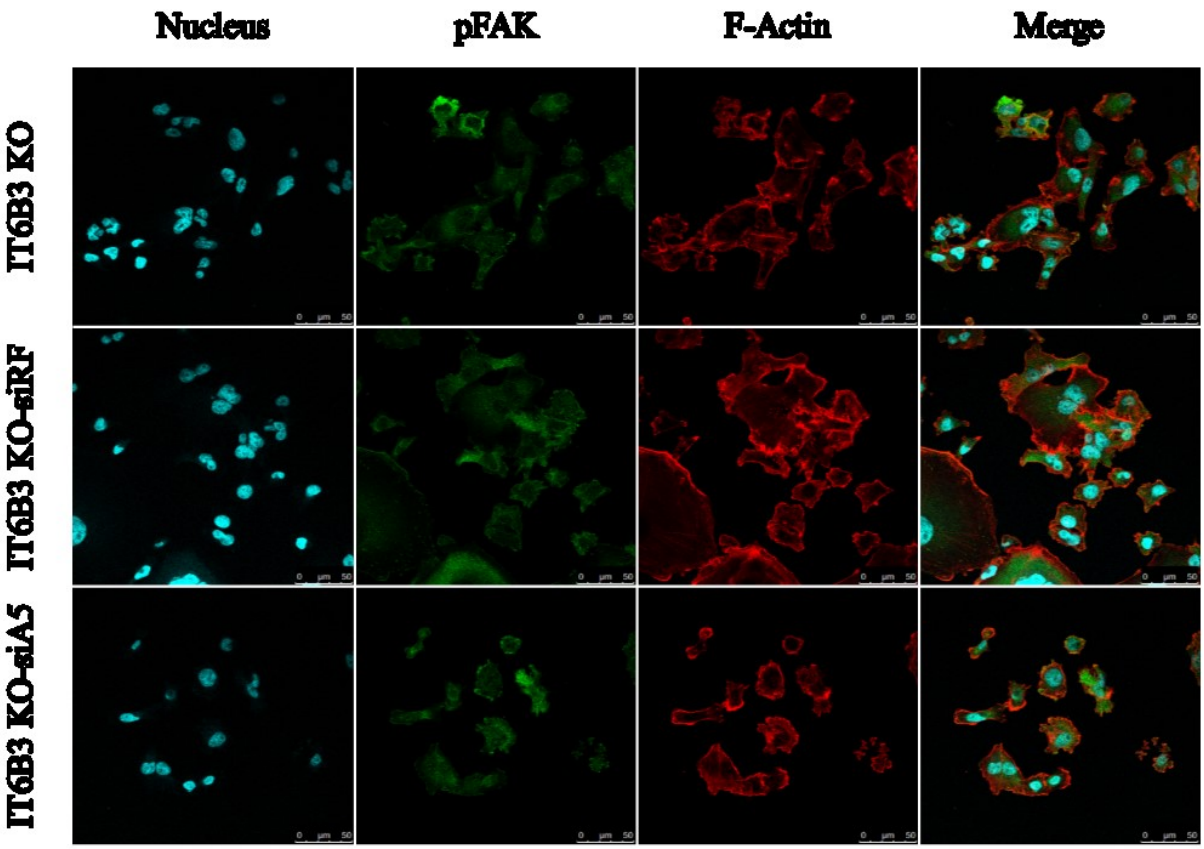
Nucleus
pFAK
F-Actin
Merge
IT6B3 KO
IT6B3 KO-siRF
IT6B3 KO-siA5

B

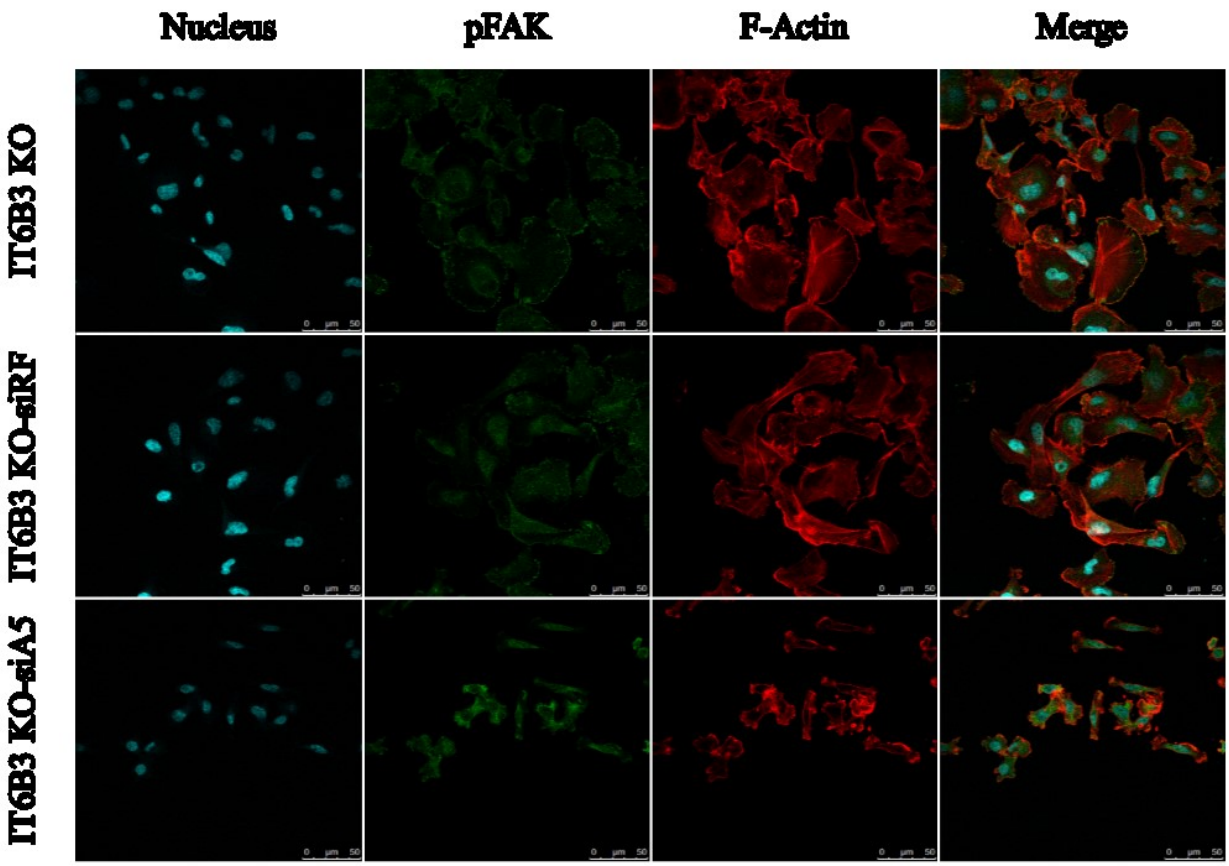

Figure 26. Immunofluorescence microscopy for p-FAK and F-Actin in MDA-MB-231 cells upon co-invalidation. ITGB3-invalidated MDA-MB-231 cells transduced with ITGB3-targeting shRNA (sh237) were non-transfected (UT) or transfected using RISC-Free control (siRF) or ITGA5-targeting (siA5). Immunofluorescence labeling was performed at 72 h post-transfection: p-FAK (green), F-actin (red) and Hoechst (blue). Scale bar = 25 µm. (A) Immunofluorescence microscopic images on uncoated surfaces. (B) Immunofluorescence microscopic images on fibronectin-coated surfaces.

V. DISCUSSION, PERSPECTIVES AND CONCLUSION

1. Discussion and perspectives

Metastasis is the leading cause of breast cancer mortality[5]. Indeed, the elucidation of the mechanism related to this process is a primordial objective to develop better diagnostic tools and treatments. Previous studies showed that the expression level of ITGA5 may modulate cell proliferation and that high levels of ITGA5 expression are required for metastasis to lymph nodes and lungs in breast cancer models[73]. Also, its expression in clinical biopsies is associated with an increased risk of mortality and was determined as an unfavorable prognosis factor[74].

MDA-MB-231 metastatic breast cancer cell line was the model chosen to characterize the role of ITGA5 in cell migration *in vitro*. To achieve this main objective, the expression of ITGA5 and ITGB3 was invalidated. Firstly, the invalidation was done using siRNA, and secondly, using shRNAs stably expressed in lentiviral-transduced cells.

The first objective of the study was to assess the efficiency of integrin invalidation. Therefore, the levels of mRNA and protein were evaluated by RT-qPCR and Western Blot analysis respectively. Also, the abundance of ITGA5 protein and its subcellular localization were evaluated using immunofluorescence labeling. Likewise, pFAK and F-actin proteins were studied by immunolabeling, in order to observe whether ITGA5 or ITGB3 invalidation would alter the formation of focal adhesions or the cell morphology.

1.1. Effective ITG-invalidation using siRNA and shRNA

In the first part, ITGA5- and ITGB3-silencing using siRNA was efficient. ITGA5 knockdown cells showed a diminution in the mRNA and in the protein levels of ITGA5. Similarly, ITGB3 knockdown cells had a lower ITGB3 mRNA level, whereas the ITGA5 mRNA level did not change. Despite this, ITGB3 knockdown cells had a significant decrease in ITGA5 protein level, that can be explained by variation in the transcription, mRNA decay, translation or protein degradation, that all together determine the protein abundance. Nevertheless, ITGA5 knockdown cells showed a slight increase in ITGB3 mRNA level, that could suggest an interconnexion between both integrins.

To proceed with a further characterization, the cells were invalidation in the long term. After performing the invalidation using shRNA and in accordance with the immunolabeling, mRNA and protein levels of ITGA5, the results demonstrated that the invalidation using sh126 was effective, but it was not using sh124. In the last case, literature was not found reporting the use of this sequence to perform the ITGA5 invalidation or its lack of effectiveness. Given that, it is suggested that could be for two reasons: first, an inefficient transduction process, or second, an off-target activity. Analyzing the first option, the transduction followed the same protocol as was done for shCtrl and sh126; therefore, it did not seem to be the cause of the infective knockdown of ITGA5. Consequently, it is more probable that it is caused as a consequence of an off-target effect.

In turn, ITGB3 was also efficiently invalidated using sh237, regarding to the results that showed a diminution in mRNA and protein levels of ITGB3.

1.2. Phenotypic variations induced by ITG-invalidation

During the second part, to validate the results obtained from the cells invalidated using sh126, another ITGA5-targeting shRNA (sh635) was tested. The strongest phenotype was observed from the invalidated cells compared to shCtrl. The cells were not able to proliferate enough to proceed for their characterization. This strong phenotype allows to hypothesize that the absence of ITGA5 could affect other important cellular processes where the integrin is involved. For example, a hypothesis in this case is that the lack of proliferation can be due to a loss of cell-surface adhesion. This idea will be developed later in the discussion. Additionally, in order to study the roles and interaction of the integrins of interest, ITGB3-invalidated cells using two different shRNA (sh236 and sh237) were also characterized.

During the study, the phenotype of ITGA5- and ITGB3-invalidated cells and the control cells did not show difference between them at a morphological level or in the formation of focal adhesion, both characteristics assessed by immunofluorescence labeling of polymerized actin (F-actin) and phosphorylation of FAK.

Nevertheless, a preceding study found a significant decrease in the focal adhesion area in the ITGA5-invalidated cells, showing a close relationship between the integrin and the formation of focal adhesion[73]. The evaluation of the formation of the focal adhesion complex could be done through the analysis of another protein downstream in the cascade. Proteins such as vinculin or paxillin could help to elucidate the relation between ITGA5 and the maturation of the complete formation of focal adhesion and later its role in the signalization that depends on that process.

1.3. Effect of ITG invalidation and FN-coating on cell phenotype

Although there were not morphologic variations, differences in cell confluence were observed in cells transduced with sh126 or sh237 compared to the control cells. After the evaluation of the cytotoxicity by LDH assay in cells transduced with ITGA5-targeting shRNA, it was concluded that was no considerable level of cytotoxicity neither in shCtrl cells nor in the invalidated cells, based on the threshold of 20%. Since cytotoxicity did not explain the lower confluence of sh126-transduced cells and knowing that integrins play a crucial role in ECM-cell and cell-cell adhesion[47], a pilot test to evaluate the cell detachment was carried out. The test was adjusted to achieve a trustable analysis of cell adhesion in MDA-MB-231 cell, but the results obtained were not conclusive. A hypothesis based on the data suggests that the difference in cell confluence could be related to not just a diminution in cell adhesion at the first moment of cell-surface interaction, but to effects in cell adhesion during cell division. In order to determine the cause of the confluence difference, this observation will be investigated further in the following part of the PACMAN project. Other adhesion assays can be used at different timings to elucidate the main cause. If the effect is due to cell-surface adhesion inhibition, it will be seen in a short time and before cell proliferation. Additionally, to confirm that the confluence difference is not because of alterations in cell proliferation itself, it is possible to do a BrdU flow cytometry, that will indicate cells that are actively replicating their DNA during the assay.

Cell adhesion also seemed to be involved in the variation or compensatory effect between the integrins. It is reflected in the difference in the mRNA level of the integrin that was not invalidated that changed along with the PPTs. The decrease in the mRNA level can be due to the fact that the cells with the strongest phenotype have less cell adhesion capacity and those cells were discarded during the process of the cell culture. Therefore, cells analyzed in the later PPTs could have been

selected and hence, displayed a less strong phenotype. Another hypothesis can be because cells adapted to the new conditions and the expression of one integrin could increase to compensate the absence of the other integrin.

Additionally, an effect of FN-coating in cell adhesion was detected through the cell size observed by Z-series. The bigger cell size observed for cells seeded on FN-coating throughout the whole work may correspond to the enhancement of cell adhesion because of the integrins activation (Annexe 144). Also, cell migration on FN-coated surfaces displayed a higher speed than in uncoated surfaces for both, control and ITG-invalidated cells. It is probably due to the increase in the cell-surface interactions.

1.4. Effects of ITG invalidation on cell migratory capacity

Since the main objective of this master thesis is to study the role of ITGA5 in cell migration in a model of metastatic breast cancer, scratch assays were performed to assess the migratory capacity of the cells using invalidated using siRNA or shRNA. First, the ITGB3 invalidation using siRNA had a marked effect reducing the relative speed of the cells to close the scratch, as was expected according to previous results obtained in the PACMAN project. Similarly, other studies showed impairment in the migratory and invasive potential of cancer cells by ITGB3 knockdown[75].

The effect of ITGA5 on cell migration has been previsouly studied, showing that ITGA5 expression promotes ITGA5-mediated cell adhesion and migration supporting breast cancer metastasis[75]. However, in this master thesis, the migration was only slightly diminished by ITGA5 silencing using siRNA. It could be assumed that the effect could not be seen because of the cells did not have enough time to adjust to the ITGA5 invalidation. Hence, with the objective to assess the effect of this integrin on this process, lentiviral vectors were used to transduce the cells with ITGA5-targeting shRNA, achieving a constitutive knockdown.

The results showed that the migratory capacity of ITGA5 knockdown cells did not differ in comparison to the control cells. This observation was performed for cells seeded on uncoated surfaces and on FN-coated surfaces. Given the microenvironment where the scratch assay was performed, a 2D model with low-FN, the results can be explained based on previous studies that reported the role of ITGA5 under similar conditions. For example, ITGA5 modulated single cell migration within a complex multicellular spheroid as well as single cell migration within 3D collagen-fibronectin gels but did not alter cell migration in 2D[73]. Also, it has been previously reported that ITGA5 can promote invasive migration and cell dispersion in FN-rich microenvironment[76], while, ITGB3 promotes migration in low-FN ECM[77]. Even if the experiment on FN-coated surfaces tried to approach to those conditions and the activation ITGA5 was observed, when the scratch is done, the FN layer is removed, preventing the possibility to evaluate the migration on FN-rich microenvironment. So, ITGA5 could not express its migratory properties under the conditions used here.

To continue with the characterization of ITGA5 and ITGB3 in cell migration, a migration test was done upon co-invalidation. The migratory capacity of the co-invalidated cells did not differ from the ITGB3 KO-siRF control. The difference in cell migration of co-invalidated and ITGB3 KO-siRF cells compared to ITGB3 KO control seems to be related to the transfection process and not to the absence of ITGA5.

Finally, results from the cell migration assay suggested that ITGA5 did not play the main role in distal cell migration in the model and conditions tested here. First, based on the analysis and results from previous researches, arise the alternative to test our cell model on FN-coated 3D models, where ITGA5 seems to have a determinant role in the migration and invasion. Our results showed that ITGA5 is not activated on uncoated surfaces, contrary as it was observed with its clusterization on FN-coated surfaces, that confirms its activation. Therefore, the ITGA5 invalidation could not have a big relevance under the conditions analyzed because when the integrin is inactive, it does not have a main role in the adhesion or migration. At the same time, for the migration assay are required more replicates and standardized method of testing and analyzing. Other assays in 2D or 3D could be used to validate the results (Annexe 15); for example, Boyden chamber or spheroid migration assay.

Second, the phosphorylation of FAK was observed in all the cases studied, even in the co-invalidated cells. The confirmation of the formation of focal adhesion supports the slight or insignificant difference of the cell migratory capacity given that focal adhesion formation has been demonstrating to correlate with 2D cancer cell motility[78]. It means that other compounds, more than FN, enhanced cell-surface interactions, activating the formation of focal adhesion and inducing cell migration, no matter the lack of ITGA5 or ITGB3. For example, it should be taken into account that the medium used in cell culture was supplemented with growth factors, that activated the epithelial growth factor receptor (EGFR). EGFR signaling can modulate adhesion by the redistribution of ITGA5 and ITGB3 and via an increase in the phosphorylation of FAK[79]. Additionally, another interesting point of future research could be to test if the MDA-MB-231 cells could produce FN by themselves and, hence, autoactivate their migration.

Based on these findings, it is possible to conclude that the migration function of ITGA5 is closely associated with the microenvironment the cells resided in and these cells can adopt a mode of migration that fits the local conditions, applying the regulation of those integrins, in this case: ITGA5 and ITGB3. That result implies that cell migration is a complex process where many actors are involved and can compensate the absence of some proteins. ITGA5 and ITGB3 are not indispensable for the formation of focal adhesion neither for the migratory cell in the model studied here. A deeper study should be carried that can establish the relation between the different actors.

1.5. Interaction and regulation between ITGA5 and ITGB3

ITGA5 knockdown cells at early PPTs showed a higher ITGB3 mRNA level than shCtrl-transduced cells, but a later diminution of that level at the increased of the PPTs. These events were also observed during the first part of the project. Likewise, the early increase in ITGB3 mRNA expression supportS the findings observed during the ITGA5 invalidation using siRNA. However, because of the duration of the experiment, the later reduction of the non-invalidated ITG mRNA level could not be seen. In addition to that, ITGB3 knockdown cells showed the same behavior for the ITGA5 mRNA levels, an overexpression at early PPTs and a continuous decreasE of that level at later PPTs.

The interactions between ITGA5 and ITGB3 that influence their gene and protein expression, have been previously described in the literature, suggesting that ITGA5 regulates the function of ITGB3 and vice versa, during some processes like migration *in vitro* or angiogenesis *in vivo*[80]. Furthermore, those interactions can vary based on the type of model studied. For example, they

are different depending on the type of cancer and the state of it. In fact, this variability increases the complexity of the study.

ITGA5 and ITGB3 bind to similar ligands but can act differently. While both promote migration, they elicit different signaling responses and cell motility outcomes. Indeed, they mutually could suppress or regulate each other in different ways[81]. To illustrate, ITGB3 and its recycling impair ITGA5 recycling and its pro-invasive activity[77]. ITGB3-recycling is promoted in the absence of FN and it stimulates directionally persistent lamellipodial migration in 2D and invasion into 3D ECM, but ITGB3-recycling pathway suppresses invasive migration in the presence of FN. Consequently, when ITGB3 or its recycling is inhibited, ITGA5 recycling drives random cell motility in 2D and promotes 3D invasion into FN-rich ECM[37]. Therefore, it is important to understand the interrelationship between these two integrins and the reciprocal influence on their gene and protein expression, specifically their role in motility of cancer cells. Given that the complex underlying mechanism of ITGA5 and ITGB3 regulation remains undetermined, one method to evaluate the effect of ITGB3 on ITGA5 could be done exposing ITGB3-invalidated cells to variation in the microenvironment conditions, such as quantity of FN or presence of other adhesion molecules, then to measure the gene and protein expression of ITGA5. In this way, determining under which specific conditions ITGB3 regulates ITGA5 could be achieved.

1.6. Perspectives

The complexity of cell migration leads to think that other integrin candidates involved in the process can be studied. In particular, integrin αvβ6 (ITGB6) has been found upregulated in many breast cancer samples and associated with poor prognosis[46]. This upregulation is caused by the abnormal high expression of MMP-9. Previous studies showed that FN can be degraded into fragments by MMP-9 *in vitro*, exposing different motifs of FN like RGD for proliferation in FNIII or IGD for migration in FNI[46]. The degradation of the ECM is a common characteristic in cancers.

Similarly, it should be taken in count that the crosstalk in processes like EMT, between different signal pathways and molecules, is crucial. To illustrate, integrins have been implicated in the communication with cadherins during cancer invasion and metastasis[82]. To elucidate that relationship between those adhesion molecules, it could be convenient to analyze epithelial and mesenchymal markers, such as E-cadherin and N-cadherin, respectively.

A study that supports the role of ITGA5 in cell migration in 3D models, found that the increased ITGA5 recycling is linked to the invasion in a FN-rich 3D microenvironment through the generation of Rho-driven invasive cellular protrusions, unique to cells in 3D to promote migration[83]. And based on the studies that exposed the difference between 2D and 3D motility in multiple contexts, further in the PACMAN project it could be interesting to characterize the role of ITGA5 related to the Rho signaling pathway in a complex 3D environment. For example, migrating cells of breast, pancreatic, and prostate cancers did not display lamellipodial structures in 3D, like spheroids, but they have unique dendritic protrusions[73].

One issue to elucidate the role of those integrins is due to the multiple functions that they have into the cell. Depending on many variables, those integrins can have a supportive or suppressive role in the cell migration regarding the literature. One possibility that should solve that problem is the use of machine learning to assess the role and the relevance that these proteins have on each state. Machine learning is a computational science that provides computers with the ability to create algorithms that can learn from and make predictions about data[84].

In the PACMAN projects, after the separation of the cell according to its migratory phenotype, and perform the single-cell RNA sequencing, that its already ongoing, machine learning could be applied in order to show the different interactions and how they differ depending on the migratory state. Also, the analysis will be specific for our breast cancer model and could bring possible therapeutic and diagnosis targets. Moreover, these targets can be specific for each phenotype. The information given by this application can be posteriorly validated by analyzing samples from the cancer biobanks. Currently, some studies already had used artificial intelligence to study breast cancer, but especially to assess the risk factors or just based on the genetic signature[85]. The application to study cell migration is just starting, like in the University of Glasgow, that has new research project that focus on using machine learning to understand the drivers of cancer spread and cell migration. An interdisciplinary collaboration could help also to understand this complex process in cancer models.

2. Conclusion

The roles of integrins in cancer have demonstrated a complex molecular mechanism involved in their biological function in different steps of cancer progression and metastasis. Integrin function and expression determine cancer cell behavior and characteristics. Integrins play a main role in metastasis because of their diverse roles in cell survival, motility, adhesion, and migration.

Even if ITGA5 and ITGB3 have been associated with cancer progression and metastasis in various types of cancer, their role has not been completely elucidated. Both integrins are involved in breast cancer metastasis, but they can act in different ways regarding the state of the disease. In MDA-MB-231 cell line, a model of metastatic breast cancer, ITGA5 did not show a significant correlation with cell migratory capacity, under the tested conditions.

Finally, the results will be validated using PACMAN surfaces (IGDQ-exposing surfaces-gradient-motogenic) and on different models that can enhance the activity of the integrin.

VI. REFERENCES

1. WHO. WHO | Cancer. *WHO* (2017).

2. Steeg, P. S. Targeting metastasis. *Nat. Rev. Cancer* **16,** 201–218 (2016).

3. NIH. Breast Cancer - National Cancer Institute. (2018). Available at: https://www.cancer.gov/types/breast/hp. (Accessed: 11th November 2018)

4. Raman, D., Foo, C. H. J., Clement, M.-V. & Pervaiz, S. Breast Cancer: A Molecular and Redox Snapshot. *Antioxid. Redox Signal.* **25,** 337–370 (2016).

5. Redig, A. J. & McAllister, S. S. Breast cancer as a systemic disease: a view of metastasis. *J. Intern. Med.* **274,** 113–126 (2013).

6. Torre, L. A. *et al.* Global cancer statistics, 2012. *CA. Cancer J. Clin.* **65,** 87–108 (2015).

7. Tao, Z. *et al.* Breast Cancer: Epidemiology and Etiology. *Cell Biochem. Biophys.* **72,** 333–338 (2015).

8. Sprague, B. L. *et al.* Variation in Breast Cancer-Risk Factor Associations by Method of Detection: Results From a Series of Case-Control Studies. *Am. J. Epidemiol.* **181,** 956–969 (2015).

9. Worsham, M. J. *et al.* Risk factors for breast cancer from benign breast disease in a diverse population. *Breast Cancer Res. Treat.* **118,** 1–7 (2009).

10. Gage, M., Wattendorf, D. & Henry, L. R. Translational advances regarding hereditary breast cancer syndromes. *J. Surg. Oncol.* **105,** 444–451 (2012).

11. Weigelt, B., Geyer, F. C. & Reis-Filho, J. S. Histological types of breast cancer: how special are they? *Mol. Oncol.* **4,** 192–208 (2010).

12. Amin, M. B., Edge, S. B. & American Joint Committee on Cancer. *AJCC cancer staging manual*.

13. Fouad, T. M. *et al.* Inflammatory breast cancer: a proposed conceptual shift in the UICC–AJCC TNM staging system. *Lancet Oncol.* **18,** e228–e232 (2017).

14. Chavez-MacGregor, M. *et al.* Incorporating Tumor Characteristics to the American Joint Committee on Cancer Breast Cancer Staging System. *Oncologist* **22,** 1292–1300 (2017).

15. Rakha, E. A. *et al.* Breast cancer prognostic classification in the molecular era: the role of histological grade. *Breast Cancer Res.* **12,** 207 (2010).

16. Mouttet, D. *et al.* Estrogen-Receptor, Progesterone-Receptor and HER2 Status Determination in Invasive Breast Cancer. Concordance between Immuno-Histochemistry and MapQuant^{TM} Microarray Based Assay. *PLoS One* **11,** e0146474 (2016).

17. Li, J., Chen, Z., Su, K. & Zeng, J. Clinicopathological classification and traditional prognostic indicators of breast cancer. *Int. J. Clin. Exp. Pathol.* **8,** 8500–5 (2015).

18. Rody, A. *et al.* A clinically relevant gene signature in triple negative and basal-like breast cancer. *Breast Cancer Res.* **13,** R97 (2011).

19. Navrátil, J. *et al.* [Triple Negative Breast Cancer]. *Klin. Onkol.* **28,** 405–15 (2015).

20. Geyer, F. C. *et al.* The Spectrum of Triple-Negative Breast Disease. *Am. J. Pathol.* **187,** 2139–2151 (2017).

21. Nik-Zainal, S. *et al.* Landscape of somatic mutations in 560 breast cancer whole-genome sequences. *Nature* **534,** 47–54 (2016).

22. Eralp, Y. The Role of Genomic Profiling in Advanced Breast Cancer: The Two Faces of Janus. *Transl. Oncogenomics* **8,** 1–7 (2016).

23. Hedenfalk, I. *et al.* Molecular classification of familial non-BRCA1/BRCA2 breast cancer. *Proc. Natl. Acad. Sci. U. S. A.* **100,** 2532–7 (2003).

24. You, D., Jung, S. P., Jeong, Y., Bae, S. Y. & Kim, S. Wild-type p53 controls the level of fibronectin expression in breast cancer cells. *Oncol. Rep.* **38,** 2551–2557 (2017).

25. Kleibl, Z. & Kristensen, V. N. Women at high risk of breast cancer: Molecular characteristics, clinical presentation and management. *The Breast* **28,** 136–144 (2016).

26. Scully, O. J., Bay, B.-H., Yip, G. & Yu, Y. Breast cancer metastasis. *Cancer Genomics Proteomics* **9,** 311–20 (2012).

27. Lawson, D. A. *et al.* Single-cell analysis reveals a stem-cell program in human metastatic breast cancer cells. *Nature* **526,** 131–135 (2015).

28. M Braden, A., V Stankowski, R., M Engel, J. & A Onitilo, A. Breast cancer biomarkers: risk assessment, diagnosis, prognosis, prediction of treatment efficacy and toxicity, and recurrence. *Curr. Pharm. Des.* **20,** 4879–98 (2014).

29. McEver, R. P. & Luscinskas, F. W. Cell Adhesion. *Hematology* 127–134 (2018). doi:10.1016/B978-0-323-35762-3.00012-3

30. Hirohashi, S. & Kanai, Y. Cell adhesion system and human cancer morphogenesis. *Cancer Sci.* **94,** 575–581 (2003).

31. Okegawa, T., Pong, R.-C., Li, Y. & Hsieh, J.-T. The role of cell adhesion molecule in cancer progression and its application in cancer therapy. *Acta Biochim. Pol.* **51,** 445–57 (2004).

32. Horstkorte, R. & Fuss, B. Cell Adhesion Molecules. *Basic Neurochem.* 165–179 (2012). doi:10.1016/B978-0-12-374947-5.00009-2

33. Lodish, H. *et al.* in *Molecular cell biology* (W. H. Freeman, 2000).

34. Cavallaro, U. & Christofori, G. Cell adhesion and signalling by cadherins and Ig-CAMs in cancer. *Nat. Rev. Cancer* **4,** 118–132 (2004).

35. Duperret, E. K., Dahal, A. & Ridky, T. W. Focal-adhesion-independent integrin-αv regulation of FAK and c-Myc is necessary for 3D skin formation and tumor invasion. *J. Cell Sci.* **128,** 3997–4013 (2015).

36. Bendas, G. & Borsig, L. Cancer cell adhesion and metastasis: selectins, integrins, and the inhibitory potential of heparins. *Int. J. Cell Biol.* **2012,** 676731 (2012).

37. Hamidi, H. & Ivaska, J. Every step of the way: integrins in cancer progression and metastasis. *Nat. Rev. Cancer* **18,** 533–548 (2018).

38. Li, Y. *et al.* Genetic depletion and pharmacological targeting of αv integrin in breast cancer cells impairs metastasis in zebrafish and mouse xenograft models. *Breast Cancer Res.* **17,** 28 (2015).

39. Giepmans, B. N. G. & van IJzendoorn, S. C. D. Epithelial cell–cell junctions and plasma membrane domains. *Biochim. Biophys. Acta - Biomembr.* **1788,** 820–831 (2009).

40. Blackstone, B. N. *et al.* Myoferlin depletion elevates focal adhesion kinase and paxillin phosphorylation and enhances cell-matrix adhesion in breast cancer cells. *Am. J. Physiol. Physiol.* **308,** C642–C649 (2015).

41. Acerbi, I. *et al.* Human breast cancer invasion and aggression correlates with ECM stiffening and immune cell infiltration. *Integr. Biol. (Camb).* **7,** 1120–34 (2015).

42. Oskarsson, T. Extracellular matrix components in breast cancer progression and metastasis. *The Breast* **22,** S66–S72 (2013).

43. Kumra, H. & Reinhardt, D. P. Fibronectin-targeted drug delivery in cancer. *Adv. Drug Deliv. Rev.* **97,** 101–110 (2016).

44. Maurer, L. M., Annis, D. S. & Mosher, D. F. IGD Motifs, Which Are Required for Migration Stimulatory Activity of Fibronectin Type I Modules, Do Not Mediate Binding in Matrix Assembly. *PLoS One* **7,** e30615 (2012).

45. Zipursky, L. B. *Molecular Cell Biology*. (W. H. Freeman, 2000).

46. LI, W., LIU, Z., ZHAO, C. & ZHAI, L. Binding of MMP-9-degraded fibronectin to β6 integrin promotes invasion via the FAK-Src-related Erk1/2 and PI3K/Akt/Smad-1/5/8 pathways in breast cancer. *Oncol. Rep.* **34,** 1345–1352 (2015).

47. Fogh, B. S., Multhaupt, H. A. B. & Couchman, J. R. Protein kinase C, focal adhesions and the regulation of cell migration. *J. Histochem. Cytochem.* **62,** 172–84 (2014).

48. Zhao, J. & Guan, J.-L. Signal transduction by focal adhesion kinase in cancer. *Cancer Metastasis Rev.* **28,** 35–49 (2009).

49. Tai, Y.-L., Chen, L.-C. & Shen, T.-L. Emerging Roles of Focal Adhesion Kinase in Cancer. *Biomed Res. Int.* **2015,** 1–13 (2015).

50. Read, R. W. in *Intraocular Inflammation* 1511–1514 (Springer Berlin Heidelberg, 2016). doi:10.1007/978-3-540-75387-2_150

51. Robert, J. [Biology of cancer metastasis]. *Bull. Cancer* **100,** 333–42 (2013).

52. Géraud, C., Koch, P. S., Damm, F., Schledzewski, K. & Goerdt, S. The metastatic cycle: metastatic niches and cancer cell dissemination. *JDDG J. der Dtsch. Dermatologischen Gesellschaft* **12,** 1012–1019 (2014).

53. O'Shaughnessy, J. Extending Survival with Chemotherapy in Metastatic Breast Cancer. *Oncologist* **10,** 20–29 (2005).

54. Polyak, K. Breast cancer: origins and evolution. *J. Clin. Invest.* **117,** 3155–63 (2007).

55. Yeung, K. T. & Yang, J. Epithelial-mesenchymal transition in tumor metastasis. *Mol.*

Oncol. **11,** 28–39 (2017).

56. Hunter, K. W., Crawford, N. P. & Alsarraj, J. Mechanisms of metastasis. *Breast Cancer Res.* **10,** S2 (2008).

57. Sone, S., Fidler, I. J., Roos, E., Kerbel, R. & Breitman, M. Activation of rat alveolar macrophages to the tumoricidal state in the presence of progressively growing pulmonary metastases. *Cancer Res.* **41,** 2401–6 (1981).

58. Li, D.-M. & Feng, Y.-M. Signaling mechanism of cell adhesion molecules in breast cancer metastasis: potential therapeutic targets. *Breast Cancer Res. Treat.* **128,** 7–21 (2011).

59. Muschel, R. J. in *Encyclopedia of Cancer* 2785–2787 (Springer Berlin Heidelberg, 2015). doi:10.1007/978-3-662-46875-3_3671

60. McSherry, E. A., Donatello, S., Hopkins, A. M. & McDonnell, S. Common Molecular Mechanisms of Mammary Gland Development and Breast Cancer. *Cell. Mol. Life Sci.* **64,** 3201–3218 (2007).

61. Kozłowski, J., Kozłowska, A. & Kocki, J. Breast cancer metastasis - insight into selected molecular mechanisms of the phenomenon. *Postepy Hig. Med. Dosw. (Online)* **69,** 447–51 (2015).

62. Larue, L. & Bellacosa, A. Epithelial–mesenchymal transition in development and cancer: role of phosphatidylinositol 3′ kinase/AKT pathways. *Oncogene* **24,** 7443–7454 (2005).

63. Thiery, J. P. & Sleeman, J. P. Complex networks orchestrate epithelial–mesenchymal transitions. *Nat. Rev. Mol. Cell Biol.* **7,** 131–142 (2006).

64. Tse, J. C. & Kalluri, R. Mechanisms of metastasis: Epithelial-to-mesenchymal transition and contribution of tumor microenvironment. *J. Cell. Biochem.* **101,** 816–829 (2007).

65. Xie, H.-Y., Shao, Z.-M. & Li, D.-Q. Tumor microenvironment: driving forces and potential therapeutic targets for breast cancer metastasis. *Chin. J. Cancer* **36,** 36 (2017).

66. Minn, A. J. *et al.* Distinct organ-specific metastatic potential of individual breast cancer cells and primary tumors. *J. Clin. Invest.* **115,** 44–55 (2005).

67. Shahi, P. K. & Pineda, I. F. Tumoral Angiogenesis: Review of the Literature. *Cancer Invest.* **26,** 104–108 (2008).

68. Hynes, R. O. Integrins: versatility, modulation, and signaling in cell adhesion. *Cell* **69,** 11–25 (1992).

69. Parvani, J. G., Gujrati, M. D., Mack, M. A., Schiemann, W. P. & Lu, Z.-R. Silencing β3 Integrin by Targeted ECO/siRNA Nanoparticles Inhibits EMT and Metastasis of Triple-Negative Breast Cancer. *Cancer Res.* **75,** 2316–2325 (2015).

70. Corvaglia, V., Marega, R., De Leo, F., Michiels, C. & Bonifazi, D. Unleashing Cancer Cells on Surfaces Exposing Motogenic IGDQ Peptides. *Small* **12,** 321–9 (2016).

71. Yano, S. *et al.* In Vivo Isolation of a Highly-aggressive Variant of Triple-negative Human Breast Cancer MDA-MB-231 Using Serial Orthotopic Transplantation. *Anticancer Res.* **36,**

3817–20 (2016).

72. Taxman, D. J., Moore, C. B., Guthrie, E. H. & Huang, M. T.-H. in *Methods in molecular biology (Clifton, N.J.)* **629,** 139–156 (2010).

73. Ju, J. A. *et al.* Hypoxia Selectively Enhances Integrin α5β1 Receptor Expression in Breast Cancer to Promote Metastasis. *Mol. Cancer Res.* **15,** 723–734 (2017).

74. Xie, J.-J. *et al.* Integrin α5 promotes tumor progression and is an independent unfavorable prognostic factor in esophageal squamous cell carcinoma. *Hum. Pathol.* **48,** 69–75 (2016).

75. Qin, L. *et al.* Steroid Receptor Coactivator-1 Upregulates Integrin 5 Expression to Promote Breast Cancer Cell Adhesion and Migration. *Cancer Res.* **71,** 1742–1751 (2011).

76. Blandin, A.-F. *et al.* Glioma cell dispersion is driven by α5 integrin-mediated cell–matrix and cell–cell interactions. *Cancer Lett.* **376,** 328–338 (2016).

77. Jacquemet, G., Humphries, M. J. & Caswell, P. T. Role of adhesion receptor trafficking in 3D cell migration. *Curr. Opin. Cell Biol.* **25,** 627–32 (2013).

78. Doyle, A. D., Carvajal, N., Jin, A., Matsumoto, K. & Yamada, K. M. Local 3D matrix microenvironment regulates cell migration through spatiotemporal dynamics of contractility-dependent adhesions. *Nat. Commun.* **6,** 8720 (2015).

79. Eberwein, P. *et al.* Modulation of focal adhesion constituents and their down-stream events by EGF: On the cross-talk of integrins and growth factor receptors. *Biochim. Biophys. Acta - Mol. Cell Res.* **1853,** 2183–2198 (2015).

80. Kim, S., Harris, M. & Varner, J. A. Regulation of Integrin $\alpha_v\beta_3$ -mediated Endothelial Cell Migration and Angiogenesis by Integrin $\alpha_5\beta_1$ and Protein Kinase A. *J. Biol. Chem.* **275,** 33920–33928 (2000).

81. Danen, E. H. J. *et al.* Integrins control motile strategy through a Rho–cofilin pathway. *J. Cell Biol.* **169,** 515–526 (2005).

82. Wu, Y. & Zhou, B. P. New insights of epithelial-mesenchymal transition in cancer metastasis. *Acta Biochim. Biophys. Sin. (Shanghai).* **40,** 643–50 (2008).

83. Jacquemet, G. *et al.* RCP-driven α5β1 recycling suppresses Rac and promotes RhoA activity via the RacGAP1–IQGAP1 complex. *J. Cell Biol.* **202,** 917–935 (2013).

84. Masuzzo, P., Van Troys, M., Ampe, C. & Martens, L. Taking Aim at Moving Targets in Computational Cell Migration. *Trends Cell Biol.* **26,** 88–110 (2016).

85. Montazeri, M., Montazeri, M., Montazeri, M. & Beigzadeh, A. Machine learning models in breast cancer survival prediction. *Technol. Heal. Care* **24,** 31–42 (2016).

VII. ANNEXES

A

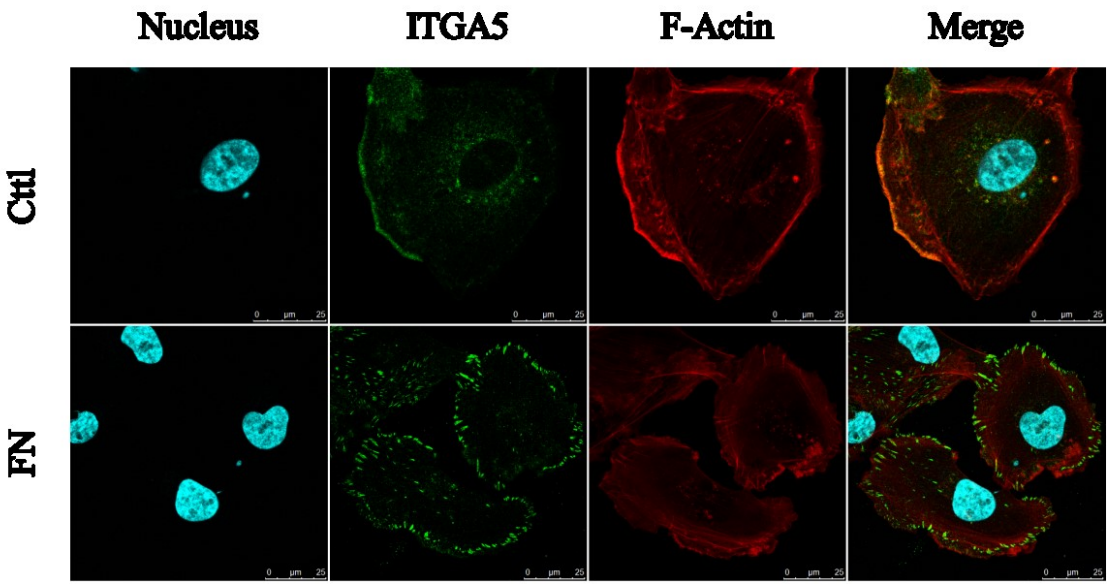

B

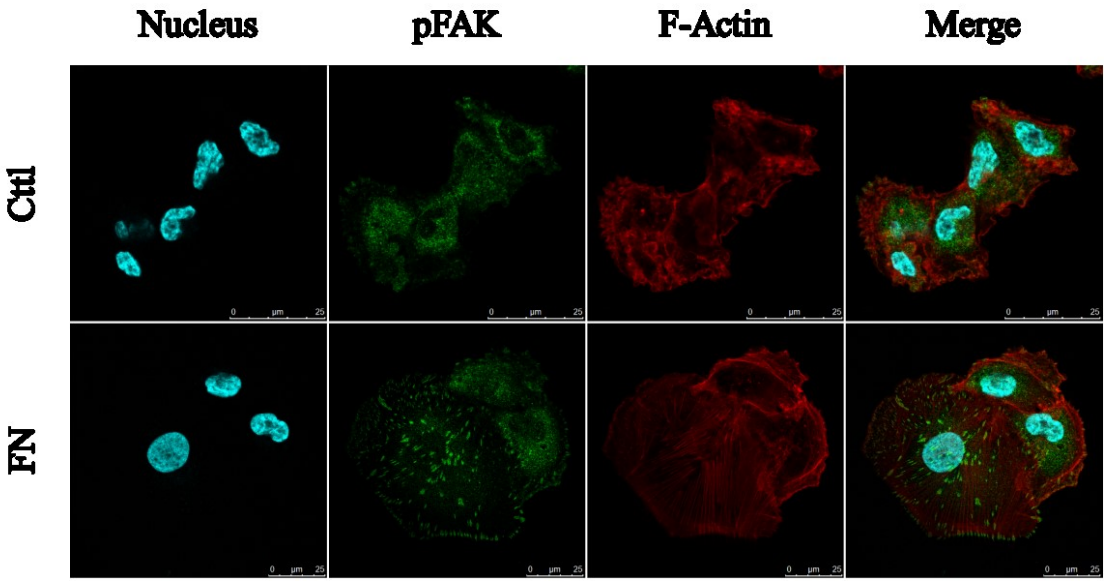

Annexe 1. Immunofluorescence microscopy for ITGA5, pFAK and F-Actin in MDA-MB-231 cells seeded on uncoated or fibronectin-coated surfaces. MDA-MB-231 cells were seeded on uncoated surfaces (Ctrl) or fibronectin-coated surfaces (FN): F-actin (red) and Hoechst (blue). Scale bars: 25 µm. (A) Immunofluorescence microscopic images for ITGA5 (green). (B) Immunofluorescence microscopic images for pFAK (green).

A

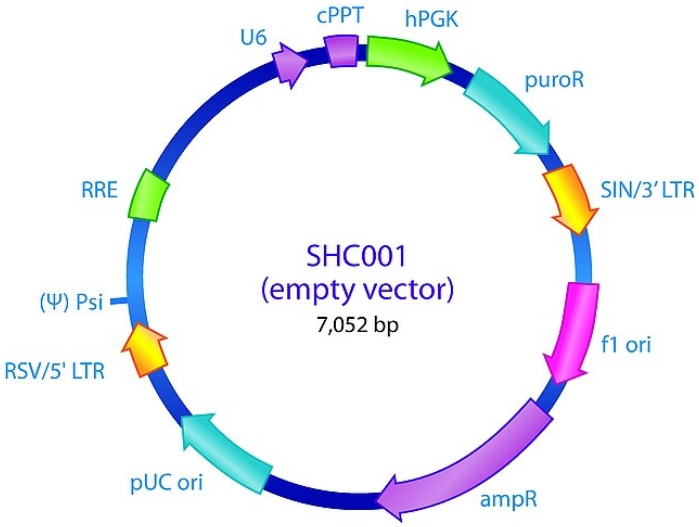

B shRNA 126
CCGGAGGCAGATCCAGGACTATATTCTCGAGAATATAGTCCTGGATCTGCCTTTTTTG
Target: 3'UTR region

C shRNA124
CCGGCATGATGAGTTTGGCCGATTTCTCGAGAAATCGGCCAAACTCATCATGTTTTTG
Target: CDC region

D shRNA 653
CCGGCTCCTATATGTGACCAGAGTTCTCGAGAACTCTGGTCACATATAGGAGTTTTT
Target: CDC region

E shRNA 236
CCGGCCTTAGCCTTTGTCCCAGAATCTCGAGATTCTGGGACAAAGGCTAAGGTTTTT
Target: 3'UTR region

F shRNA 237
CCGGGATGCAGTGAATTGTACCTATCTCGAGATAGGTACAATTCACTGCATCTTTTT
Target: CDC region

Annexe 2. SHC001 vector and short hairpin RNA sequences for ITGA5 or ITGB3 knockdown. Cells were transduced with lentiviral particles containing the SHC001 vector (A). Lentiviral construct integrates into the host genome and provides stable expression of the short hairpin RNA that target ITGA5 mRNA (shRNA 126, shRNA 124 or shRNA653) or ITGB3 mRNA (shRNA 236 or shRNA 237). Sequences shRNA 126 (B), shRNA124 (C), shRNA653 (D), shRNA236 (E), and shRNA237 (F).

A

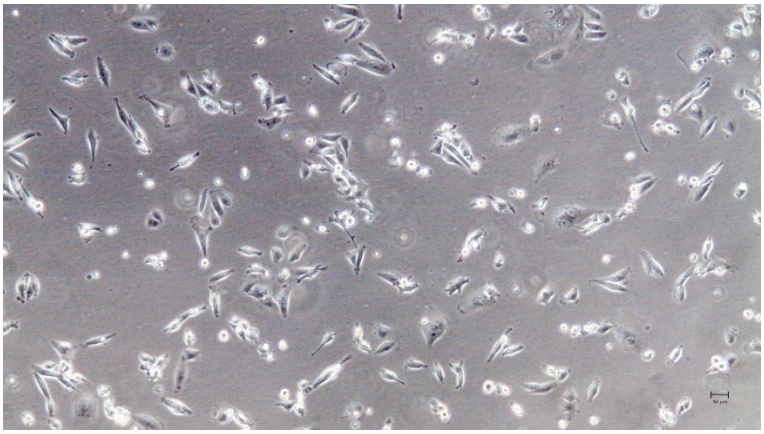

B

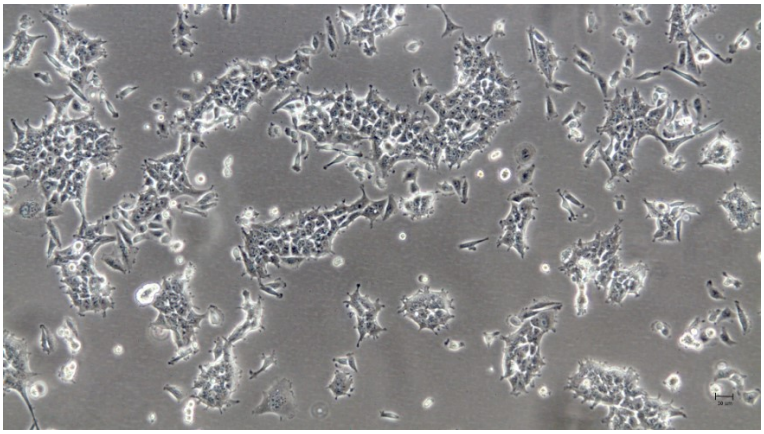

Annexe 3. MDA-MB-231 cell transduced using sh126. Cell morphology of cells transduced with sh126 (A). at PPT7 and (B). at PPT21. Cells presented differences in morphology probably because cells diverged at late PPT.

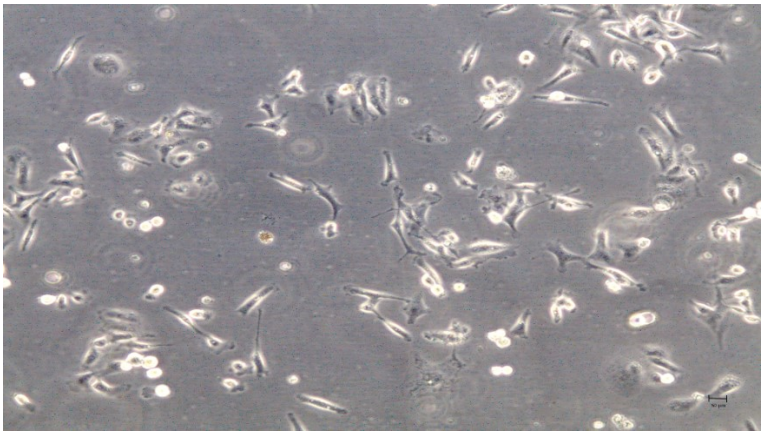

Annexe 4. MDA-MB-231 cell transduced using sh635. Strong cell phenotype at PPT2 after the invalidation of ITGA5 using sh635, that did not allow to achieve the confluence required to perform the characterization of the cells. Picture taken after 5 days of cell seeding

A

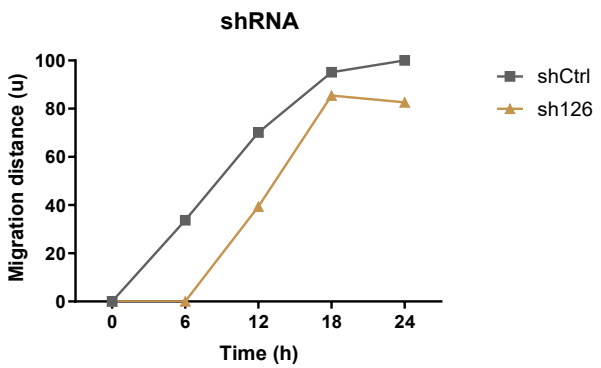

B

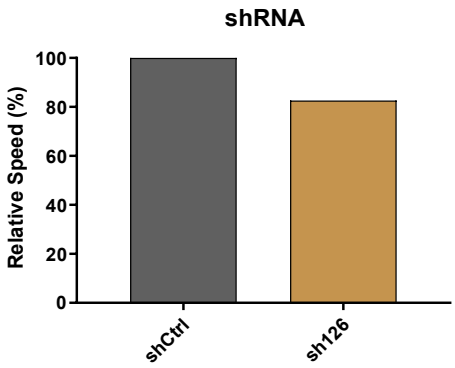

C

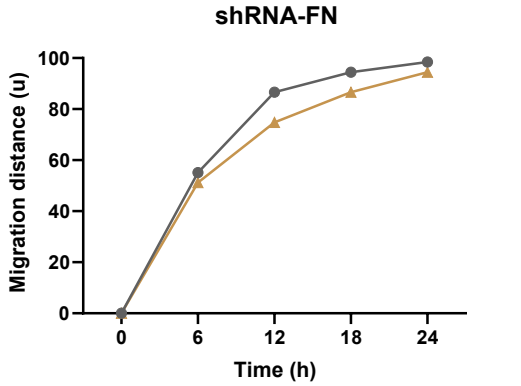

D

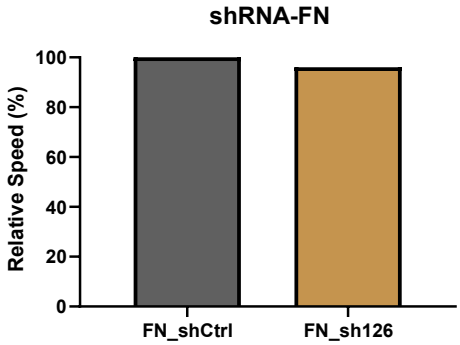

Annexe 5. Effects of ITGA5 knockdown on the migratory capacity of MDA-MB-231 cells seeded on uncoated or FN-coated surfaces. Scratch assay was performed to assess the effects of ITGA5 knockdown using shRNA on the migratory capacity of MDA-MB-231 cells seeded on uncoated surfaces (A and B) or on FN-coated surfaces (C and D). Cell migration quantification of pictures was assessed by imaging processing and it is represented by Migration distance (u), that follows an arbitrary scale (A, C). The relative speed of migration is expressed after being normalized to the corresponding control (B, D).

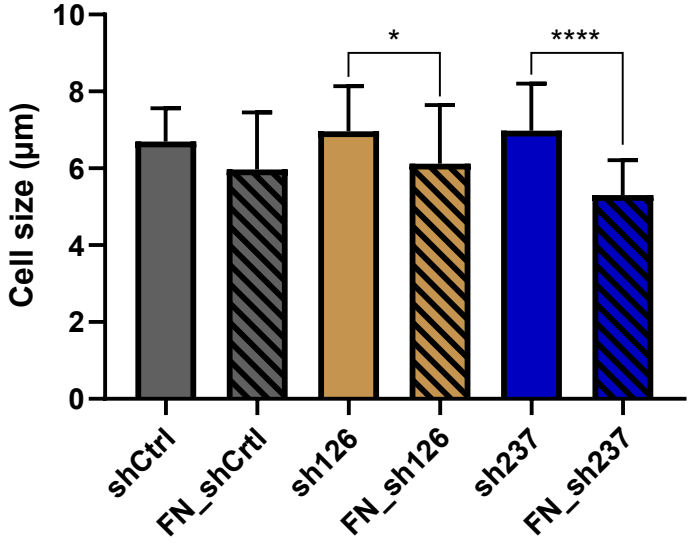

Annexe 6. Cell sizes measured by confocal microscopy of MDA-MB-231 cells. MDA-MB-231 cells were transduced with empty vector shC001 (shCtrl), ITGA5-targeting shRNA (sh126) or ITGB3-targeting shRNA (sh237). Cell sizes were measured by z-series stacking at the passages post transduction (PPT) 13 on uncoated and FN-coated surfaces. Results represent the mean of independent replicates (n = 30). Statistical significance was determined by two-way ANOVA; *$p < 0.05$; **$p < 0.01$; ***$p < 0.001$; ****$p < 0.0001$.

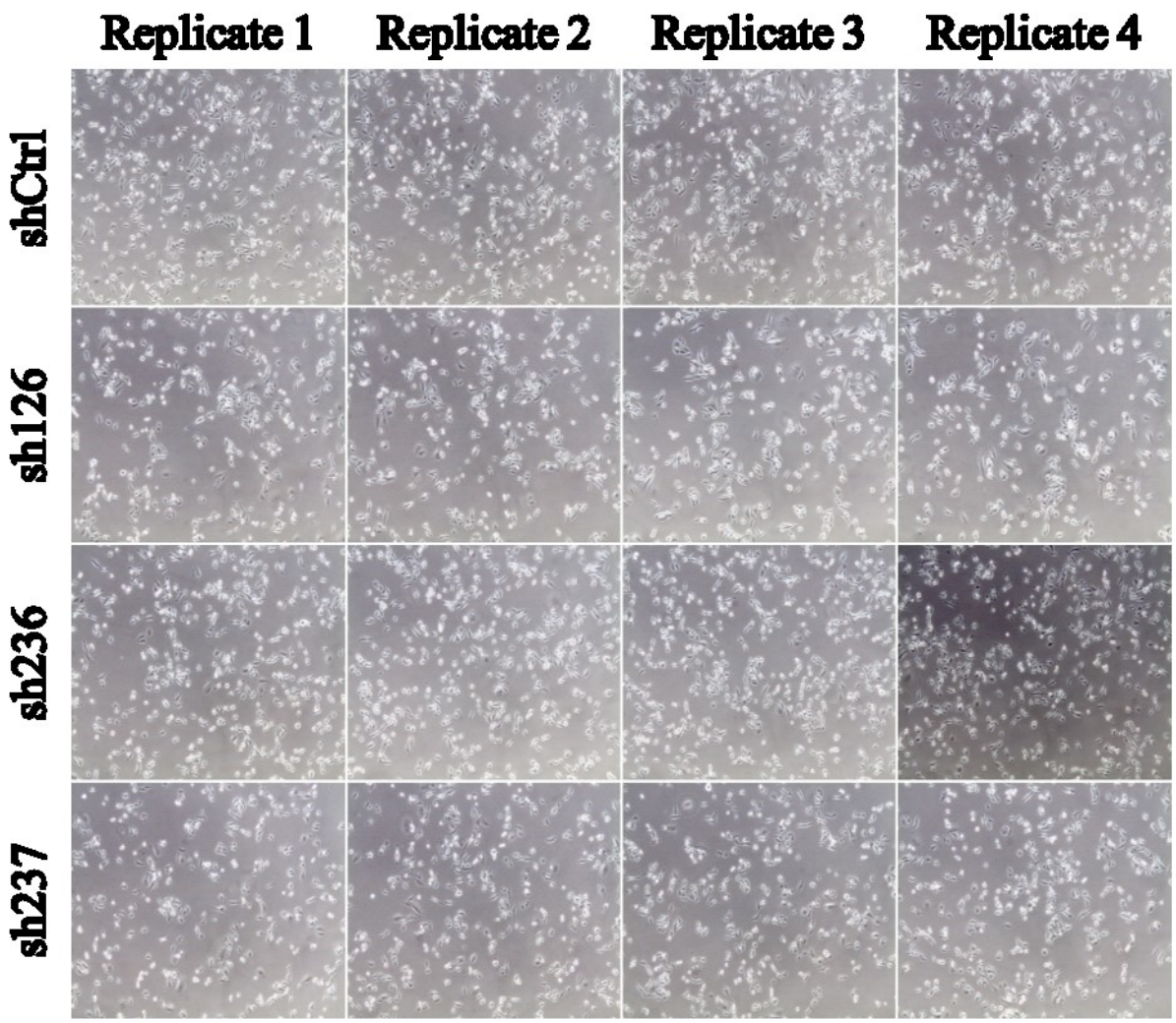

Annexe 7. Difference in confluence between the samples of MDA-MB-231 cells. MDA-MB-231 cells were transduced with empty vector shC001 (shCtrl), ITGA5-targeting shRNA (sh126) or ITGB3-targeting shRNA (sh237 or sh236). Pictures taken at PPT8.

A

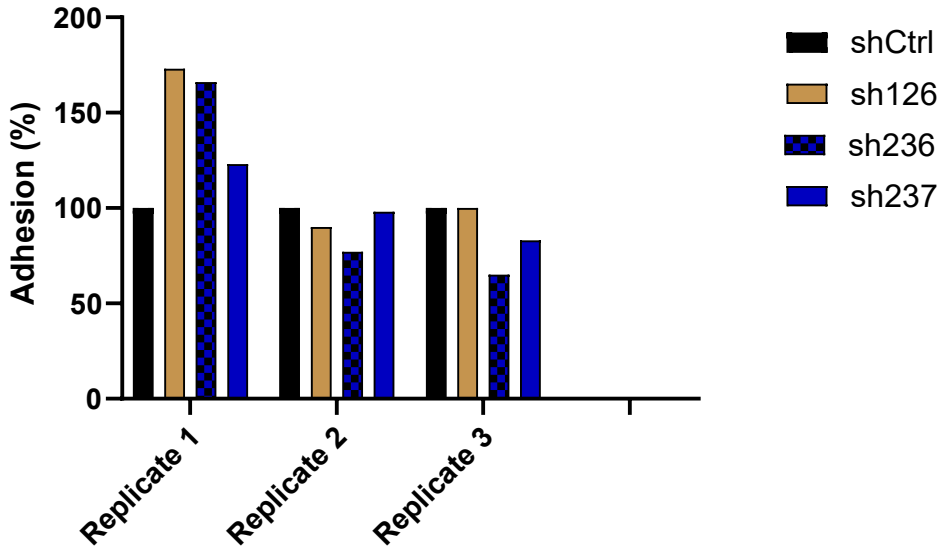

B

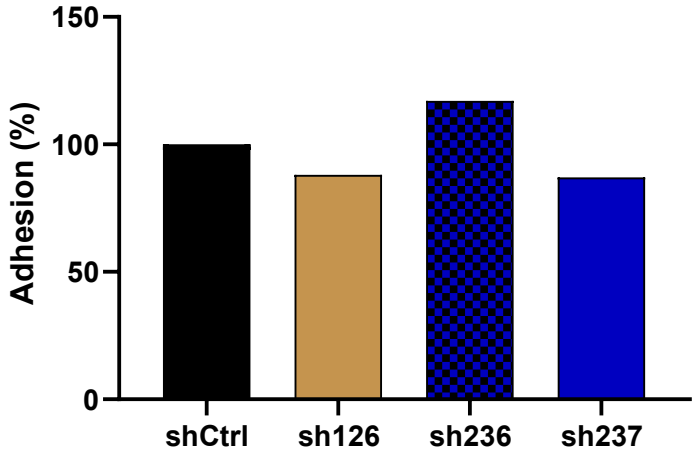

Annexe 8. Adhesion assay for MDA-MB-231 cells. MDA-MB-231 cells were transduced with empty vector shC001 (shCtrl), ITGA5-targeting shRNA (sh126) or ITGB3-targeting shRNA (sh237 or sh236). Adhesion capacity analyzed (A) 1.5 hours and (B) 24 hours after the seeding of the labeled cells.

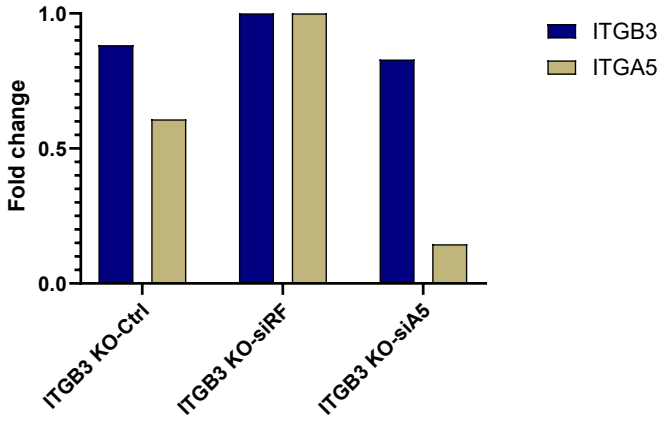

Annexe 9. Gene expression of ITGA5 and ITGB3 in MDA-MB-231 cells upon co-invalidation. ITGB3-invalidated MDA-MB-231 cells transduced with ITGB3-targeting shRNA (sh237) were non-transfected (ITGB3 KO-Ctrl) or transfected using RISC-Free control (ITGB3 KO-siRF) or ITGA5-targeting (ITGB3 KO-siA5). 72 hours post-transfection, the mRNA levels of ITGA5 and ITGB3 were measured by RT-qPCR using α-tubulin as house-keeping gene. Results are expressed in fold change after being normalized to the reference condition (UT) (n = 1).

A

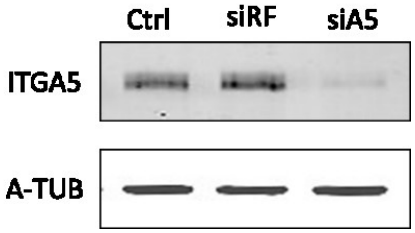

B

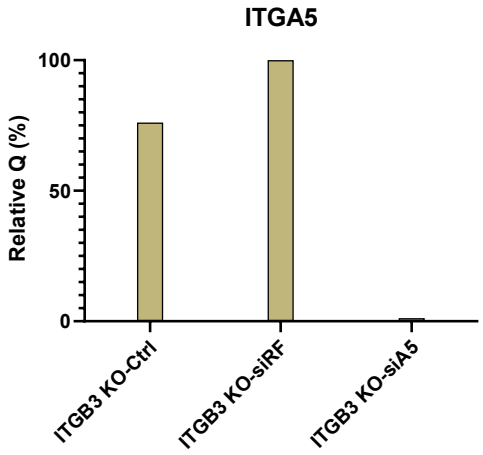

Annexe 10. Protein level of ITGA5 in control cells, in MDA-MB-231 cells upon co-invalidation. ITGB3-invalidated MDA-MB-231 cells transduced with ITGB3-targeting shRNA (sh237) were non-transfected (ITGB3 KO-Ctrl) or transfected using RISC-Free control (ITGB3 KO-siRF) or ITGA5-targeting (ITGB3 KO-siA5). 72 hours post-transfection, the protein level of ITGA5 was assessed by Western Blot analysis and α-tubulin was used as the loading control. Results are expressed in relative quantity after being normalized to the reference condition (UT) (n = 1). (A) Western blotting. (B) Relative quantification.

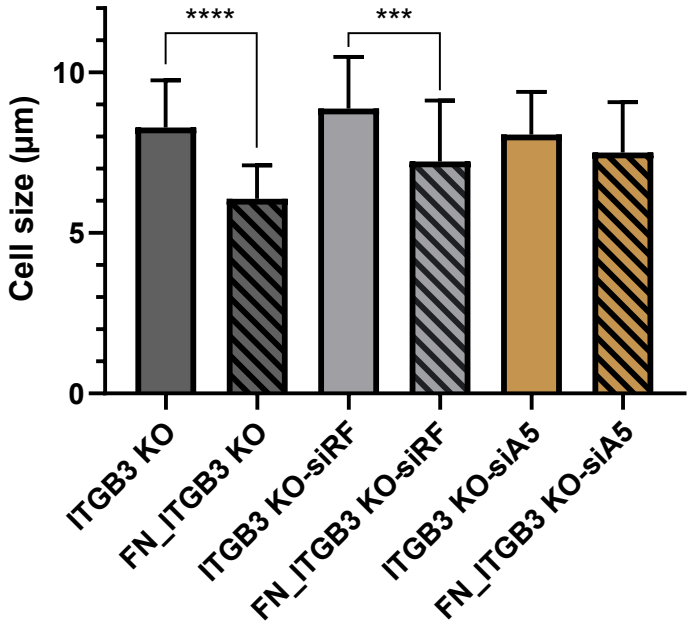

Annexe 11. Cell sizes measured by confocal microscopy of MDA-MB-231 cells upon co-invalidation. ITGB3-invalidated MDA-MB-231 cells transduced with ITGB3-targeting shRNA (sh237) were non-transfected (ITGB3 KO-Ctrl) or transfected using RISC-Free control (ITGB3 KO-siRF) or ITGA5-targeting (ITGB3 KO-siA5). Cell sizes were measured by z-series stacking at 72 hours post-transfection on uncoated and FN-coated surfaces. Results represent the mean of independent replicates (n = 30). Statistical significance was determined by two-way ANOVA; *$p < 0.05$; **$p < 0.01$; ***$p < 0.001$; ****$p < 0.0001$.

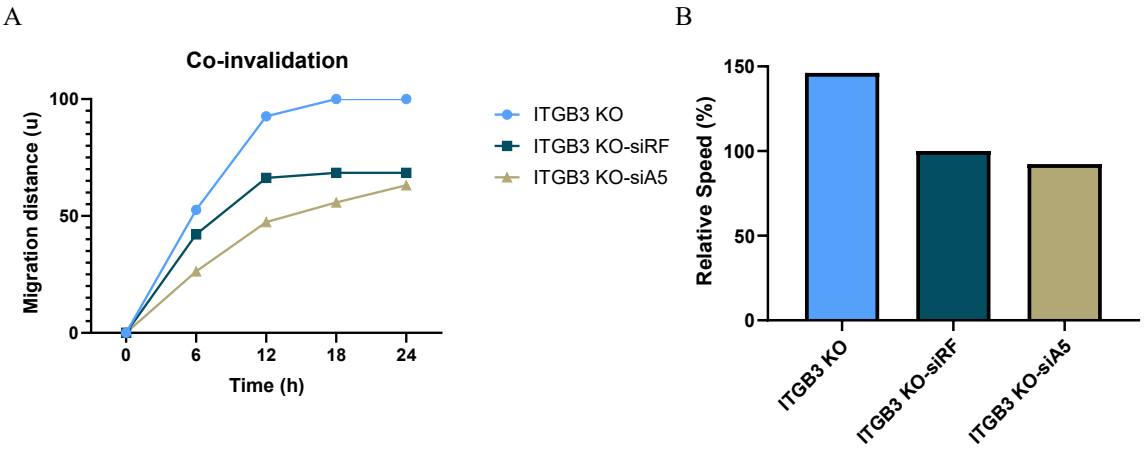

Annexe 12. Effects of ITGA5 knockdown on the migratory capacity of MDA-MB-231 cells after co-invalidation test. ITGB3-invalidated MDA-MB-231 cells transduced with ITGB3-targeting shRNA (sh237) were non-transfected (ITGB3 KO-Ctrl) or transfected using RISC-Free control (ITGB3 KO-siRF) or ITGA5-targeting (ITGB3 KO-siA5). 72 hours post-transfection, scratch assay was performed to assess the effects of ITGA5-silencing and ITGB3-silencing on the migratory capacity of MDA-MB-231 cells. Cell migration quantification of pictures was assessed by imaging processing and it is represented by Closed area (Scratch), that follows an arbitrary scale. The relative speed of migration is expressed after being normalized to the corresponding control.

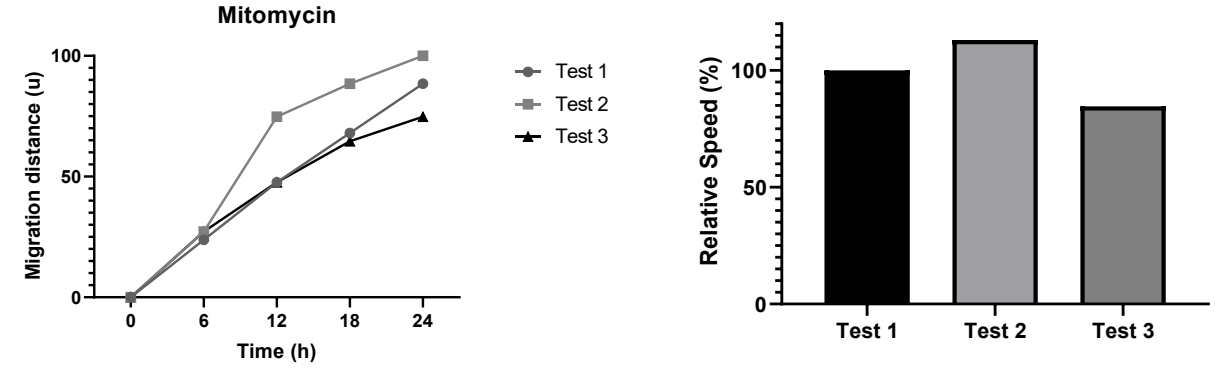

Annexe 13. Effects of mitomycin treatment on the migratory capacity of MDA-MB-231 cells. Scratch assay was performed to assess the effects of mitomycin treatment (see Material and Methods) on the migratory capacity of MDA-MB-231 cells. Test 1: after the scratch is done, the debris was removed with the medium and 3 mL of fresh serum-starved medium with mitomycin were added. Test 2: mitomycin was added 3 hours before performing the scratch and removed from the new media. Test 3: mitomycin was added 3 hours before doing the scratch and kept within the new media. Cell migration quantification of pictures was assessed by imaging processing and it is represented by Closed area (Scratch), that follows an arbitrary scale. The relative speed of migration is expressed after being normalized to the corresponding control.

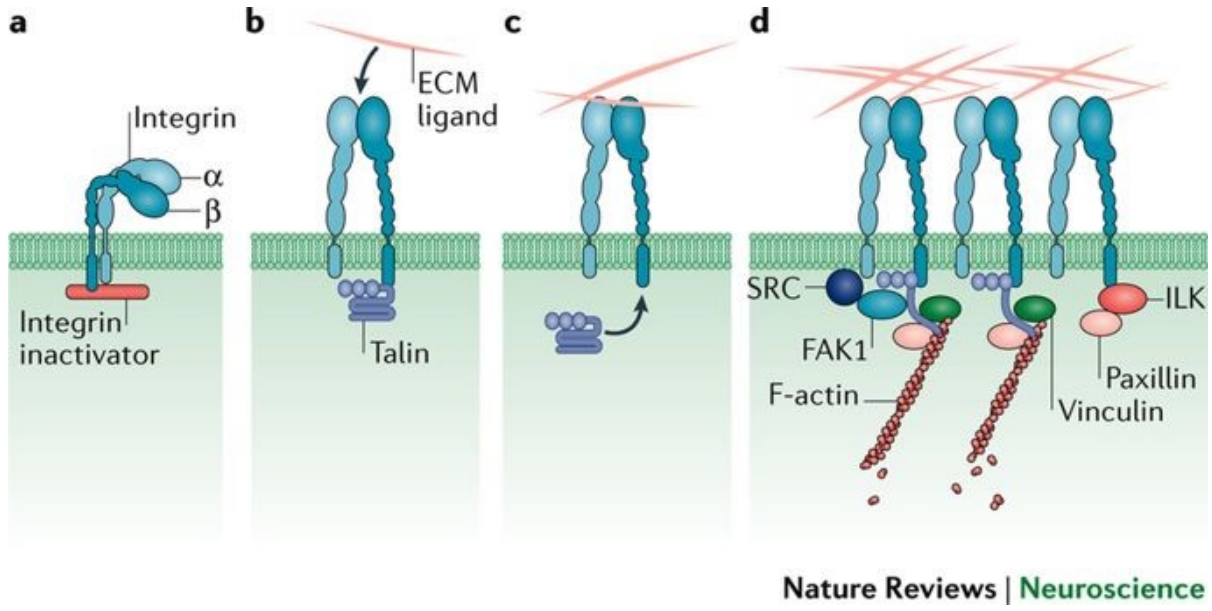

Annexe 14. Integrin activation and signaling. Low-affinity integrin has an inactive, bent, conformation (a). Integrin activation by cytoplasmic proteins or via ECM ligand (b), both lead to complete extension of the extracellular domains (c). High-affinity activated integrin and formation of focal adhesion (d). From Kyung Park and Goda, Nature reviews (2016).

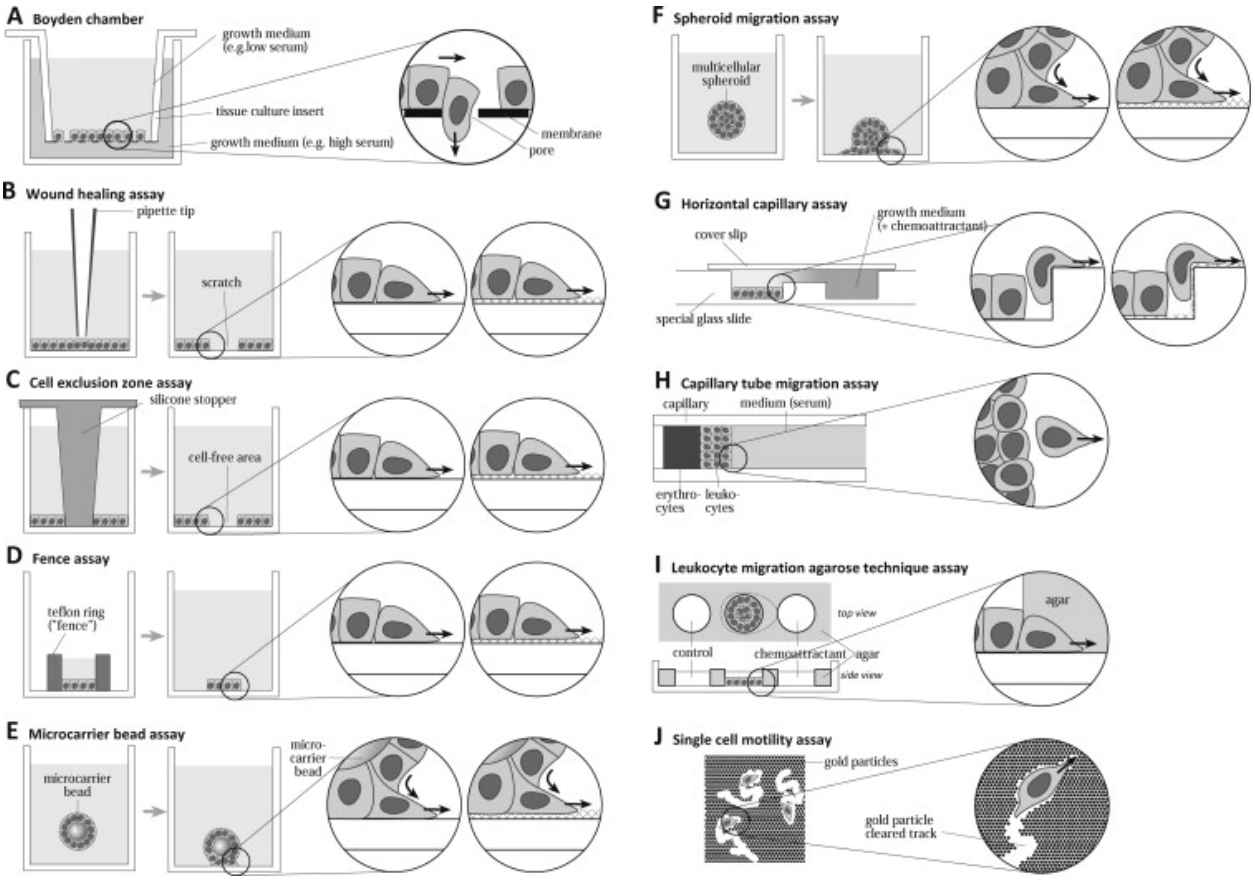

Annexe 15. Schemes of commonly used migration assays. From Kramer, et al, Mutational Research (2013).